

*The role of the pro-inflammatory cytokine
Interleukin-18, its processing enzyme
Caspase-1, and potential alternative IL-18-
activating pathways in atherosclerosis*

Inaugural-Dissertation

zur

Erlangung des Doktorgrades

der Mathematisch-Naturwissenschaftlichen Fakultät

der Universität zu Köln

vorgelegt von

Norbert Gerdes

aus Altenberge

Köln 2005

This work was performed between September 2001 and May 2005 under supervision of Professor Dr. Uwe Schönbeck in the group of Professor Dr. Peter Libby at the Division of Cardiovascular Medicine, Department of Medicine, Brigham & Women's Hospital and Harvard Medical School in Boston, Massachusetts, United States of America. The work was mentored by Professor Dr. Helmut W. Klein, Institute for Biochemistry, University of Cologne, Germany.

Referees (Berichterstatter): Prof. Dr. Helmut W. Klein, University of Cologne
Prof. Dr. Jens Brüning, University of Cologne
Prof. Dr. Uwe Schönbeck, Harvard Medical School

Day of disputation: 5. July 2005

For Christin

And

My family

Table of contents

Table of Abbreviations	5
Zusammenfassung (German summary)	7
Summary.....	8
1. Introduction	9
1.1. Cardiovascular disease and atherosclerosis.....	9
1.2. Atherosclerosis: An inflammatory disease	10
1.3. Matrix metalloproteinases in atherosclerosis.....	14
1.4. Cytokines in atherosclerosis	15
1.5. The pro-inflammatory cytokine IL-18.....	16
1.6. Caspase-1.....	17
1.7. IL-18 and atherosclerosis.....	18
1.8. Clinical association of IL-18 with cardiovascular disease and its risk factors...	20
1.9. Aim of this thesis	21
2. Materials and Methods	22
2.1. Materials	22
2.2. Expression of IFN γ in atheroma-associated cell types	22
2.3. Murine atherosclerosis model.....	30
2.4. Western blot analysis of mouse tissue lysates.....	40
2.5. MMP-mediated processing of proIL-18.....	42
3. Results	45
3.1. IL-18 induces IFN γ in macrophages and smooth muscle cells.....	45
3.2. Deficiency of IL-18 decreases development of atherosclerosis in mice....	51
3.3. The role of IL-18R in aterogenesis.....	65
3.4. Caspase-1 deficiency does not limit aterogenesis in hyperlipidemic mice....	71
3.5. Caspase-1 independent processing of proIL-18.....	78
4. Discussion	90
5. References	103
Acknowledgments	118
Statement of Research	120
Curriculum vitae.....	122

Table of Abbreviations

APMA	p-aminophenylmercuric acetate
ApoE	Apolipoprotein E
<i>apoe</i> ^{-/-}	Apolipoprotein E-deficient (mouse)
bp	Base pair
BCA	Bicinchoninic Acid
BMI	Body mass index
BMT	Bone marrow transplantation
BSA	Bovine serum albumin
CAD	Coronary artery disease
Caspase	Cysteine aspartate protease
<i>casp1</i> ^{-/-}	Caspase-1-deficient (mouse)
CD	Cluster of differentiation
CRP	C-Reactive protein
CO ₂	Carbon dioxide
CVD	Cardiovascular disease
DMEM	Dulbecco's modified eagle medium
DNA	Deoxyribonucleic acid
dNTP	Deoxynucleotide triphosphate
DTT	Dithiothreitol
EC	Endothelial cells
ECGF	Endothelial cell growth factor
ECM	Extracellular matrix
EDTA	Ethylenediaminetetraacetic acid
ELISA	Enzyme-linked immunosorbent assay
FACS	Fluorescence activated cell sorting
FBS	Fetal bovine serum
FITC	Fluorescein isothiocyanate
GAPDH	Glyceraldehyde 3-phosphate dehydrogenase
GM-CSF	Granulocyte/macrophage-colony stimulating factor
Gy	Gray (SI unit for radiation dose; 1 Gy = 1 J / kg = 100 Rad)
HBSS	Hanks' balanced salt solution
HCD	High cholesterol diet
HRP	Horse radish peroxidase
ICAM-1	Intercellular adhesion molecule 1
ICE	Interleukin-1 β -converting enzyme (= Caspase-1)
IGIF	Interferon gamma-inducing factor
IFN γ	Interferon gamma
IgG	Immunoglobulin class G
IHC	Immunohistochemistry
IL	Interleukin
IL-1 β	Interleukin-1 beta
IL-18BP	Interleukin-18 binding protein
IL-1RacPL	Interleukin-1 receptor accessory protein-like
IL-1Rrp	Interleukin-1 receptor related protein
IL-18R	Interleukin-18 receptor
<i>il1rl</i> ^{-/-}	Interleukin-1 receptor type 1-deficient (mouse)
<i>il18rl</i> ^{-/-}	Interleukin-18 receptor alpha-deficient (mouse)
ISH	In situ hybridization
JNK	c-Jun N-terminal kinase

IRAK	Interleukin receptor associated kinase
LC-MS/MS	Liquid chromatography mass spectrometry/mass spectrometry
LPS	Lipopolysaccharide (= endotoxin)
kb	Kilo base
kDa	Kilo dalton
LDL	Low density lipoprotein
LDLR	LDL receptor
MAPK	Mitogen-activated protein kinase
MCP-1	Monocyte chemoattractant protein 1
MHC I	Major histocompatibility complex class I
MIP-1	Macrophage inflammatory protein 1
MMP	Matrix metalloproteinase
MØ	Mononuclear phagocytes, Macrophage
M-CSF	Macrophage colony-stimulating factor
MI	Myocardial infarction
MyD88	Myeloid differentiation primary response gene 88
NFκB	Nuclear factor kappa B
NK cells	Natural killer cells
PBS	Phosphate-buffered-saline
PDGF	Platelet-derived growth factor
PE	Phycoerythrin
PMSF	Phenylmethylsulfonyl fluoride
pNA	p-Nitroaniline
PR-3	Proteinase-3
proIL-1/proIL-18	IL-1/ IL-18 precursor
(m)RNA	(messenger) Ribonucleic acid
RPMI	Rockwell park memorial institute
RT-PCR	Reverse transcriptase-polymerase chain reaction
SCID	Severe combined immuno deficiency
SD	Standard deviation
SDS-PAGE	Sodium-dodecylsulfate-polyacrylamide gelectrophoresis
SEM	Standard error of the mean
SMC	Smooth muscle cells
STAT5	Signal transducer and activator of transcription factor 5
TAE	Tris-acetate-EDTA
TF	Tissue factor
TGFβ	Transforming growth factor beta
T _H	T helper (lymphocytes)
TMB	Tetramethylbenzidine
TNFα	Tumor necrosis factor alpha
TNFR	TNF receptor
TIMP	Tissue inhibitor of matrix metalloproteinases
TFPI-2	Tissue factor pathway inhibitor-2
TRAF	TNF Receptor Associated Factor
UV	Ultraviolet
VCAM-1	Vascular cell adhesion molecule 1

Zusammenfassung

Die Arteriosklerose mit ihren klinischen Komplikationen ist eine der häufigsten Todesursachen in den westlichen Industrienationen. Abstandnehmend vom klassischen Verständnis als Erkrankung des Fettstoffwechsels mit konsekutiver Einlagerung von Lipiden in der Gefäßwand und hierdurch provozierten mechanischen Komplikationen, geht man heute vielmehr von einem komplexen dynamischen Krankheitsbild aus. Dabei sind insbesondere inflammatorische und immunologische Prozesse von entscheidender pathophysiologischer Bedeutung. In der Tat beinhalten arteriosklerotische Läsionen eine Vielzahl immunologisch aktiver Zellen. Diese produzieren verschiedenste proinflammatorische Mediatoren, welche ihrerseits die Atherogenese unterhalten und letztlich zum Auftreten klinischer Symtome führen, wie etwa der instabilen Angina, des Mykardinfarktes oder des Schlaganfalls. Unlängst konnten wir das proinflammatorische Zytokin Interleukin-18 (IL-18) als neuen, potentiellen Mediator der Arteriosklerose identifizieren.

Auf diesen Ergebnissen aufbauend besteht das Ziel der vorliegenden Arbeit darin, die *in vivo* Rolle von IL-18 und seiner aktivierenden Protease Caspase-1 in der Arteriosklerose am Mausmodell zu evaluieren. Interressanterweise führte die IL-18-Defizienz zu einer signifikanten Reduktion früher arteriosklerotischer Läsionen, während spätere Stadien der Erkrankung unbeeinflusst blieben. Diese Studien verdeutlichen, dass IL-18 über seine klassische Funktion, der Induktion von Interferon- γ (INF- γ), hinausgehend von pathophysiologischer Bedeutung für die Progression der Arteriosklerose ist. Weiterführende Experimente an durch Knochenmarktransplantation erhaltenen chimären Mäusen mit IL-18R α defizienten hämatopoetischen bzw. vaskulären Zellen ergaben, dass die proatherogenen Effekte von IL-18 nicht über den IL-18R α vermittelt werden. Ferner vermochte die Caspase-1 Defizienz überraschender Weise nicht die Atherogenese zu beeinflussen, ein Ergebnis, welches alternative Mechanismen der IL-18 Aktivierung nahelegte. Im Folgenden durchgeführte Experimente untersuchten, ob Matrixmetalloproteininasen (MMPs), welche in arteriosklerotischen Plaques überexprimiert werden, einen solchen alternativen Aktivierungsweg darstellen könnten. In der Tat bewirkten mehrere rekombinante MMPs die proteolytische Spaltung von pro-IL-18. Insbesondere MMP-2 und MMP-8 prozessiertes proIL-18 zeigte biologische Aktivität. Sequenzanalysen des prozessierten proIL-18 identifizierten Schnittstellen, die von der klassischen Schnittstelle von Caspase-1 differierten. Abschließend gelang der Nachweis von prozessiertem IL-18 in Caspase-1 defizienten Mäusen. Dieser Befund unterstreicht die biologische *in vivo* Relevanz eines solchen alternativen MMP-vermittelten Aktivierungsweges.

Zusammenfassend zeigt die vorliegende Arbeit die proatherogene Rolle von IL-18 *in vivo* auf und weist deren Unabhängigkeit von IL-18R α und Caspase-1 nach. Der letztere Befund ist überraschend und trägt wesentlich zum besseren Verständnis der biologischen Funktion von IL-18 bei. Die dargestellten Ergebnisse haben potentiell tiefgreifende Konsequenzen für gegenwärtige Strategien zur therapeutischen Intervention dieser biologischen Kaskaden.

Summary

Atherosclerosis is the predominant underlying pathology of cardiovascular disease, the most common cause of premature death in the industrialized world. Recent research attributed inflammation a crucial role in atherosclerosis. Indeed, atherosclerotic lesions are characterized by abundance of immune cells and their effector molecules, accelerating atherogenesis and eventually leading to clinical symptoms such as unstable angina, myocardial infarction, or stroke. We have recently implicated the pro-inflammatory cytokine interleukin (IL)-18 as a novel mediator in this disease.

The present work aims to evaluate the *in vivo* role of this cytokine and its activating protease Caspase-1 in atherosclerosis. Interestingly, IL-18-deficiency limited early lesion development in hyperlipidemic mice but did not affect atherogenesis after prolonged hyperlipidemia. These studies suggest a direct role for IL-18 in disease progression extending beyond the classical function of this cytokine, the induction of interferon gamma. Additional experiments employing chimeric mice, that lacked the IL-18R α on either the hematopoietic or the vascular cells, generated by bone-marrow transplantation, revealed that IL-18R α does not participate in the pro-atherogenic effects of IL-18.

Surprisingly, deficiency of Caspase-1 did not diminish atherogenesis, thus suggesting alternative mechanisms of IL-18 activation during atherosclerosis.

Subsequent experiments tested whether matrix metalloproteinases (MMPs), enzymes prominently expressed in atherosclerotic lesions mediate the maturation of the IL-18 precursor (proIL-18). Indeed, several recombinant MMPs proteolytically cleaved the precursor *in vitro*, and MMP-2- and MMP-8 processed proIL-18 exhibited IL-18 activity.

Sequence analysis of processed proIL-18 demonstrated that cleavage sites of MMP-2 and MMP-8 differ from that of Caspase-1. Finally, the presence of mature/processed IL-18 in atherosclerotic tissue of Caspase-1-deficient mice highlighted the potential *in vivo* relevance of such an alternative, MMP-mediated IL-18 activation mechanism for this pro-inflammatory disease.

In sum, this work directly demonstrates the pro-atherogenic role of IL-18 independent of IL-18R α or Caspase-1. These surprising observations provide a novel understanding of IL-18 biology and may foster re-thinking of current approaches for the therapeutic intervention of this pathway in prevalent inflammatory diseases.

1. Introduction

1.1. Cardiovascular disease and atherosclerosis

Cardiovascular disease (CVD) continues to lead as a principal cause of death in developed countries,^{1,2} accounting for approximately 38 % and 42 % of deaths in the United States and the European Union, respectively.^{3,4} The total economic burden of CVD exceeds \$390 billion and €165 billion annually for these regions, respectively.^{3,4} Due to containment of many infectious diseases and increasing adoption of western lifestyles, this trend is projected to extend worldwide by 2020.^{2,5} The vast majority of CVD-related deaths is attributed to a disease of arterial blood vessels, known as ‘atherosclerosis’.³

Derived from the Greek words *athera* (gruel) and *scleros* (hard), atherosclerosis has been viewed for decades as a mere deposition of lipids along arterial walls. In the progression of the disease, these accumulations were thought to gradually narrow the lumen and finally lead to occlusion of the vessel, thus interrupting blood flow and oxygen supply to vital organs such as the heart and brain.⁶ This dogma was commonly accepted until studies in the late 1980s revealed that 60-70% of acute myocardial infarctions result from non-occlusive atherosclerotic lesions.⁷⁻⁹ Further research identified plaque disruption and subsequent thrombus formation rather than gradually developing stenosis as the final pathologic steps that cause acute clinical events such as myocardial infarction or stroke.^{10,11} Despite its considerable impact, the pathological mechanisms underlying this vascular dysfunction remain incompletely understood.

Research during the past two decades has focused on the cellular and molecular mechanisms responsible for the development and destabilization of atherosclerotic plaques. Indeed, numerous studies demonstrated that most plaques did not consist of mere acellular lipid depositions, but rather harbored active inflammation characterized by accumulation of immune-competent cells.¹²⁻¹⁷ The current view of atherosclerosis hypothesizes that complex processes, that include molecular and cellular components of the immune system, successively decrease plaque stability and provoke its rupture, thus exposing highly pro-

coagulant mediators to the blood stream and resulting in thrombosis and its subsequent clinical symptoms.¹⁸⁻²⁰ Hence, immune mechanisms that regulate integrity and stability as well as formation of atherosclerotic plaques have gained considerable attention among vascular biologists.¹⁴⁻¹⁷

1.2. Atherosclerosis: An inflammatory disease

The development of human atherosclerosis usually extends over decades.^{13,21,22} Two independent studies found fatty streaks, the earliest visible atherosclerotic lesions, ubiquitous among teenagers.^{23,24} These studies revealed that atherosclerosis starts rather early in life although clinical symptoms precipitate most commonly in people of advanced age. The initial triggers of the atherogenic process still remain undetermined. Among other factors, i.e., response to endothelial injury or microbial infection, elevated levels of plasma lipoproteins such as low-density lipoproteins (LDL) are considered prerequisite for atherosgenesis. Hyperlipidemia, commonly caused by environmental and/or genetic factors,²⁵⁻²⁷ can lead to the accumulation of LDL within the vessel wall, where it can undergo modifications such as glycation or oxidation within the intima (Figure 1).^{28,29} Subsequently, such modified LDL can activate endothelial cells (EC), preferably at sites of hemodynamic strain,^{30,31} promoting recruitment of circulating T lymphocytes and monocytes from the blood via the expression of adhesion molecules (e.g., P-selectin, vascular cell adhesion molecule-1 (VCAM-1), and intercellular adhesion molecule-1 (ICAM-1)).¹⁴⁻¹⁷ Upon adhesion, monocytes and T lymphocytes, attracted by EC-derived chemokines (e.g., monocyte chemoattractant protein-1 (MCP-1) and macrophage inflammatory protein-1 α (MIP-1 α)), transmigrate into the intima.^{16,17} Resident monocytes, termed macrophages, within the inflamed vessel wall can incorporate native or modified LDL via phagocytic or receptor-mediated mechanisms.^{14,17} Following uptake, cholesterol can not be mobilized sufficiently and might instead accumulate as cytosolic droplets of cholesterol esters. These lipid-laden macrophages, also termed ‘foam cells’ due to their microscopic appearance, characterize early atherosclerotic lesions, also known as fatty streaks (Figure 1).^{16,17} The

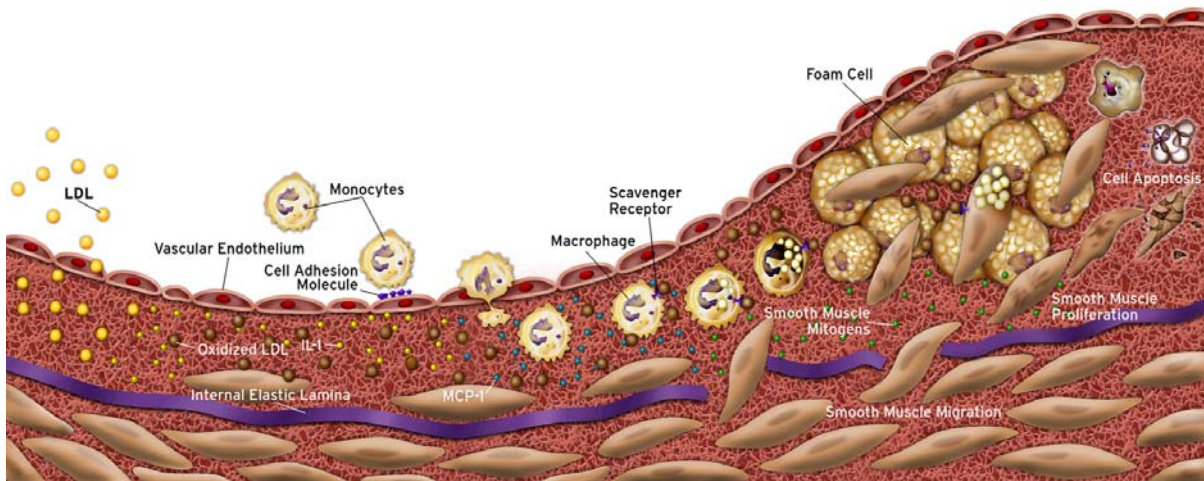


Figure 1: Cellular mechanisms during atherosclerotic plaque evolution.

The earliest changes preceding the formation of atherosclerotic lesions take place in the endothelium. Increased endothelial permeability to lipoproteins leads to accumulation of low density lipoprotein (LDL) in the intima. Modification, particularly oxidation, of these particles induces local cytokine elaboration, which enhances in turn the expression of adhesion molecules and chemokines, e.g., monocyte chemoattractant protein 1 (MCP-1). Attracted by chemokines peripheral blood monocytes enter the lesion and express scavenger receptors in response to cytokine stimulation. These receptors mediate the uptake of modified lipoprotein particles by macrophages promoting the development of foam cells. Macrophage-derived foam cells are a source of further cytokines, smooth muscle cells (SMC) proliferative factors, and matrix metalloproteinases. SMC proliferate and can migrate from the media into the intima. Proliferation and synthesis of extracellular matrix assist establishing the fibrous cap, which separates the lesion from the blood stream. Continued influx and activation of macrophages, which release metalloproteinases, can cause degradation of extracellular matrix, eventually leading to rupture of the fibrous cap, thrombus formation, and occlusion of the artery (not shown).

Modified from: Libby. P. *The vascular Biology of Atherosclerosis*. Heart Disease: A Textbook of Cardiovascular Medicine. Braunwald, Zipes, and Libby Eds., 2001.

accumulation of lipids, particularly their oxidatively modified derivatives furnish a strong trigger of pro-inflammatory responses.^{32,33} Sustained lipid uptake and accumulation causes production of pro-inflammatory cytokines, such as interleukin- (IL-)1 β and tumor necrosis factor (TNF) α .^{14,16,17} Notably, these mediators might activate in an autocrine and paracrine fashion not only other macrophages, but also EC, smooth muscle cells (SMC), and T-lymphocytes within the lesion, thereby accelerating the inflammatory process in a positive feedback loop.^{14,16,17,34} Additionally, overexpressed growth factors, such as macrophage colony-stimulating factor (M-CSF), in the inflamed arterial wall function as survival and mitogenic stimulus for the inflammatory cells.³⁵

During lesion progression, foam cells in these early lesions can undergo apoptosis.^{16,36} This process, thought mediated in part by the Fas/FasL pathway,^{37,38} contributes to the development of the lipid-rich, acellular core of the plaque (Figure 1). The lipid core contains large amounts of pro-coagulants, particularly tissue factor (TF) synthesized by foam cells and potentially released during their death.²⁰ Furthermore, SMC migrate into the lesion in response to signals provided by platelet derived growth factor (PDGF) and other chemoattractant mediators from the media, establishing the plaque's fibrous cap, which segregates the pro-thrombotic lipid core from the lumen. SMC proliferate and contribute to formation of the fibrous cap by synthesis of extracellular matrix proteins, particularly interstitial collagen.³⁹ The thickness and collagen content of the fibrous cap positively correlates with the plaque's biomechanical stability.^{40,41} Certain pro-inflammatory cytokines such as interferon gamma (IFN γ) inhibit proliferation and collagen synthesis of SMC and can trigger apoptosis of these cells, eventually contributing to the thinning of the fibrous cap and rendering the plaque prone to rupture.^{16,38,39,42}

Rupture of the atherosclerotic plaque, often occurring in the macrophage-enriched shoulder region, the junction between the atheroma and the normal vessel wall, exposes the pro-coagulant content of the lesion to coagulation factors of the blood,¹⁶ resulting in thrombus formation (Figure 2)^{16,18,43} In subclinical plaque rupture, the thrombus does not completely occlude the lumen of the vessel and may eventually resorb. Growth factors released during the subsequent wound healing process can lead to SMC proliferation and thickening of the fibrous cap, yielding a constriction of the lumen and restriction of blood flow. Under increased cardiac demand this can lead to ischemia, provoking symptoms such as *angina pectoris*.¹⁶ However, if plaque rupture causes an occlusive thrombus formation it may lead to acute clinical complications, such as myocardial infarction (MI) and stroke.^{16,44} Therefore, the strength of the fibrous cap is considered a key determinant of atherosclerotic plaque stability.^{40,41} Accordingly, histological studies classify atherosclerotic lesions into those with features of 'stable' and 'unstable' (vulnerable) plaques (Figure 2). An unstable atheromatous plaque typically displays a large lipid core containing high amounts of pro-thrombotic tissue factor overlaid by a thin fibrous cap and accompanied by an accumulation of inflammatory cells, particularly in the shoulder region.^{16,18,21,44} In contrast, a stable fibrous

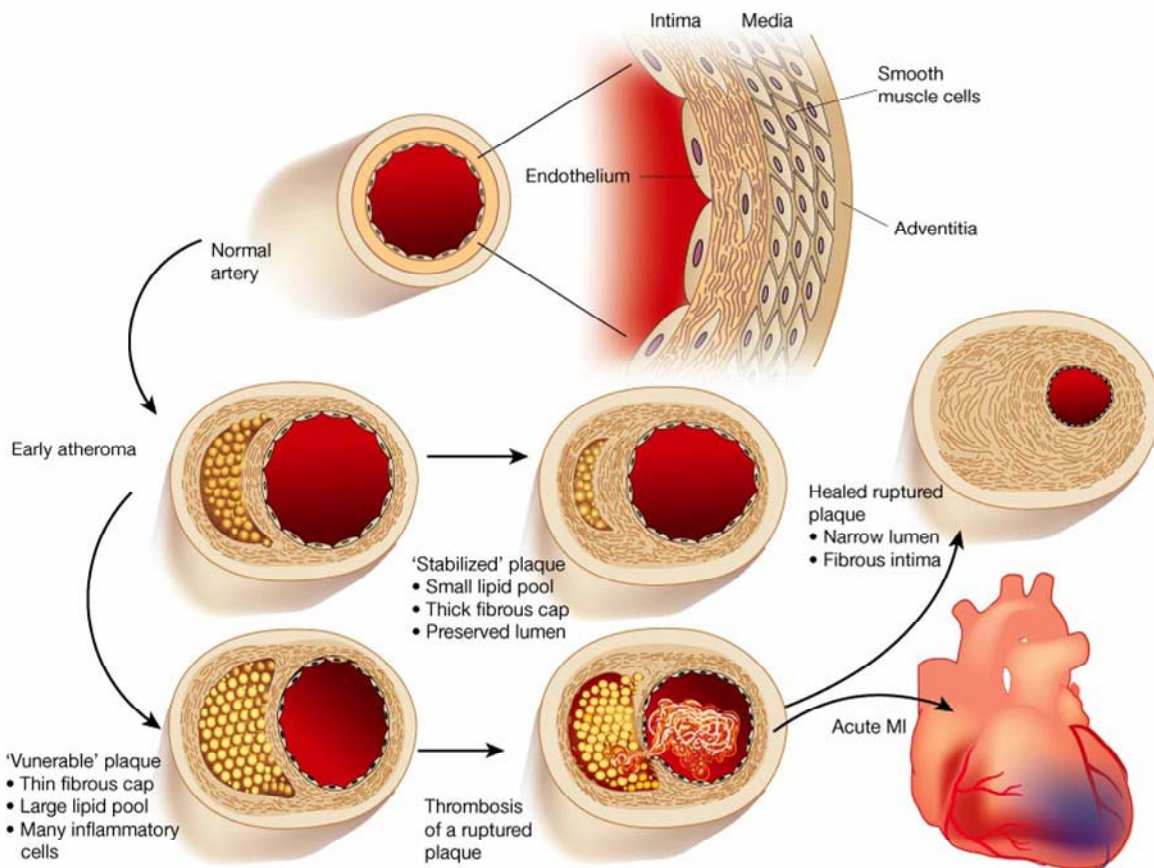


Figure 2: Schematic of the life history of an atheroma.

The normal human artery has a trilaminar structure. The endothelial cells separate the bloodstream from the intima, which contains a smattering of smooth muscle cells scattered with extracellular matrix. The media consists of much more tightly packed smooth muscle cells embedded in matrix rich in elastin as well as collagen. In early atherogenesis recruitment of inflammatory cells and accumulation of lipids lead to the formation of the lipid-rich core, as the artery enlarges to accommodate the expansion of the intima. Persistent inflammatory conditions cause further growth of the lipid core, degradation of extracellular matrix by proteases secreted by activated leukocytes, and reduced de-novo synthesis of collagen. These changes can thin the fibrous cap and leave it susceptible to rupture. Upon rupture, blood coming in contact with the thrombogenic content in the plaque coagulates and triggers thrombus formation. If the thrombus occludes the vessel persistently, an acute myocardial infarction (MI) can result. The thrombus may eventually resorb as a result of endogenous or therapeutic thrombolysis. However, growth factors released during the subsequent wound healing process can lead to smooth muscle cell proliferation and thickening of the fibrous cap, which can cause an inward directed growth of the intima, yielding a constriction of the lumen and restriction of blood flow. Increasing cardiac demand can lead to ischemia, provoking symptoms such as *angina pectoris*. Lipid lowering may reduce lipid content and calm the intimal inflammatory response, yielding a more “stable” plaque with a thick fibrous cap and, hence, less prone to rupture.

Modified from: Libby P., Inflammation in atherosclerosis. *Nature* 2002;420:868-74

lesion features a well-developed fibrous cap and moderate lipid/leukocyte content (Figure 2).^{16,18,21,44}

Nonetheless, the progression from fatty streak to advanced, complex lesions likely does not occur inevitably and continuously over time.¹⁶ Clinical observations rather suggest that many human lesions develop discontinuously, featuring “bursts” of growth and progression of atheroma.^{16,45} Therefore, comprehensive understanding of the mechanisms that cause plaque progression and destabilization is crucial for the future treatment of the disease and prevention of acute clinical events.

1.3. Matrix metalloproteinases in atherosclerosis

Matrix metalloproteinases have gained particular interest as potential mediators of plaque destabilization. These enzymes constitute a family of zinc-endopeptidases that share variations on a basic five-domain structure and are generally classified after their particular substrate (e.g., collagenases, gelatinases, elastases).^{46,47} Notably, atheromatous plaques overexpress MMP-1, -2, -3, -7, -8, -9, -10, 12, and -13.⁴⁶⁻⁵⁵

Within the fibrous cap, SMC express a mixture of structural proteins, including collagen, gelatin, laminin, and elastin, that comprise the extracellular matrix (ECM).^{46,47} The amount of collagen, the most abundant ECM protein in the fibrous cap contributing to its strength, is modulated by two mechanisms: *de novo* synthesis and degradation.^{47,56} Pro-inflammatory conditions can abrogate synthesis of collagen by SMC and simultaneously enhance the expression of MMPs, increasing collagen catabolism and, in turn, decreasing plaque stability.¹⁸ During lesion progression macrophages and T-cells continue to enter the lesion and aggregate particularly in the shoulder region.^{16,18,43} The continued activation of macrophages and T-cells as well as EC and SMC by inflammatory cytokines enhances expression and activity of MMPs.^{18,47} Members of two subfamilies of MMPs are considered particularly relevant to atherosclerosis and plaque stability. Interstitial collagenases (MMP-1, -8, and -13) mediate the initial breakdown of collagen fibrils, while gelatinases (MMP-2 and -9) can facilitate further degradation.^{47,48,51,55,57} Notably, endogenous inhibitors such as

members of the TIMP family (tissue inhibitor of matrix metalloproteinases)^{46,47,58} and TFPI-2 (tissue factor pathway inhibitor-2),⁵⁹ regulated MMP activity. However, chronic inflammation may cause an imbalance of MMPs and their endogenous inhibitors, thereby promoting elevated MMP activity, a characteristic of atherosclerosis and other inflammatory diseases.^{18,46,47} Indeed, expression of these proteases localizes with sites of collagenolysis in advanced atherosclerotic lesions,⁵³ supporting the hypothesis that imbalanced MMP regulation contributes to lesion destabilization by decreasing fibrous cap strength, thus rendering the plaque prone to rupture.

1.4. Cytokines in atherosclerosis

Substantial evidence suggests that the cytokine network orchestrates the complex cellular and inflammatory interactions underlying atherogenesis. The net pro- or anti-atherogenic function of cytokines relates to their ability to augment or antagonize inflammation, although this classification certainly oversimplifies the complex pathologic scenario of atherosclerosis. IL-1 β and TNF α are classical pro-inflammatory cytokines and mediate pro-atherogenic functions,^{16,17} whereas IL-4 and IL-10 are considered anti-inflammatory cytokines and accordingly promote mostly anti-atherogenic pathways.^{16,17,60,61} Macrophages and T-cells, the dominant lymphocyte subpopulation within the atherosclerotic plaque, may partially modulate the antagonism between pro- and anti-atherogenic cytokines within the lesion and their polarization into a type 1 or type 2 helper T-cell (T_H1) or (T_H2) phenotypes. Lacking distinct surface markers, T_H1 lymphocytes are characterized by secretion of IFN γ and TNF α ,^{62,63} whereas T_H2 polarization favors secretion of IL-3, IL-4, IL-5, IL-10, and IL-13, which promote B-cell differentiation and immunoglobulin production,^{62,63} processes not commonly associated with atherosclerosis. In accord with the observed pro- or anti-inflammatory functions, expression of T_H1 cytokines indeed dominates over T_H2 cytokines in human atherosclerotic lesions *in situ*.^{60,64} Moreover, lack of T_H1 cytokines generally diminishes the extent of atheroma in animal models,⁶⁵⁻⁶⁸ whereas deficiency of T_H2 cytokines promotes atherogenesis.^{61,68}

IFN γ crucially mediates the T H 1-dominated pathways that lead to macrophage activation and the induction of a plethora of pro-inflammatory factors such as chemokines, cytokines, and growth factors from vascular as well as immune cells.^{16,17,63,69} In addition, IFN γ might contribute to plaque destabilization by inhibiting SMC-proliferation and collagen synthesis, as discussed above.⁷⁰ Accordingly, IFN γ - or IFN γ receptor-deficiency leads to reduced severity of atherosclerosis in hyperlipidemic mice.^{65-67,71,72} Nonetheless, the underlying mechanisms that elicit IFN γ expression in atherosclerosis remained largely unknown until recently.

1.5. The pro-inflammatory cytokine IL-18

IL-18 is a member of the IL-1 cytokine family. Originally designated as Interferon gamma-inducing factor (IGIF) IL-18 was initially discovered as a potent inducer of IFN γ in T H 1-cells and Natural Killer (NK) cells.⁷³⁻⁷⁵ The human IL-18 gene consists of six exons, spanning approximately 19.5 kb.⁷⁶ In both humans and mice, IL-18 expression in macrophages is enhanced either directly by bacterial and viral antigens or in an auto- and paracrine manner by stimulation with IFN α , - β , or - γ .^{77,78} Furthermore, pro-inflammatory cytokines such as IL-1 β or TNF α enhance expression of IL-18.^{78,79} Initially identified in Kupffer cells and activated macrophages,⁷⁵ a variety of other cell types express IL-18, including osteoblasts,⁸⁰ chondrocytes,⁸¹ epidermal keratinocytes,⁸² dendritic cells,⁸³ as well as intestinal and airway epithelial cells.^{84,85}

IL-18 expression and function has been associated with a variety of chronic inflammatory disorders, including cancer, rheumatoid arthritis, Crohn's disease, psoriasis, and pulmonary sarcoidosis.^{79,86-89} Recently, anti-viral and anti-tumor properties were ascribed to IL-18 in addition to its role in innate immunity against bacterial infection.^{77,90}

In contrast to most cytokines, the IL-18 gene contains only one RNA-destabilizing element, conferring unusual stability on IL-18 mRNA that highlights the importance of post-transcriptional regulation of IL-18 activity.⁷⁸ Translation results in the synthesis of an 193 amino acid precursor (proIL-18) of 24 kDa, revealing 65% sequence identity with the 192

amino acid murine proIL-18.⁷⁴ Similar to its analogue proIL-1 β , proIL-18 lacks a conventional signal sequence and requires processing by Caspase-1, also termed IL-1 β -converting enzyme (ICE), into the active, 18 kDa mature form.⁹¹⁻⁹³ Cleavage via Caspase-1 occurs between Asp³⁶ and Tyr³⁷ for human proIL-18 and between Asp³⁵ and Asn³⁶ for the murine homologue, respectively.^{78,93} In addition, Caspase-3 has been reported to cleave proIL-18 at different sites than Caspase-1, resulting in inactive forms of the cytokine and implicating Caspase-3 in negative regulation of IL-18 activity.⁹⁴ Since the IL-18 mRNA is unusually stable, as discussed above, and thus appears to evade stringent transcriptional regulation, the post-translational regulation of IL-18 activity by proteases such as Caspase-1 and -3 is considered particularly relevant to determination of the activity of this cytokine.⁷⁸

1.6. Caspase-1

Caspase-1 represents the founding member of a family of cysteine proteases termed Cysteine requiring ASPartate proteASE (Caspase), sharing the active site cysteine and aspartate binding clefts.⁹⁵ Originally isolated and cloned from cells of the monocytic lineage^{96,97} and traditionally considered the enzyme responsible for maturation of IL-1 β precursor,⁹⁶ Caspase-1 was identified in 1997 as the protease that mediates the activation of proIL-18.^{91,92} As the prototypical activator of these two prominent cytokines, Caspase-1 may participate in a number of inflammatory diseases and has received considerable attention as a potential target for therapeutic intervention.^{98,99}

A variety of cell types express Caspase-1 including EC, SMC, fibroblasts, epithelial and epidermal cells.¹⁰⁰⁻¹⁰³ Although caspases are widely recognized as a family of enzymes primarily involved in apoptosis, the role of Caspase-1 in programmed cell death appears rather limited, hence, is considered a member of the subfamily of inflammatory caspases.^{93,104-106}

Typically, Caspase-1 is synthesized as an inactive 45 kDa precursor that is autocatalytically processed to an active tetrameric complex consisting of the 10 kDa and 20 kDa subunits ((p20/p10)₂).¹⁰⁷ However, detection of mature immunoreactive Caspase-1

protein does not always correspond to its biological activity.^{100,108} Indeed, regulation of Caspase-1 activity remains incompletely understood. Interestingly, intracellular processing of the precursors by Caspase-1 and the secretion of IL-1 β and IL-18 seem at least in part independently regulated.¹⁰⁹ Besides passive release from dead cells, proIL-1 β and proIL-18 can be actively secreted from live cells or,^{93,109,110} highlighting the relevance of additional regulatory control through extracellular proteases.

1.7. IL-18 and atherosclerosis

Work performed during my diploma thesis implicated the macrophage-derived cytokine IL-18 as a potent inducer of IFN γ expression and other pro-inflammatory mechanisms in atherogenesis.^{111,112} Besides initially demonstrating the presence of IL-18 in human atherosclerotic lesions, I also provided evidence for the expression of both subunits of the IL-18R in this tissue as well as in atheroma-associated cell types *in vitro*. Notably, IL-18 localized only with macrophages of atherosclerotic lesions, whereas all three atheroma-associated cell types expressed IL-18R α , namely EC, SMC, and macrophages (Figure 3).¹¹² After demonstrating the expression of both receptor subunits on EC, SMC, and macrophages, additional experiments revealed several IFN γ -independent pro-atherogenic functions of IL-18 on these cells, including enhanced expression of ICAM-1, of the cytokines IL-6 and IL-8, and of MMPs.¹¹²

Although IL-18 is a sufficient stimulus synergism with IL-12 enhances induction of its classical downstream mediator IFN γ .^{73,74} Reciprocal induction of the respective receptor^{113,114} as well as modulation of different signaling pathways leading to IFN γ promotor activation and IFN γ release may cause co-stimulatory induction of IFN γ by IL-18 and IL-12.^{78,115,116}

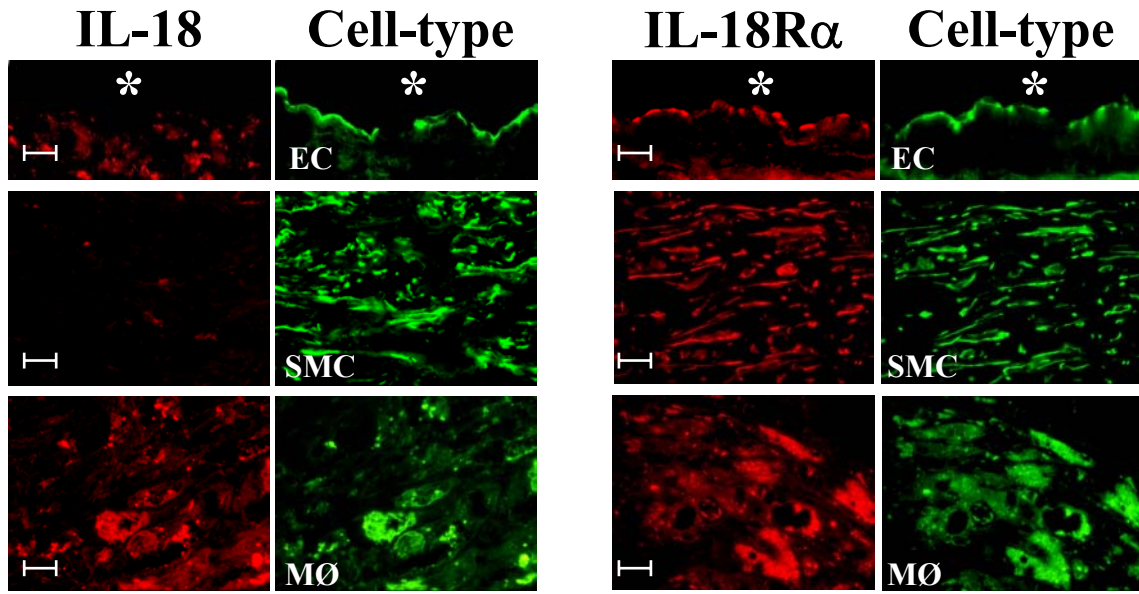


Figure 3: Differential expression of IL-18 and IL-18R α in human atherosclerotic lesions.

Double-immunofluorescence staining co-localized IL-18 (red, *left panels*) or IL-18R α (red, *right panels*) with endothelial cells (EC, anti-CD31), smooth muscle cells (SMC; anti- α -actin), or mononuclear phagocytes (MØ, anti-CD68) within human carotid atherosclerotic plaques. Analysis of three atheroma from different donors showed similar results. The asterisk indicates the lumen of the vessel. The bar corresponds to 10 μ m.

Modified from: Gerdes N. et al.: Expression of interleukin (IL)-18 and functional IL-18 receptor on human vascular endothelial cells, smooth muscle cells, and macrophages: implications for atherogenesis. *J Exp Med* 2002;195:245-57.

Apart from this prototypical function, IL-18 induces the expression of additional inflammatory mediators including the cytokines IL-1 β , IL-6, and TNF α , the chemokines IL-8, MCP-1, and MIP-1 α , as well as adhesion molecules, such as VCAM-1 and ICAM-1.^{78,81,117,118} Furthermore, IL-18 stimulation augments Fas/FasL-mediated cytotoxicity, as well as expression of perforin and granulocyte macrophage colony stimulating factor (GM-CSF), all of which contribute to cell death and local inflammation.^{79,81,119-121}

IL-18 exerts its functions by binding to the heterodimeric IL-18 receptor, comprised of the IL-1 receptor-related protein (IL-1Rrp), termed IL-18R α , and the IL-1 receptor accessory protein-like (IL-1RacPL), termed IL-18R β .¹²²⁻¹²⁴ Both receptor subunits belong to the IL-1R family. While IL-18R α represents the ligand binding chain, IL-18R β appears to assist the formation of a high affinity complex and mediates intracellular signals.^{78,124} Binding of IL-18

to the receptor complex results in recruitment of the adaptor protein MyD88, which subsequently recruits IL-1R-associated kinase (IRAK)-1 and IRAK-4 to the receptor complex.¹²⁵ After activation, IRAK-1 translocates to the TNFR-associated factor 6 (TRAF-6)-containing protein complex,¹²⁶ inducing downstream signals including nuclear factor kappa b (NF- κ B) and various mitogen activated phosphatase kinase (MAPK) pathways (e.g., c-Jun N-terminal kinase (JNK)).^{78,124,127} Indeed, IL-18 signal transduction requires this common cascade, as demonstrated by gene-targeting studies showing that MyD88, IRAK-1, and IRAK-4 play critical roles in IL-18 responses.^{125,128,129}

IL-18R α is expressed in a variety of tissues and cell types including myeloid, monocytic, and lymphocytic cell lines.^{78,130} Interestingly, the T_H1 lymphocyte subpopulation, a hallmark cell type in atherosclerotic lesions,¹⁷ but not T_H2 cells, mediators of which were considered anti-atherogenic, express the IL-18 receptor.¹³¹ Of note, inflammatory cytokines overexpressed in human atheroma, such as TNF α and IL-12,^{16,17,60} enhance the expression of both IL-18R chains on lymphocytes, thereby increasing the responsiveness to IL-18.^{78,113,130}

1.8. Clinical association of IL-18 with cardiovascular disease and its risk factors

Following our initial identification of IL-18 as a novel pro-atherogenic mediator,¹¹² several clinical studies demonstrated the correlation of elevated plasma IL-18 levels with cardiovascular risk. In a cohort of 10,600 European men followed for 5 years, IL-18 plasma concentrations in subjects who experienced MI, death, or angina were significantly higher than those in age-matched controls, independent of other inflammatory markers, such as C-reactive protein (CRP), IL-6 or fibrinogen.¹³² Moreover, IL-18 levels are elevated in patients with stable and unstable angina,¹³³ and are higher in patients with MI compared to those with unstable angina.¹³⁴ IL-18 plasma levels have also been associated with mortality in patients with coronary artery disease (CAD), independently of CRP, IL-6, and fibrinogen.¹³⁵ Furthermore, elevated plasma IL-18 concentrations reportedly accompany acute coronary syndromes,¹³⁶ a finding corroborated in an experimental model of MI in mice.¹³⁷ Finally, IL-18 correlates with parameters of myocardial dysfunction,¹³⁶ dilated and ischemic cardiomyopathy,¹³⁸ and severity of congestive heart failure.^{139,140}

The predictive value of IL-18 plasma levels extends beyond CVD to related dysfunctions such as metabolic syndrome. IL-18 plasma concentrations correlate with body mass index (BMI) and waist to hip ratio, and show an inverse correlation to weight loss.¹⁴¹⁻¹⁴³ Furthermore, IL-18 plasma concentrations correlate with hyperglycemia and associate inversely with insulin sensitivity.¹⁴³⁻¹⁴⁵ In accord, several groups have reported susceptibility and occurrence of type 2 diabetes mellitus associated with elevated plasma IL-18.^{146- 149} In sum, these clinical data demonstrate a strong correlation between elevated levels of IL-18 and several manifestations of CVD and risk factors, highlighting the potential of IL-18 as a clinical marker as well as a target for therapeutic intervention.

1.9. Aim of this thesis

Increased expression of IL-18 and its receptor in atherosclerotic tissue together with its pro-inflammatory function on atheroma-associated cells *in vitro* suggest a prominent atherogenic role for this molecule. To verify the role of IL-18 *in vivo* in atherosclerosis this thesis used an experimental model of atherosclerosis in mice. Quantification of atherosclerosis in mice lacking IL-18 in comparison to control animals will allow for assessment of IL-18's contribution to the disease.

Furthermore, it remains uncertain whether the lack of Caspase-1 limits development of atherosclerosis even more efficiently. Considering that Caspase-1 is the activating enzyme for both, IL-1 β and IL-18, Caspase-1 deficiency in hyperlipidemic mice might lead to an even greater reduction of lesion development than could be attributed to lack of either substrate alone.

In sum, this thesis will evaluate the contribution of IL-18 and IL-1 signaling as well as Caspase-1 to experimental atherosclerosis and assess their potential as targets for therapeutic intervention. Furthermore, identification of cell types that participate in IL-18 signaling may provide valuable information to guide future research on IL-18-mediated mechanisms of atherogenesis and other inflammatory diseases.

2. Materials and methods

2.1. Materials

The commercial sources for recombinant proteins and other reagents are listed in Table 1.

Table 1: Recombinant proteins

Reagent	Company	Cat.-#
recombinant human IL-18	MB International, Woburn, MA	B-003-5
recombinant human IL-12	R&D Systems, Minneapolis, MN	219-IL
recombinant human IL-1 β	Pierce-Endogen, Cambridge, MA	R-IL1B-25
recombinant human TNF α	Pierce-Endogen	R-TNF-50
recombinant human IFN γ	Pierce-Endogen	R-IFN-100
recombinant human TNF α	Pierce-Endogen	R-TNF-50
Polymyxin B	Sigma , St. Louis, MO	P4932

2.2. Expression of IFN γ in atheroma-associated cell types

2.2.1. Cell isolation and culture

All human cells were obtained according to protocols approved by the Human Investigation Review Committee at Brigham & Women's Hospital.

2.2.1.1. Endothelial Cells

Human vascular EC were isolated from saphenous veins by collagenase treatment, as originally described by Jaffe et al.¹⁵⁰ Saphenous veins were rinsed three times using syringe and cannula with Hanks' buffered salt solution (HBSS). Veins were clamped on one end with a hemostat, filled with 0.1 % (w/v) collagenase (Worthington Biochemicals, Freehold, NJ) solution in phosphate buffered saline (PBS), and were clamped on the other end. After incubation (30 min, 25°C), the EC-containing collagenase solution was flushed out by three washes with HBSS. Collagenase treatment was repeated twice. All fractions were collected and EC precipitated (5 min, 300 x g, 25°C). Subsequently, cells were resuspended in EC-

culture medium (see below) and grown (37°C , 5% CO₂) in 60 cm² cell culture dishes (Becton Dickinson, Franklin Lakes, NJ). Medium was changed for the first time after 24 h and then routinely every 3 days. Cells were later cultured in 150 cm² cell culture flasks (Corning, Corning, NY) and used through passages 3-4. For cell passage, confluent layers of EC were washed twice with HBSS and subsequently treated (37°C) with trypsin-EDTA-solution (500 µg/ml trypsin and 200 µg/ml EDTA; Cambrex, cat.-#:17-161E) until cell detachment. Trypsin was inactivated by addition of 10 % volume of fetal bovine serum (FBS; Hyclone, Logan, Utah) and cells were precipitated (5 min, 300 x g, 25°C). Finally, 5000 cells/cm² were sub-cultured in fresh medium in the desired culture vessels. For the experiments, EC were cultured in 60 cm² cell culture dishes and medium was changed 24 h before experiments to serum-free starvation medium (see below). All culture dishes and flasks for EC were coated with gelatin. For this purpose, culture surface area was covered for 1 min with 0.1 % (w/v) gelatin (Becton Dickinson, Sparks, MD) solution in PBS and, after removal of the solution, dried for 30 min at 37°C .

EC were characterized by immunohistochemical staining with mouse-anti-CD31 (Dako, Carpinteria, CA, cat.-#: M 0823). Contamination with SMC, macrophages, or T lymphocytes was excluded by employing mouse-anti-muscle actin (Enzo Diagnostics, Farmingdale, NY, cat.-#: C34931), mouse-anti-CD68 (Dako, cat.-#: M 0823), and mouse-anti-CD3 (Dako, cat.-#: T 0629) antibody, respectively, yielding no specific staining.

2.2.1.2. Smooth Muscle Cells

Human vascular SMC were isolated from saphenous veins by the explant-outgrowth method.¹⁵¹ Veins were cut longitudinally and adventitia and intima were removed with a scalpel. The remaining media was cut in 2 x 2 mm pieces, transferred in 60 cm² cell culture dishes, and incubated for 30 min (25°C) without medium. Subsequently, SMC culture medium (see below) was carefully added to cover the tissue. After the first outgrowing SMC were observed microscopically, medium was changed every 3 days and the tissue pieces were removed after a confluent SMC culture was established (approximately 3 weeks after isolation). Cells were sub-cultured, as described above for EC, with 3000 cells/cm². SMC were used through passages 3-4. For the experiments cells were cultured in 60 cm² cell culture dishes and medium was changed 24 h before stimulation to serum-free medium (see

below). SMC were characterized by immunohistochemical staining and contamination with EC, macrophages, or T-lymphocytes was excluded as described above for EC, yielding no specific staining.

2.2.1.3. Monocytes and macrophages

Monocytes were isolated by density gradient centrifugation from freshly prepared leukocyte concentrates (Leukopac) from healthy donors obtained from the Brigham & Women's Hospital/Dana Faber Cancer Institute blood donor center. One volume (10 ml) of Lymphocyte separation medium (ICN Biomedicals, Aurora, OH) was gently overlaid with 4 volumes of leukocyte concentrate. Following 45 min centrifugation (450 x g, 25°C, without brake), the upper phase was aspirated and the leukocyte containing interphase was transferred into fresh tubes, while avoiding interference with the granulocyte- and erythrocyte-containing bottom phase.

Leukocytes were washed three times with HBSS. Cells were precipitated by centrifugation for 10 min (300 x g, 25°C) between each washing step. After the final washing step, the number of viable cells was determined by staining with trypan blue (0.4 % (w/v); Sigma), and subsequent counting in a hematocytometer (Neubauer chamber; Reichert, Buffalo, NY). Trypan blue penetrates membranes of non-viable cells and thus yields blue intracellular staining, whereas viable cells do not stain.

For purification purposes, 1×10^6 cells/cm² in monocyte medium were (see below) plated in 60 cm² cell culture dishes. After one hour of incubation (37°C, 5% CO₂), plates were vigorously washed three times with HBSS to remove non-adherent cells. Macrophages were cultured (37°C, 5% CO₂) in macrophage culture medium supplemented with 2 % (v/v) human serum (see below) for 10 days. Medium was changed every 3 days, and differentiated macrophages (day 10) were cultured 24 h before stimulation in serum-free medium. The purity of macrophages was $\geq 96\%$, as determined routinely by FACS analysis (PE-conjugated mouse-anti-human CD68; 20 µl/0.5 x 10⁶ cells; PharMingen; San Diego, CA).

2.2.1.4. *Limulus amoebocyte assay*

All culture media, FBS, and human serum contained less than 40 pg endotoxin/ml, as determined by the chromogenic *Limulus amoebocyte assay* following the instructions of the

manufacturer (QCL-1000[®] Chromogenic LAL Kit; Cambrex, cat.-# 50-647U). Endotoxin derived from gram-negative bacteria catalyses the activation of a pro-enzyme in the *Limulus Amoebocyte Lysate*. In the second reaction step, the activated enzyme catalyses the cleavage of p-nitroaniline (pNA) from a colorless substrate. The pNA released can be measured photometrically at 405 nm after the reaction is stopped with stop reagent (25% (v/v) glacial acetic acid). The concentration of endotoxin in a sample was calculated from the absorbance values of a serial dilution of a known concentration of endotoxin standard.

2.2.1.5. Cell culture media

Culture medium for EC

Medium M199 (Cambrex)

Supplemented with:

5 % (v/v)	Fetal Bovine Serum (FBS; Hyclone)
250 µg/ml	Endothelial Cell Growth Factor (ECGF; kindly provided by Dr. M Muszynski, Brigham & Women's Hospital)
100 U / 100 µg/ml	Penicillin/streptomycin (Cambrex)
1.25 µg/ml	Amphotericin (Fungizone; Apothecon, Princeton, NJ)
100 µg/ml	Heparin (Sigma)

Starvation medium for EC

Same as Culture medium for EC but without FBS and ECGF

Culture medium for SMC

Dulbecco's Modified Eagle Medium (DMEM; Cambrex)

Supplemented with:

10 % (v/v)	FBS
100 U / 100 µg/ml	Penicillin/streptomycin
1.25 µg/ml	Amphotericin
200 µM	L-glutamine (Cambrex)

Starvation medium for SMC

Same as Culture medium for SMC but without FBS

Culture medium for macrophages

Rockwell Park Memorial Institute medium 1640 (RPMI 1640; Cambrex)

Supplemented with:

100 U / 100 µg/ml	Penicillin/streptomycin
1.25 µg/ml	Amphotericin
2 % (v/v)	Human serum (ICN Biomedicals, heat-inactivated (30 min/56°C) before use)

Culture medium for monocytes (also used for starvation of differentiated macrophages)

Same as Culture medium for macrophages but without human serum

2.2.2. Enzyme-Linked Immunosorbent Assay (ELISA)

Release of IFN γ from EC, SMC, monocytes/macrophages, and KG-1 cells was measured by ELISA. Cell supernatants (50 µl) were added for 2 h to 96-well Maxisorb plates (Nunc, Rochester, NY) pre-coated with a monoclonal IFN γ capturing antibody (Pierce-Endogen; 1.5 µg/ml in PBS, 4°C, overnight). The plates were subsequently washed three times with PBS 0.1% (v/v) Tween-20 in an automatic plate washer, and the respective biotin-labeled anti-human IFN γ antibody (Pierce-Endogen; 0.5 µg/ml diluted in 2% (w/v) bovine serum albumin (BSA) in PBS) was added for 1 h (25°C, shaking). Following incubation for 30 min at room temperature with Horse-radish peroxidase (HRP)-conjugated Streptavidin (Pierce-Endogen; 0.125 µg/ml in PBS/2%BSA) and three washing steps, antibody binding was detected by the addition of tetramethylbenzidine (TMB) solution (Pierce-Endogen) and measuring absorbance at 650 nm in a plate reader (Molecular Devices, Spectra Max plus 384). The concentration of IFN γ was calculated from a standard curve prepared from recombinant IFN γ (Pierce-Endogen). Samples were assayed in duplicates.

2.2.3. In situ hybridization (ISH)

In situ hybridization was performed according to the instructions of the manufacturer (Innogenex, San Ramos, CA). Briefly, frozen tissue sections as well as cultures of SMC and macrophages on 4-chamber slides were fixed in cold acetone, air-dried, and incubated (10 min, 65°C; subsequently 2 h, 37°C) with a mixture of FITC-labeled IFN γ (5'-CATCGTTCCGAGAGAATTAAGCCAAAGAAGTTGAAATCA-3'; 5'-AAGAGAA CCCAAAACGATGCAGAGCTGAAAAGCCAAGATA-3'; 5'-TTTTCTGTCACTCTCCT CTTCCAATTCTTCAAAATGCCT-3') antisense oligomers, or the respective sense (control) oligomers (all 4 μ g/ml, final concentration) in hybridization-buffer. Finally, slides were washed 3 times, incubated with biotinylated mouse-anti-FITC antibody (1 h), followed by alkaline phosphatase-conjugated streptavidin (30 min) and NBT/BCIP chromogen solution (1 h). Adjacent sections were analyzed for SMC, macrophage, and T-cell content by immunohistochemistry as described below.

2.2.4. Immunohistochemistry (IHC)

Serial cryostat sections (6 μ m) of surgical specimens of human carotid atheroma (n=3), normal carotids from autopsies, and non-diseased aorta from cardiac transplantation donors (n=3) were cut, air dried onto microscope slides, fixed in acetone (-20°C, 5 min), and pre-incubated with PBS containing 0.3% hydrogen peroxide. Subsequently, sections were incubated (30 min) with primary mouse-anti-human muscle actin mAb for SMC (1:200; Enzo Diagnostics), mouse-anti-human CD31 mAb for EC (1: 35; Dako, Carpinteria, CA), mouse-anti human CD68 for macrophages (1:500; Dako), mouse-anti-human CD3 mAb for T cells (1:500; Dako), or control antibody (mouse myeloma protein MOPC-21; 0.25 μ g/ml; Sigma), diluted in PBS supplemented with 5% appropriate serum, and processed according to the recommendations provided by the supplier (Universal Dako LSAB Kit, Dako).

2.2.5. Reverse Transcription-Polymerase Chain Reaction (RT-PCR)

2.2.5.1. RNA isolation

SMC were washed twice with PBS and total RNA was isolated from SMC cultures under RNase-free conditions employing RNazolTM B reagent (Tel-Test, Friendswood, TX) according to the instructions from the manufacturer. Nucleic acids were subsequently visualized by UV-transillumination and bands for the 18S and 28S ribosomal RNA examined for possible indications of degradation. Concentration was determined by employing a spectrophotometer. RNA degradation observed on the gels or an OD₂₆₀/OD₂₈₀ value of less than 1.7 led to disqualification of these samples. The total RNA yield ranged between 10 and 30 µg/60 cm² cell culture dish. Samples were stored at - 80°C until use.

2.2.5.2. Reverse Transcription and PCR

All reagents used for this reaction were obtained from Invitrogen (Carlsbad, CA), if not stated otherwise. Total RNA (2 µg) was equilibrated at 11 µl and 1 µl of Oligo (dT)₁₂₋₁₈ (500 ng/µl; cat.-#: N42001) was added. Mixture was incubated for 10 min at 70°C and quickly chilled on ice. Subsequently, 4 µl of 5 X First Strand Buffer, 2 µl of 100 mM DTT, 1 µl of 10 mM (each) dNTP mix were added, and mix was incubated for 2 min at 42°C, followed by addition of 1 µl of reverse transcriptase (Superscript II; 200 U/µl) and total incubation for 1 h at 42°C. Reaction was stopped by heat inactivation of the enzyme at 70°C for 15 min. RT reaction products (2 µl) were added to a 50 µl total PCR reaction. 5 µl PCR-buffer (10 X), 1 µl dNTP mix (10 mM), 1.5 µl MgCl₂ (50 nM), 1 µl Platinum *Taq* DNA polymerase (5 U/µl), 1 µl sense primer (20 µM), 1 µl antisense primer (20 µM), and 38 µl H₂O were added to 2 µl cDNA. Primer pairs for either IFNγ or glyceraldehyde-3-phosphate dehydrogenase (GAPDH) were obtained from Integrated DNA Technologies (Coralville, IA). The sequence and expected fragment sizes of these primers are shown in Table 2.

Table 2: Primer and conditions for RT- PCR

Primer		Sequence (5'-3')	Fragment	(X)	(Y)
IFN γ	sense	TTTAGCTCTGCATGTGGTAGC	375 bp	60°C	35
	antisense	CATGTATTGCTTGCGTTGG			
GAPDH	sense	GTCAGTGGTGGACCTGACCT	247 bp	60°C	25
	antisense	TGCTGTAGCCAAATCGTTG			

X = Annealing temperature; Y = cycle number

PCR reaction mix was applied to the general protocol of Y cycles at 94°C (60 s), X°C (60 s), and 72°C (90 s), where Y refers to the number of PCR-cycles and X to the annealing temperature for each individual primer pair (listed in Table 2). PCR reaction was performed in a PTC-200 DNA Engine™ Thermal Cycler (MJ Research, Waltham, MA).

Aliquots (10 µl) of the PCR products were mixed with 2.5 µl DNA loading buffer (5 X) (Sigma, St. Louis), applied to ethidium bromide-containing 1.5% agarose gel in TAE-buffer, and subsequently visualized by UV-transillumination. Fragment size was verified by comparison to a 100 bp standard (Invitrogen).

2.2.6. Flow Cytometry (FACS)

To determine activity of the IFN γ released by SMC, supernatants of SMC cultures (1:2 diluted in M199) were applied (48 h) in absence or presence of neutralizing mouse-anti-human IFN γ antibody (5 µg/ml; R&D Systems) to confluent cultures of human vascular EC. Cells were washed with ice-cold PBS, harvested by trypsinization, fixed (PBS/4% paraformaldehyde, 15 min), and subsequently washed once with PBS/0.2% BSA before being incubated (1 h, 4°C) with PE-conjugated control IgG, mouse-anti-human MHC I, or mouse-anti-human MHC II antibody (Coulter, Miami, FL; 1h, 4°C). Subsequently, cells were washed with PBS/0.2% BSA and analyzed in a Becton Dickinson FACScan® flow cytometer employing CellQuest® software (Becton Dickinson; San Jose, CA). At least 20,000 viable cells per condition were analyzed.

2.3. Murine atherosclerosis model

The initial mouse study, which tested the relevance of IL-18 for atherosclerosis also served the goal to establish the experimental model of atherosclerosis for the subsequent studies. In particular, choosing the appropriate duration of high cholesterol diet (HCD) and the vascular location for analysis proved invaluable for the succeeding *in vivo* studies. The three most common vascular locations for the analysis are the aortic sinus, the aortic arch, and the thoracic/abdominal aorta (Figure 4). Whereas the earliest signs of atherosclerosis are commonly observed in the aortic sinus, lesion development in the aortic arch requires hypercholesterolemia for at least 6 weeks.^{152,153}

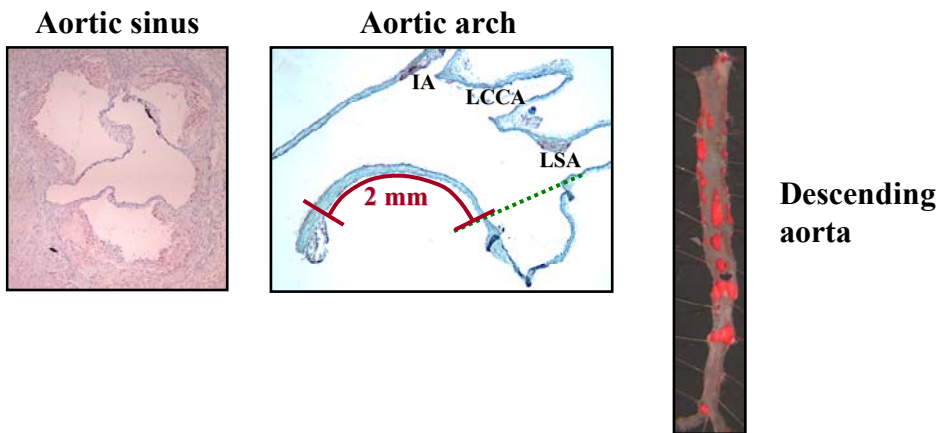


Figure 4: Common vascular locations employed for analysis of atherosclerosis.

Analysis of atherosclerosis frequently employs quantification of lesion development in the aortic sinus (left), the aortic arch (middle), or the descending aorta (right). While histological analysis can analyze several sections of the vessel in aortic sinus and aortic arch, en face analysis of Oil Red O-stained aorta is limited to two-dimensional analysis. Within the aortic arch, a 2 mm segment of the inner curvature was defined for analysis proximal of the perpendicular drawn from the distal side of the left subclavian artery origin. IA = Innominate artery; LCCA = Left common carotid artery; LSA = Left subclavian artery.

Analysis of atherosclerosis in the abdominal and thoracic aorta, however, requires prolonged hypercholesterolemia. Furthermore, the Oil Red O-stained *en face*-preparation of the aortae allow only very limited conclusion regarding the atherogenic properties of a certain gene or protein, since this method only determines the lipid deposition in a two-dimensional fashion,

in contrast to the histological studies, which facilitate analysis of multiple markers and parameters of atherosclerosis, including gross morphology, content of macromolecules, and expression of proteins on sections of multiple layers.^{152,153}

Of note, the prolonged duration of lesion initiation observed in the experiments employing chow diet compared to HCD (see *Results*) is in accord with previous studies.^{72,154-156} In addition, previous studies demonstrated that different conclusion could be drawn regarding the atherogenic role of certain mediators, depending on vascular location chosen for analysis.¹⁵⁷ Thus, it was of particular importance to thoroughly establish and optimize the methodology for analyzing atherosclerosis in mice and determine a common endpoint for the initial (IL-18-deficiency) and the following *in vivo* studies. In view of the profound changes of lesion development following 8 weeks of HCD (see *Results*), this treatment protocol was adopted for the subsequent studies, however, the prolonged hypercholesterolemia (18 weeks) was included as a second endpoint, to account for potentially differentially affected atherosclerosis in IL-18, IL-18R α , IL-1R1, or Caspase-1-deficient mice.

2.3.1. Animal housing and welfare

Mice were housed in specific pathogen-free animal facilities according to guidelines from the *Office of Laboratory Animal Welfare at the National Institutes of Health*. In addition, all experimental procedures were approved by the *Institutional Animal Care and Use Committee (IACUC)* at Harvard Medical School. Animals were under constant observance of veterinarians from *The Center for Animal Resources and Comparative Medicine (ARCM)* at Harvard Medical School. When necessary, veterinary services were provided. Mice were kept under 12 h dark / 12 h light cycles with no more than 4 mice per standard cage (0.03 m^2) and were administered fresh water and pellet food *ad libitum*. If not indicated otherwise mice consumed a regular chow diet (Labdiet Inc., St. Louis, MO, cat. #5001, 0.02 % cholesterol, 4.5 % total fat, 0 % cholate).

2.3.2. Generation of compound gene-deficient mice

There are two common experimental models of atherosclerosis in mice. In 1992 two independent groups generated mice deficient for ApoE.^{158,159} ApoE is the ligand on remnant lipoproteins required for their hepatic clearance and its lack leads to severe hypercholesterolemia with accumulation of chylomicrons and very low density lipoprotein (VLDL) particles even when mice are fed a normal diet. This leads to development of atherosclerotic lesion as early as at 10 weeks of age, and this process is further accelerated when these mice consume HCD. In contrast, wild type mice on the C57Bl/6 background do not develop appreciable plaques even when administered HCD.

The second most common model of atherosclerosis was developed in 1993 by targeting the gene for the LDL receptor (LDLR), leading to accumulation of cholesterol mostly in the form of LDL.¹⁶⁰ There are several advantages and disadvantages of each of these models, which are discussed vividly among vascular biologists.¹⁵² However, the fact that the genes for LDLR and IL-18 are both located on chromosome 9 in the mouse,^{75,160} accordingly led to the decision to choose the ApoE model for the generation of hyperlipidemic compound mutant mice. Since the ApoE gene is located on chromosome 7,^{158,159} the genes should be non-linked, resulting in double-deficient offspring in the F2-generation according to the expected Mendelian ratios. To facilitate comparison between results of this initial *in vivo* study using *il18^{-/-}apoe^{-/-}* mice and all following studies, other double-deficient mice were also generated in the ApoE-deficient model.

ApoE-deficient (B6.129P2-*Apoe^{tm1Unc}*/J; *apoe^{-/-}*)¹⁵⁸, IL-1 receptor type I (IL-1RI)-deficient mice (B6.129S7-*Il1rl^{tm1Imx}*/J; *il1rl^{-/-}*)¹⁶¹, IL-18R α -deficient mice (B6.129P2-*Il18rl^{tm1Aki}*/J; *il18rl^{-/-}*)¹⁶², and mice carrying the common CD45.1 (B6.SJL-*Ptprc^a* *Pep3^b*/BoyJ; *cd45^{1/1}*)¹⁶³ were obtained from The Jackson Laboratory (Bar Harbor, ME). IL-18-deficient mice (B6.129P2-*Il18^{tm1Aki}*/J; *il18^{-/-}*)¹⁶⁴ were acquired from Dr. S. Akira (Osaka University, Suita, Japan). Caspase-1-deficient (*casp1^{-/-}*) mice¹⁶⁵ were kindly provided by Dr. W. Wong (Abbott, Worcester, MA). All mouse strains have been previously backcrossed to the C57BL/6 background for at least 8 generations.

Compound-deficient mice were generated by crossbreeding the respective single gene-deficient mice and interbreeding the resulting heterozygous F1 generation. Genotypic identification of the resulting F2-offspring was performed employing PCR.

2.3.3. Genotypic identification

Genomic DNA was obtained from tail tip biopsies employing the DNeasy tissue kit (Qiagen, Hilden, Germany) following the instructions of the manufacturer. Genotyping for ApoE, IL-1R1, IL-18, and IL-18R α was performed employing Hotmastermix (2.5X) (Eppendorf, Hamburg, Germany) according to Table 3 and 4. Genotyping for Caspase-1 was performed employing Platinum Taq DNA Polymerase kit (Invitrogen, Carlsbad, CA) according to Table 5.

Table 3: PCR reactions for genotyping of *apoe*, *il1r1*, *il18*, and *il18r1*

Gene	<i>apoe</i>	<i>il18</i>	<i>il18r1</i>	<i>il1r1</i>	
Allele	+/+ and -/-	+/+ and -/-	+/+	+/+	-/-
Hotmastermix (2.5X)	10	10	10	10	10
Primer A (20 μ M)	0.5	0.5	0.5	0.5	-
Primer B (20 μ M)	0.5	0.5	0.5	0.5	0.5
Primer C (20 μ M)	0.5	0.5	-	-	0.5
H ₂ O	12.5	12.5	13	13	13
Template DNA	1	1	1	1	1
Total	25	25	25	25	25
All volumes in μ l					

Table 4: PCR reactions for genotyping of *casp1*

Gene	<i>casp1</i>	
Allele	+/+	-/-
PCR beads	-	-
PCR buffer (10X)	2.5	2.5
MgCl ₂ (50 mM)	0.75	0.75
dNTP-mix (10 mM)	0.5	0.5
Platinum Taq (5 U/ μ l)	0.25	0.25
Primer A (20 μ M)	0.5	-
Primer B (20 μ M)	0.5	0.5
Primer C (20 μ M)	-	0.5
H ₂ O	19	19
Template DNA	1	1
Total	25	25
All volumes in μ l		

Table 5: PCR reactions for genotyping of *apoe*, *il1r1*, *il18*, *il18r1*, and *casp1*

Gene	<i>apoe</i>	<i>il18</i>	<i>il18r1</i>	<i>il1r1</i>	<i>casp1</i>
Allele	+/+ and -/-	+/+ and -/-	+/+	+/+ and -/-	+/+ and -/-
1. Initial denaturation: 94°C	120s	120s	180s	120s	120s
2. Denat.: 94°C	30s	30s	30s	30s	45s
3. Annealing: X°C	67°C, 60s	67°C, 60s	58°C, 60s	68°C, 90s	60°C, 60s
4. Elongation: 72°C	120s	120s	60s	120s	120s
Go to step 2	34x	34x	29x	39x	39x
5.Final Elong.: 72°C	10 Min.	10 Min.	2 Min.	10 Min.	10 Min.
6. Cool down: 10°C	Indefinite	Indefinite	Indefinite	Indefinite	Indefinite

Table 6: Primers used for genotyping of *apoe*, *il1r1*, *il18*, *il18r1*, and *casp1*

Allele	Primer	Sequence (5'-3')	Resulting fragments
<i>apoe</i>	A	GCC TAG CCG AGG GAG AGC CG	A+B result in 155bp band
	B	TGT GAC TTG GGA GCT CTG CAG C	for +/++; B+C result in 245bp
	C	GCC GCC CCG ACT GCA TCT	band for -/-
<i>il18</i>	A	TAA TGG GTG GTC TTC TCA TCT CTG TGT	A+B result in 682bp band
	B	GGA AAA GAA CTG GTC TAG TGT GGT GGC	for +/++; B+C result in
	C	ATC GCC TAC TAT CGC CTT CTT GAC GAG	~900bp band for -/-
<i>il18r1</i>	A	TAC CTG ATA TCC CAG GCC ATG T	A+B result in ~150bp band
	B	GTG TCT CGT CTC TTT CCG CTA T	for +/+
<i>il1r1</i>	A	GAG TTA CCC GAG GTC CAG TGG	A+B result in ~1,150bp
	B	CCG AAG AAG CTC ACG TTG TCA AG	band for +/++; B+C result in
	C	GAA TGG GCT GAC CGC TTC CTC G	860bp band for -/-
<i>casp1</i>	A	ATC CAG GAG GGA ATA TGT GG	A+B result in 700bp band
	B	CCT GGT GTT GAA GAG CAG AA	for +/++; B+C result in
	C	TGC TCC TGC CGA GAA AGT AT	~1,400bp band for -/-

The respective primers obtained from Integrated DNA Technologies are indicated in Table 6. PCR reaction was performed in a PTC-200 DNA Engine™ Thermal Cycler. Aliquots (10 µl) of the PCR products were mixed with 2.5 µl DNA loading buffer (5 X) (Sigma, St. Louis), applied to ethidium bromide-containing 1.5% agarose gel in TAE-buffer, and subsequently visualized by UV-transillumination. Fragment size was verified by comparison to a 100 bp standard (Invitrogen) and genotype determined based upon the presence of the respective wild type (+/+) or mutated allele (-/-).

2.3.4. Bone marrow reconstitution

Recipient mice (either *il18r1^{-/-}apoe^{-/-}* or *il18r1^{+/+}apoe^{-/-}*) were lethally irradiated (2 x 7 Gy, >3 hours apart) at the age of 6-8 weeks and randomly assigned to receive bone marrow derived from *il18r1^{-/-}apoe^{-/-}* or *il18r1^{+/+}apoe^{-/-}* donor mice 6-8 weeks of age.

For isolation of bone marrow, femurs, tibias, and humeri were removed from donor mice, placed in RPMI with 5% FBS on ice, and subsequently cleaned using scissors and gently wiping off muscle tissue with a paper tissue. Bones were washed twice with RPMI 1640 containing 5% FBS. Under sterile conditions both condyles of the bone were cut off and bone marrow was flushed out with RPMI 1640/5% FBS using a 27G needle attached to a syringe. Pooled bone marrow (2-6 mice) was homogenized using a 19G needle, centrifuged (5 min, 800 x g, 4°C) and resuspended in 3-5 ml of 0.155 M NH₄Cl for 3 min, 4°C to lyse erythrocytes. 30 ml of HBSS was added, mixed by inverting, and centrifuged (5 min, 800 x g, 4°C). The Pellet was resuspend in 20 ml HBSS and filtered through a cell strainer (>70 µm

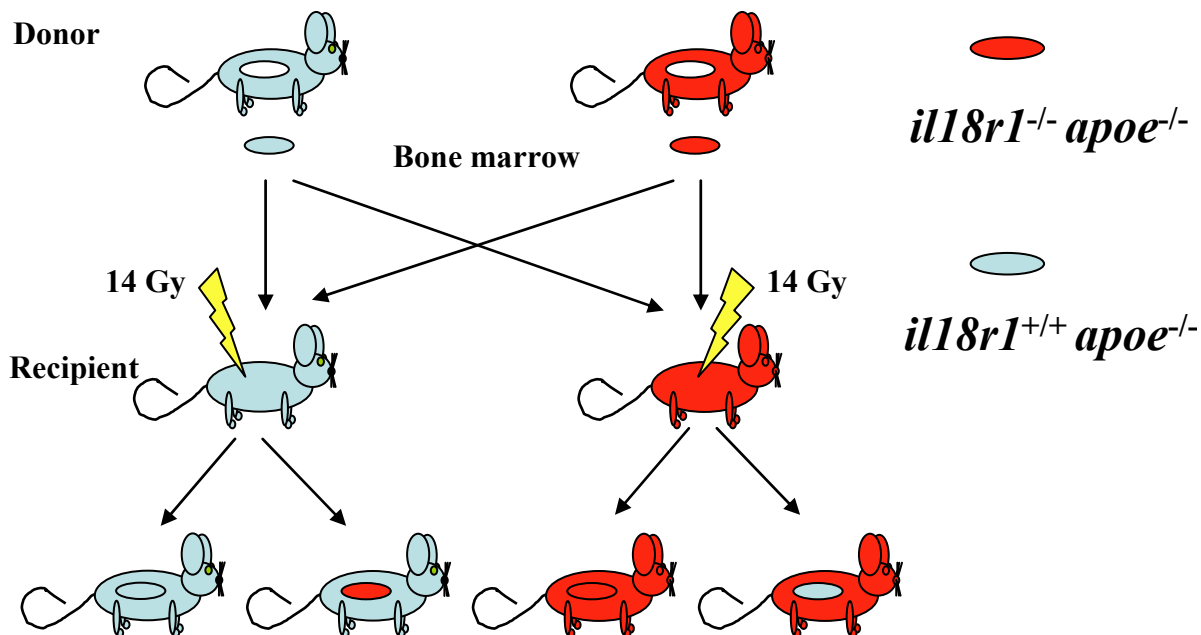


Figure 5: Schematic of the generation of IL-18R α chimeric mice using bone marrow transplantation.

Bone marrow of donor *il18r1^{-/-}apoe^{-/-}* or *il18r1^{+/+}apoe^{-/-}* mice was injected i.v. in previously lethally irradiated recipient *il18r1^{-/-}apoe^{-/-}* or *il18r1^{+/+}apoe^{-/-}* mice generating chimeric mice either globally deficient or competent for IL-18R α or lacking IL-18R α selectively on cells of the hematopoietic or non-hematopoietic origin.

exclusion, Becton Dickenson). Cells were centrifuged (5 min, 800 x g, 4°C), counted and resuspended to a concentration of 1×10^8 cells/ml. 5×10^7 cells (200 µl), adjusted to room temperature, were injected (30G needle) into the tail vein following the second dose of radiation (Figure 5).

Following bone marrow transplantation (BMT) mice were housed in microisolator cages and provide acidified water (pH 2.5; adjusted with hydrochloric acid) and allowed to recover for 6 weeks, before start of HCD.

In additional experiments bone marrow transplantation employed mice carrying the CD45.1 isoform of the common leukocyte antigen (CD45) as both donors and recipients. Mice of the C57/Bl6 background commonly carry the CD45.2 allele, making leukocytes of *cd45^{1/1}apoe^{-/-}* easily distinguishable from *cd45^{2/2}apoe^{-/-}* and *cd45^{2/2}il18rl^{-/-}apoe^{-/-}* by FACS analysis of peripheral blood thus allowing an estimate of reconstitution success (see also *Results*).

2.3.5. Experimental procedure for induction of atherogenesis

At the age of 6-8 weeks, littermate male or female mice of the respective gene-deficient and control strain were either assigned to a high-cholesterol diet (HCD; Research Diets, New Brunswick, NJ, cat.-#D12108, 1.25 % cholesterol, 20 % total fat, 0 % cholate) or were continued on the chow diet for either 8 or 18 weeks. Bone marrow transplanted mice were 12-14 weeks of age at the start of the study since they had a 6 week recovery period following BMT. Blood samples were obtained and body weight was recorded prior to diet assignment and immediately before study end. Mice were kept in groups of 2-4 animals and consumed diet and water *ad libitum*.

2.3.6. Analysis of atherosclerosis

2.3.6.1. Mouse harvesting

Following 8 or 18 weeks of diet, mice were anesthetized by i.p.-injection of 2,2,2-tribromoethanol (Sigma; 250 mg/kg) and the vascular tree was perfused with PBS under physiologic pressure. Subsequently, the heart and aorta were removed, the arch and abdominal portions of the aorta were separated, and the heart and aortic arch were embedded and snap-frozen in OCT compound (Tissue-Tek, Torrance, CA), as described previously.¹⁶⁶ The descending (thoracic and abdominal) aortae were fixed in 10% buffered formalin, as described previously.

2.3.6.2. En face analysis of descending aorta

Aortae, fixed and stored in 10 % buffered formalin solution were washed overnight in PBS. Subsequently, aortae were dehydrated in propylene glycol for 2 min, stained with 0.5 % Oil Red O in propylene glycol for 2-4 h at room temperature, differentiated by 3 washing steps in 85 % propylene glycol and finally washed overnight in PBS. Aortae were opened longitudinally to the aortic bifurcation, pinned on black silicon-elastomere dishes using 0.2-mm stainless steel pins while covered with PBS. Dishes were drained, dehydrated with propylene glycol for 2 min, and aortae were stained again with 0.5 % Oil Red O in propylene glycol for 2-4h at room temperature. Finally, dishes were washed three times with 85 % propylene glycol and three times with PBS, and digital image was captured with a CCD camera.

2.3.6.3. Histological analysis of aortic sinus and aortic arch

Serial longitudinal cryostat-sections (6 µm) of the aortic arches were used for immunohistochemical-, Oil Red O-, and Picosirius Red-staining. Within the aortic arch, a 2 mm segment of the inner curvature was defined proximal of the perpendicular drawn from the distal side of the left subclavian artery origin (Figure 4) Serial cryostat-sections (6 µm) of the aortic sinus (cross-sections) at the level of all three leaflets of the aortic valve, immediately proximal to the right coronary artery ostium (Figure 4) were applied to similar staining as outlined for those of aortic arches above and detailed in the following.

2.3.6.4. Picosirius Red-staining for collagen

Formalin-fixed frozen sections were incubated for 4 hours in a freshly prepared 0.1% solution of Sirius Red F3BA (Polysciences Inc., Warrington, PA) in saturated aqueous picric acid. After rinsing twice in 0.01 N hydrochloric acid and distilled water, sections were briefly dehydrated in 70% ethanol and mounted in Permount (Vector Laboratories). Sirius red staining was analyzed by polarization microscopy.

2.3.6.5. Oil Red O staining for lipids

Frozen sections were fixed in 10 % buffered formalin solution (10 min.), rinsed with H₂O, and dehydrated in propylene glycol for 2 min. Subsequently, slides were incubated in 0.5 % Oil Red O solution in propylene glycol (25 min, 60°C), rinsed with H₂O, counterstained with hematoxylin (see below) and coverslipped with glycerol gelatin (Sigma).

2.3.6.6. Immunohistochemical staining

For immunohistochemical analysis, sections of the aortic arch or sinus were fixed in acetone (-20°C, 10 min), air dried, and incubated with 0.3 % H₂O₂ for 15 min to inhibit endogenous peroxidase activity. Subsequently, sections were blocked with 4 % normal rabbit serum in PBS (30 min, RT) and incubated (90 min, RT) with the following primary antibodies diluted in blocking solution: rat-anti-mouse Mac-3 (for macrophages; BD Pharmingen, San Diego, CA, cat. #553322, 5 µg/ml); rat-anti-mouse MHC II (BD Pharmingen, cat. #556999, 2.5 µg/ml); rat-anti-mouse IFNγ (BD Pharmingen, cat. #551216, 5 µg/ml); rat-anti-mouse VCAM-1 (BD Pharmingen, cat. #553330, 0.2 µg/ml). Slides were washed, incubated (45 min, RT) with biotinylated rabbit-anti-rat IgG antibody (Vector, Burlingame, CA, cat. #BA4001, 2.5 µg/ml), and applied to the Vectastain ABC kit (avidin-biotin complex) according to the instructions of the manufacturer (Vector, cat. #PK-6100).

The reaction was visualized employing 3-amino-9-ethyl carbazole as substrate (AEC substrate chromogen; DAKO, cat. #K3464), and the sections were counterstained with Gill's hematoxylin solution (Sigma, cat. #GHS-3-32), differentiated with 0.25 % ammonia in water and coverslipped with glycerol gelatin. To verify specificity of the antibodies, staining with the respective isotype-matched IgG (BD Pharmingen/ DAKO) was performed.

Staining of α -actin for SMC employed a slightly modified protocol. Sections were fixed 10 min in chilled acetone at -20°C, air-dried, and incubated in 0.2% H₂O₂ in 100% methanol for 15 min at room temperature. Following 3 x washing for 5 min in PBS sections were incubated in 5% horse serum diluted in PBS for 20 min. Subsequently, slides were incubated with primary antibody (α -smooth muscle-FITC conjugate; Sigma cat-# F-3777) diluted 1:1000 in 1% BSA/0.1 %Tween20 in PBS for 1 h followed by 3 washes in PBS and anti-FITC-biotin conjugated antibody (Sigma, cat # B0287) for 45 min. After that step, the staining continued as described above with the Vectastain ABC kit and subsequent steps.

2.3.6.7. Computer-assisted image analysis and statistical analysis

Total vessel wall area, total intima area, and relative positive stained (Oil Red O, Sirius Red, Immunohistochemistry) areas of sections of the aortic sinus and arch as well as Oil Red O positive area on the thoracic/abdominal aortae employed ImagePro Plus software (Media Cybernetics, Silver Springs, MD). Image analysis was performed independently by two blinded investigators.

Data are presented as mean \pm standard error of the mean (SEM) and were compared between study groups using the non-parametric Mann-Whitney U-test. A *p*-value of <0.05 was considered statistically significant. Statistical analysis utilized the Statistical Package for Social Sciences (SPSS; SPSS Inc., Chicago, IL).

2.3.7. Plasma cholesterol and triglyceride analysis

Blood samples of mice starved for at least 8 hours were obtained prior to diet assignment under methoxyfluorane-anesthesia (Medical Developments Australia Ltd., Springvale, Australia) by puncture of the retro-orbital venous plexus using heparinized glass capillaries (Fisher Scientific). Blood was allowed to clot for at least 30 min, centrifuged at 1,500 x g for 15 min. Subsequently, plasma was removed and stored at -80°C until further analysis. Plasma total cholesterol and triglyceride concentrations were determined employing enzymatic assays (cat.-#401 and cat.-#343, respectively; Sigma) according to the recommendations of the manufacturer, however, adopted for use in 96-well plates.

2.3.8. Leukocyte count

Freshly drawn blood was diluted 1:1,000 in 10 ml of PBS. Three drops of Zap-Oglobin II lytic reagent (Beckman Coulter, Fullerton, CA) were added and cell suspension was mixed for 10 seconds. Total leukocyte count was estimated using a Z2 particle count & size analyzer (Beckman Coulter) limiting particle size from 4-11 μm .

2.3.9. Flow cytometry (FACS)

50 μl of mouse blood was diluted 1:1 in FACS Buffer (2 % BSA, 0.1 % sodium azide in PBS) and incubated with 2 μl of Fc-block (ebioscience, San Diego, CA) for 30 min., at room temperature. Subsequently, the fluorescent labeled antibodies were added for another 30 min. at room temperature. Finally, 1ml of FACS lysis buffer (Becton Dickinson) was added for 10 min., cells were washed twice with FACS buffer and analyzed in a Becton Dickinson FACScalibur[®] flow cytometer employing CellQuest[®] software (Becton Dickinson). At least 20,000 viable cells per condition were analyzed. Antibodies for CD45.1-PE, CD45.2-PE, CD45.2-FITC, CD11b-FITC, CD19-PECy5, CD3-APC as well as the isotype-matched, fluorescent-labeled control antibodies were purchased from ebioscience.

2.4. Western blot analysis of mouse tissue lysates

2.4.1. Preparation of tissue lysates

Under anesthesia with 2,2,2 tribromoethanol and following perfusion with PBS the aortae of mice were removed and immediately frozen in liquid nitrogen and stored at -80°C until further use. To extract proteins 0.5 ml of pre-chilled tissue lysis buffer (40 mM Tris base, 120 mM sodium chloride, 0.5 % (v/v) Nonident P40, 1 mM sodium vanadate, 5 mM EDTA, 1 mM PMSF (added < 10 min before use), and Complete[®] protease inhibitor cocktail (Roche, Indianapolis, IL; cat# 1873580)) was added per one aorta and tissue was homogenized using a Polytron homogenizer (Kinematica, Littau, Switzerland; model-# PT 10/35 with PTA7 aggregate) for 30-60 sec at medium speed and 4°C. Subsequently, homogenates were centrifuged for 10 min, (13,000 x g, 4°C) to pre-clear the lysates.

Supernatants were transferred into fresh tubes and protein concentration was determined using the BCATM protein assay kit (Pierce, Rockford, IL, cat.-# FF70699) according to the instructions of the manufacturer. The absorbance was measured at 562 nm in a 96-well plate spectrophotometer and compared to a standard of bovine serum albumin.

2.4.2. SDS-PAGE and Western Blot analysis of tissue protein extracts

Protein extracts from atherosclerotic tissue (50 µg total protein/lane) were mixed with reducing SDS-PAGE sample buffer (5 X; 100 mM Tris base, 30 % (v/v) glycerol, 2 % (w/v) SDS, 10 % (v/v) β-mercaptoethanol, 0.02 % (w/v), bromophenol blue), boiled 5 min at 95°C, spun down briefly, and loaded on 15 % SDS-PAGE gel. As a reference Precision Plus Protein Dual Color Standard[®] (Bio-Rad, Hercules CA; cat.-#: 161-0374) was used to allow for later identification of approximate molecular weight. Gels were run (1.5 - 2 h, 125 V, current limited to 0.04 A/ chamber) in a SDS-PAGE gel chamber (Mini Trans-Blot[®], Bio-Rad, Hercules, CA) in Tris/Glycine/SDS buffer (Bio-Rad, cat.-#: 161-0732). Gels were blotted using a semi-dry blotting apparatus (Trans-Blot SD cell[®], Bio-Rad; 50-60 min, 25 V, current limited to 0.8 A/cell) to polyvinylidene difluoride (PVDF) membranes (Perkin Elmer Life Sciences, Boston, MA, cat.-#: NEF 1002). Membranes were blocked for 1 h (25°C, shaking) in Western blot blocking solution (5 % dry milk /0.1% Tween-20 in PBS). Subsequently, the following primary antibodies were applied in 10 ml total volume of Western blot blocking solution (overnight, 4°C, shaking): rabbit-anti-mouse IL-18 (Cell Sciences, Canton, MA, cat# CPI103; 1 µg/ml final concentration); rabbit-anti-human IL-1β (Santa Cruz, Santa Cruz, CA, cat# sc-7884; 0.5 µg/ml; cross-reacts with mouse IL-1β); rabbit-anti-mouse Caspase-1_{p10} (Santa Cruz,; 0.8 µg/ml). Membranes were washed 3 x for 5 min (25°C, shaking) with 0.1% (v/v) Tween-20 in PBS and subsequently incubated with peroxidase-conjugated goat-anti-rabbit IgG antibody (Jackson Immunoresearch, West Grove, PA, cat# 111-035-0034; 0.05 µg/ml) for 1 h (25°C, shaking) in Western blot blocking solution. Membranes were washed 3 x for 5 min (25°C, shaking) with 0.1% (v/v) Tween-20 in PBS and immunoreactive proteins were visualized using the Western LightningTM Chemiluminescence Reagent Plus (Perkin Elmer, cat.-#: NEL 105; 1 min, 25°C, shaking), capturing the luminescent signal on a film (Scientific imaging film; Kodak, Rochester, NY, cat.-#: KP 112078).

2.5. MMP-mediated processing of proIL-18

2.5.1. MMP activation

All recombinant human MMPs (MMP-1, -2, -3, -7, -8, -9, -10, -12, and -13) were obtained as recombinant zymogens from R&D Systems. MMPs were activated by incubation with APMA (p-aminophenylmercuric acetate; 1 mM) at 37°C for 1 h (MMP-1, -2, -7, and -8), 2 h (MMP-10 and -13) or 24 h (MMP-3 and -9), as recommended by the supplier. MMP-12 was provided as a catalytic domain and did not require APMA activation. Activation was verified by adding MMP-1, -2, -7, -8, -9, -12, and -13 to the fluorogenic substrate Mca-Pro-Leu-Gly-Leu-Dpa-Ala-Arg-NH₂ (R&D Systems) and adding MMP-3 and -10 to the fluorogenic substrate Mca-Arg-Pro-Lys-Pro-Val-Glu-Nval-Trp-Arg-Lys(Dnp)-NH₂ (R&D Systems). The substrate (10 µM) and defined concentrations of the respective MMP were incubated for 1-5 minutes at room temperature before fluorescence intensity was determined every 5 minutes for 30 minutes using a fluorescence spectrometer (excitation 320 nm, emission 405 nm, Spectra Max M2; Molecular Devices, Sunnyvale, CA). To determine activity, the fluorescence intensity of the quenched substrate was set as the baseline. The standard curve was constructed by applying serial dilutions of known concentrations of the pre-cleaved fluorogenic peptide fragment (Mca-Pro-Leu-OH; Calbiochem, San Diego, CA).

2.5.2. Pro-IL-18 processing assay

Caspase-1 (EMD, San Diego, CA) was used at a concentration of 0.5 µg/ml, determined during this study to be optimal for the proIL-18 processing assay employed. TCNB buffer (50 mM Tris, pH 7.5, 10 mM CaCl₂, 150 mM NaCl and 0.05% Brij35) was used in all processing assays to maintain an optimal pH for the recombinant MMPs.

APMA-activated MMPs were tested for concentration- and time-dependent processing of proIL-18. In the concentration-dependent assays, MMPs were incubated at 0-10 µg/ml with proIL-18 (2.5 µg/ml; kindly provided by Vertex Pharmaceuticals Inc., Cambridge, MA) for 1 and 24 h. In the time-dependent assays, MMPs were incubated at a concentration of 1 µg/ml with proIL-18 (2.5 µg/ml) for 0-24 h. Processing assays were performed in a total volume of 40 µl and under sterile conditions at 37°C.

2.5.3. SDS-PAGE and Western Blot analysis of pro-IL-18 processing

For analysis of pro-IL-18 processing, reaction mixtures from the processing assay (equivalents of 100 ng pro-IL-18/lane) were stopped after the indicated time by adding reducing SDS-PAGE sample buffer (5 X) and applied to SDS-PAGE analysis as described above for tissue protein extracts.

Unprocessed recombinant proIL-18 was applied either alone or following Caspase-1 treatment (0.5 µg/ml, 1 h, 37°C) as a negative and positive control, respectively. Western blot analysis employed rabbit-anti-human IL-18 primary antibody (Serotec, Raleigh, NC, cat.# AHP456; 1:1000 dilution) for 1 h (25°C, shaking) and followed the procedure as described above for tissue protein extracts.

2.5.4. IL-18 bioactivity assay

KG-1 cells (ATCC, Manassas, VA, cat.-# CCL-246) were maintained by sub-culturing every third day at 400,000 cells/ml in RPMI-1640 medium (Cambrex, Walkersville, MD, cat.# 12-702F) containing 20 % fetal bovine serum (HyClone, Logan, UT, cat.# SH30070.03) with penicillin and streptomycin (Cambrex, cat.# 17-602E; 100 U/ml and 100 µg/ml, respectively). For experiments, KG-1 cells (500,000 cells/ml) were plated in a 48-well plate in 0.5 ml/well RPMI-1640 medium without serum. Cells were pre-stimulated with TNF α (Pierce, Rockford, IL, cat.# M303; 10 ng/ml) for 24 h to induce expression of the IL-18 receptor, thus rendering the cells more responsive to IL-18. MMP- or Caspase-1-processing mixtures co-incubated with proIL-18 for 1 or 24 h were applied in part (50 ng of IL-18/well) to KG-1 cells. The cells were incubated for 24 h prior to collection and analysis of supernatants. Supernatants were assayed for IFN γ by ELISA as described above.

2.5.5. Mass Spectrometry and Protein Sequence Analysis

MMP-2 or MMP-8 (5 µg/ml) were incubated with pro-IL-18 (12.5 µg/ml) for 24 h. Mixtures were prepared for SDS-PAGE analysis as described above. Processing assay samples (equivalent to 500 ng of proIL-18) were separated by SDS-PAGE under reducing conditions on an 18 % gel. Gels were applied to Coomassie Brilliant Blue (Gel Code® Blue Stain Reagent; Bio Rad) and Silver staining (Silver Stain Plus; Bio-Rad).

Mass spectrometric analysis was performed at the Department of Pathology Functional Proteomics Center, Harvard Medical School by Eric Spooner. Coomassie-stained gel bands were excised and subjected to enzymatic digestion (overnight) with modified trypsin (20 ng/µl, 37°C; Sigma-Aldrich) after reduction by dithiothreitol (DTT) (10 mM; 30 min; Sigma-Aldrich) and alkylation by iodoacetamide (100 mM; 30 min; Sigma-Aldrich). Trypsin cleaves only to the C-terminal site of Arginine (Arg, R) and Lysine (Lys, K), however does not cleave if Arg or Lys is preceded by Proline (Pro, P). Thus, any peptides derived from this analysis not featuring an Lys or Arg at the C-terminus potentially indicate a MMP-cleavage site. Peptides were subsequently extracted from the digests by treatment with a mixture of 50 % acetonitrile/ 45% water/ 5% formic acid. Employing a speedvac, volume was reduced to 20 µl, of which 5 µl were subjected to reverse phase high performance liquid chromatography (RP-HPLC; CapLC XE, Waters, Milford, MA) with a C-18 column (Waters; 3 µm pore size, 0.75 mm x 100 mm) coupled to a electrospray ionization (ESI) tandem-mass spectrometer (MS/MS; Micro-Q-Tof, Micromass, Beverly, MA) operated in a data dependent fashion. The analytical gradient was 5% buffer B (Acetonitrile with 0.1% Formic Acid) to 45 % buffer B in 35 minutes.

The resulting data were analyzed using a database search algorithm (Mascot, Matrixscience, Boston, MA) to identify the peptides of interest. Theoretical molecular weights of peptide fragments were determined during reverse sequence search for analysis of the MMP-8 cleavage site.

3. Results

3.1. IL-18 induces production of the pro-inflammatory cytokine IFN γ in mononuclear phagocytes and in vascular smooth muscle cells

Work summarized in my diploma thesis demonstrated expression of IL-18 in human atherosclerotic lesions, providing the initial implication for this cytokine in atherogenesis.^{111,112} This work also identified several novel pro-atherogenic functions of IL-18, such as enhanced expression of adhesion molecules and MMPs in human vascular EC and SMC as well as macrophages. Subsequently, I investigated whether IL-18 also mediates its originally recognized function, the induction of IFN γ expression, in these atheroma-

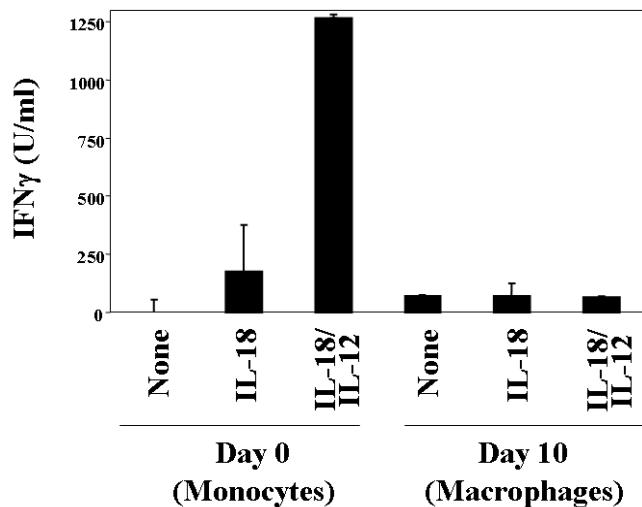


Figure 6: IL-18 induces IFN γ from freshly isolated human monocytes.

Human peripheral blood-derived monocytes were either stimulated immediately after isolation or cultured for 10 days in medium containing 5% human serum. Cells were serum-starved for 12 h and subsequently stimulated with IL-18 [50 ng/ml] alone or in combination with IL-12 [10 ng/ml] for 36 hours. Subsequently, concentrations of IFN γ in the supernatant were measured by ELISA. Data represent mean \pm SD of data obtained in four independent experiments using cells from different donors.

associated cell types. Indeed, IL-18, particularly in synergism with IL-12, elicited IFN γ protein and transcript in macrophages (Figure 6) and, even more surprisingly, in human vascular SMC, a cell type previously not implicated in the synthesis of this cytokine. These observations were validated on the protein (ELISA, Figure 7) and RNA level (*in situ* hybridization, Figure 8A; RT-PCR, Figure 8B). Of note, addition of Polymyxin B did not diminish the expression of IFN γ transcripts or protein, whereas heat-inactivation of the recombinant IL-12/IL-18 abolished this function, indicating that endotoxin contamination did not account for the IFN γ expression (Figure 7 and 8B).

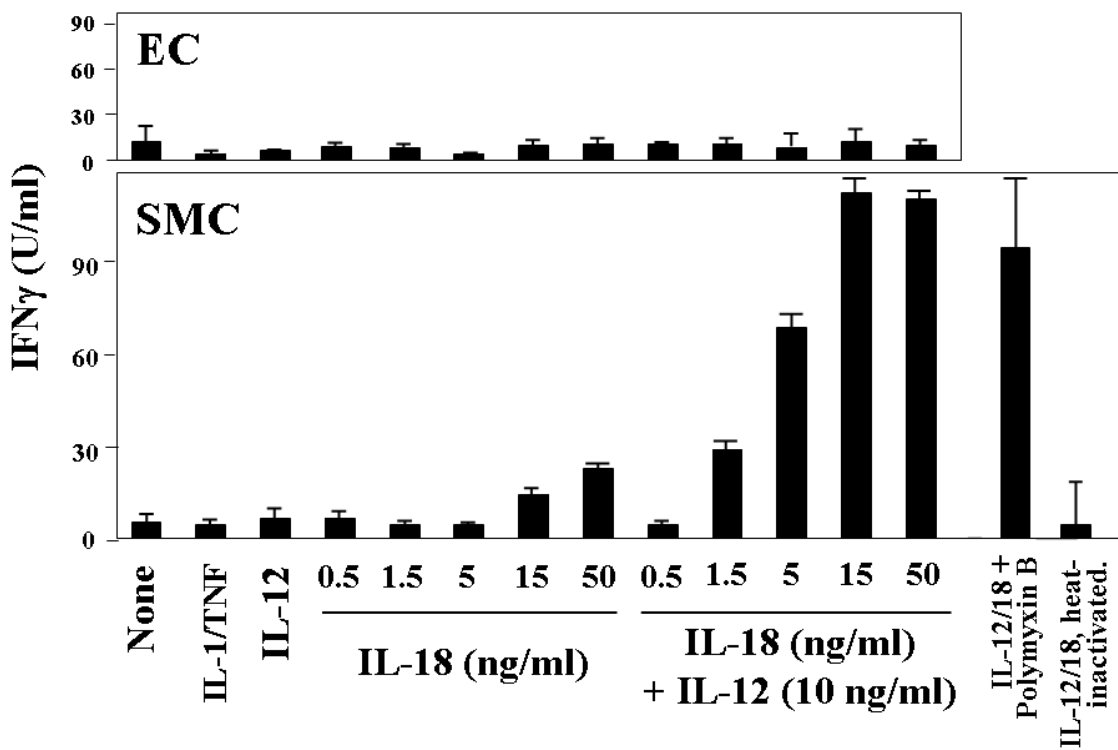


Figure 7: IL-18 induces IFN γ expression in human vascular smooth muscle cells.

Human saphenous vein smooth muscle cells (SMC) or endothelial cells (EC) were stimulated (36 h) with either IL-1 β /TNF α [10/50 ng/ml], IL-12 [10 ng/ml], respective concentrations of IL-18, or combinations of the latter two, and supernatants were analyzed by ELISA for IFN γ . Polymyxin B [1 μ g/ml] and heat treated (95°C, 10 min) IL-12/IL-18 were tested to exclude activation via endotoxin contamination. Data represent mean \pm SD. Similar results were obtained five independent experiments employing cells of different donors.

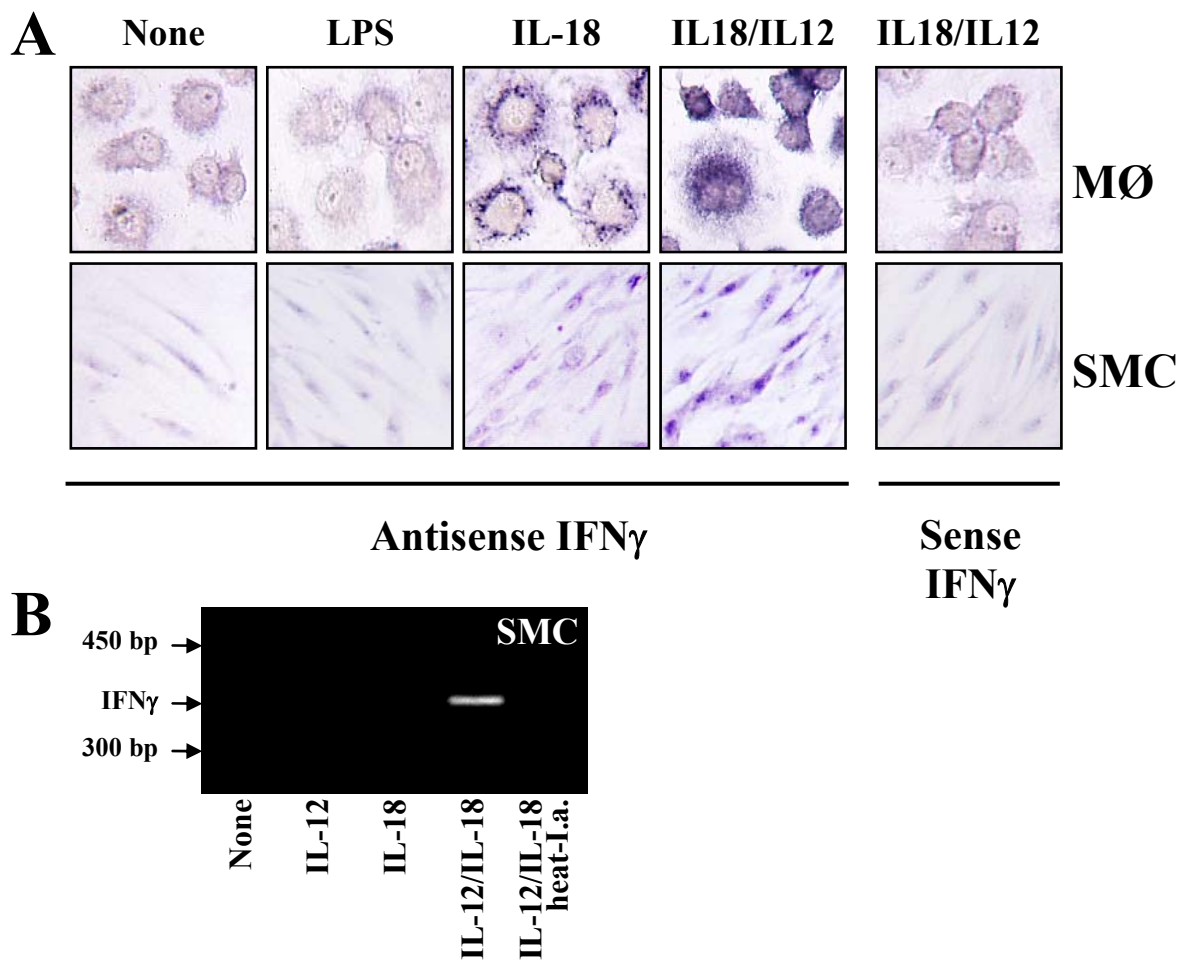


Figure 8: IL-18 induces IFN γ expression in human monocytes and vascular smooth muscle cells.

(A) Mononuclear phagocytes (MØ, top) or smooth muscle cells (SMC, bottom) cultured to confluence on 4-well chamber slides and subsequently incubated with medium alone (None), IL-12 [10 ng/ml], IL-18 [50 ng/ml], or combinations thereof, were analyzed for the expression of IFN γ transcripts by *in situ* hybridization employing the respective antisense or sense (control) oligomers. Magnification is 40x. (B) Total RNA obtained from cultured SMC cultured with medium alone (None), IL-12 [10 ng/ml], IL-18 [50 ng/ml], or combinations thereof, was analyzed by RT-PCR for IFN γ transcripts. Heat-treated rec. IL-12/IL-18 (95°C, 10 min) were applied to exclude activation via endotoxin contamination. Similar results were obtained in three independent experiments employing cells of different donors.

Moreover, other pro-inflammatory cytokines such as IL-1 β or TNF α did not induce expression of IFN γ in these cell types, demonstrating specificity of IL-18 function. The SMC cultures employed expressed smooth muscle α -actin but did not yield a signal for CD14 by RT-PCR or for CD3, CD4, CD31, CD64, or CD68 by immunohistochemical or FACS analysis (data not shown), demonstrating that the SMC cultures employed, indeed contained negligible if any T-lymphocytes, EC, or macrophages. Of note, vascular SMC demonstrated a donor-specific expression pattern for IFN γ . Within the total of 15 different donors, SMC cultures from five donors did not show detectable induction of IFN γ compared to supernatants of non-stimulated cultures (1.4 ± 1.8 U IFN γ /ml), even when maximal

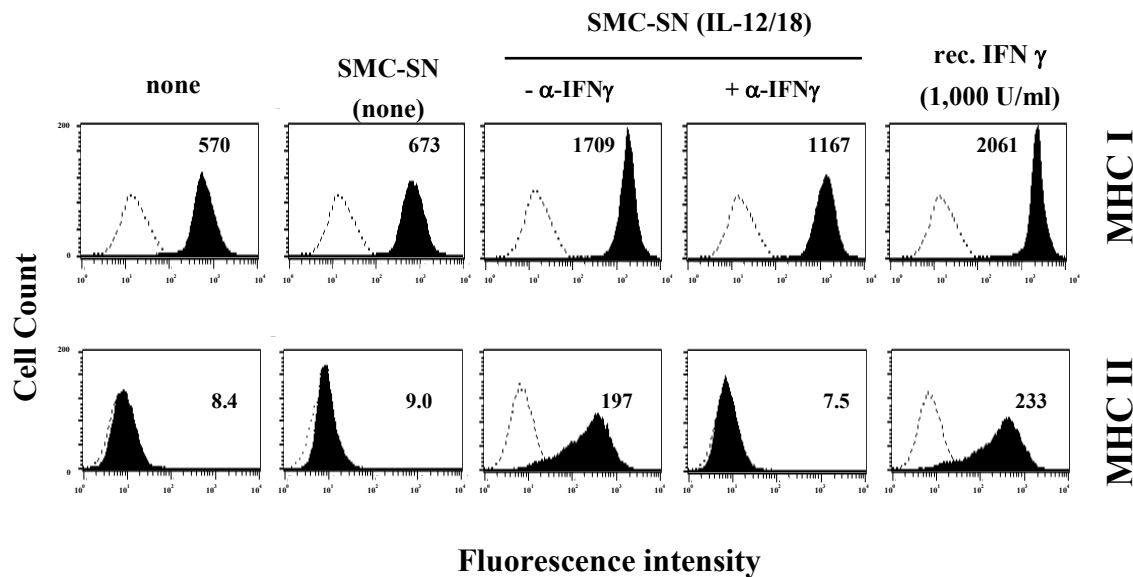


Figure 9: IFN γ secreted from human smooth muscle cells exhibits biologic activity.

Supernatants of smooth muscle cell cultures stimulated with medium alone (SMC-SN (none)) or combination of IL-12 [10 ng/ml] and IL-18 [50 ng/ml] (SMC-SN (IL-12/18)) were applied in absence or presence of neutralizing α -IFN γ antibody (SMC-SN (IL-12/18) + α -IFN γ) to confluent endothelial cell (EC) cultures for 48 hours and MHC I (top) and MHC II (bottom) expression was compared to unstimulated (none) or IFN γ -stimulated (rIFN γ , 1000 U/ml) EC by FACS analysis. Staining (solid histograms) was compared to isotype control (dotted line). At least 20,000 viable cells were analyzed for each staining. Values of geometric mean fluorescence are indicated in each panel. Similar results were obtained in three independent experiments.

concentrations of IL-18 or IL-12/IL-18 were applied. Within the group of ten experiments yielding significantly ($p \leq 0.05$) enhanced IFN γ expression upon stimulation with IL-12/IL-18 combination, low and high “responders” were identified. Five donors yielded an average of 16.5 ± 12.9 U IFN γ /ml and the remaining five donors of 260 ± 115 U IFN γ /ml (Figure 7). Although the cause remains unknown, neither gender nor age of the cell donor nor passage number of the cells appeared to account for this observed variation. In contrast to SMC, macrophages expressed IFN γ more uniformly following stimulation with IL-12/IL-18 (120 ± 43 U IFN γ /ml; n=4). EC did not express IFN γ in response to any of the stimuli or combinations thereof tested, supporting the cell type specificity of the finding (Figure 7).

In view of the unexpected expression of IFN γ by SMC, I further tested the ability of medium conditioned by IL-12/IL-18-stimulated SMC to exhibit a IFN γ -characteristic biological activity of IFN γ , such as enhancing the expression of major histocompatibility complex (MHC) class I or II. Indeed, incubation with culture supernatants derived from IL-12/IL-18-stimulated SMC enhanced the expression of MHC I and MHC II (Figure 9) in EC compared to those cultured with supernatants of non-treated SMC, as demonstrated by FACS analysis. Addition of neutralizing anti-IFN γ antibody to the culture medium abrogated induction of MHC I and MHC II on EC, further validating the surprising finding that IFN γ secreted by SMC exhibits biological activity.

To demonstrate the potential relevance of SMC-derived IFN γ to the pathogenesis of atherosclerosis, we performed *in situ* hybridization studies on sections of human atheroma. In support of the *in vitro* observations outlined above, mRNA for IFN γ in atherosclerotic lesions localized with T-cells, but also within macrophage- and SMC-enriched areas, which were T-cell-deprived (Figure 10). In contrast, non-atherosclerotic tissue did not contain detectable levels IFN γ mRNA (not shown). Moreover, application of sense oligomers did not yield detectable signals. Unavailability of appropriate antibodies hampered extension of these *in situ* results to the protein level (see *Discussion*).

These studies add to the pro-inflammatory role of IL-18 and further highlight its potential relevance for atherosclerosis. In particular, the unexpected finding of IFN γ expression by SMC, ascribing this cell type additional immune functions, may have far-reaching implications considering the abundance of this cell-type in atherosclerosis.

Nonetheless, these experiments limited the evaluation of the role of IL-18 in atherogenesis *in vitro*, thus rendering its relevance for atherosclerosis *in vivo* unexplored.

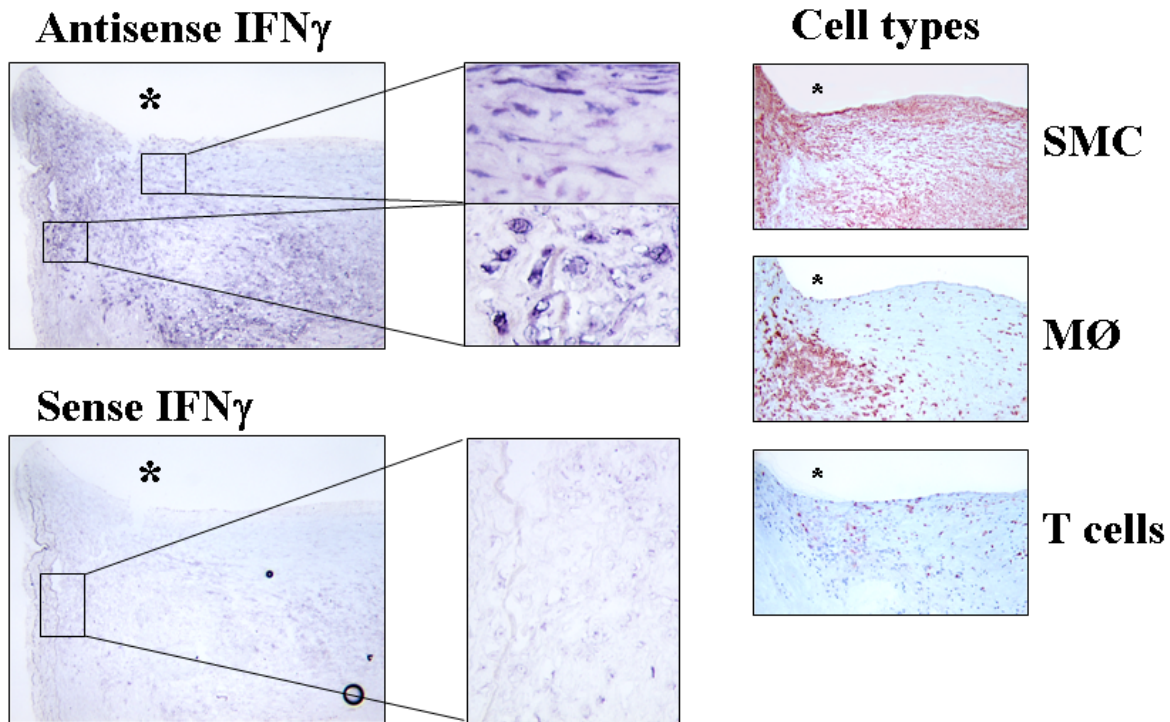


Figure 10: IFN γ mRNA localizes in macrophage- and smooth muscle cell-rich regions of atherosclerotic lesions.

Serial cryostat sections of frozen specimens of carotid atheroma were analyzed for the expression of IFN γ transcripts by *in situ* hybridization employing the respective antisense (*top left panels*) or sense (*bottom left panels*) oligomers. Low (4x, *left*) and high (40x, *right*) magnifications are shown. The asterisk indicates the lumen of the vessels. Adjacent sections were stained for SMC (anti- α -actin), macrophages (MØ; anti-CD68), or T-lymphocytes (anti-CD3) (*right panels*).

3.2. Deficiency of IL-18 decreases development of atherosclerosis in mice

3.2.1. IL-18, IL-18R α , and Caspase-1 are expressed in murine atherosclerotic lesions

After the initial observation of IL-18 and IL-18R expression in human atherosclerotic lesions and demonstration of pro-atherogenic functions of IL-18 in cells implicated in atherosclerosis, I proposed to test whether this cytokine indeed aggravates atherosclerosis *in vivo*. To ensure that IL-18 is also expressed in atherosclerotic lesion of mice, similar to human atheroma, Western blot analysis of protein extracts obtained from murine atherosclerotic aortas was performed. Indeed, aortae of ApoE-deficient mice fed an atherogenic diet for 8 weeks contained both the 24 kDa precursor and 18 kDa mature form of IL-18 (Figure 11). Additional experiments revealed Caspase-1 expression in these aortae, further displaying the inflammatory conditions induced by hyperlipidemia in mice. Of note, the antibody directed against the p10-subunit detects the precursor (~45 kDa) and the p10

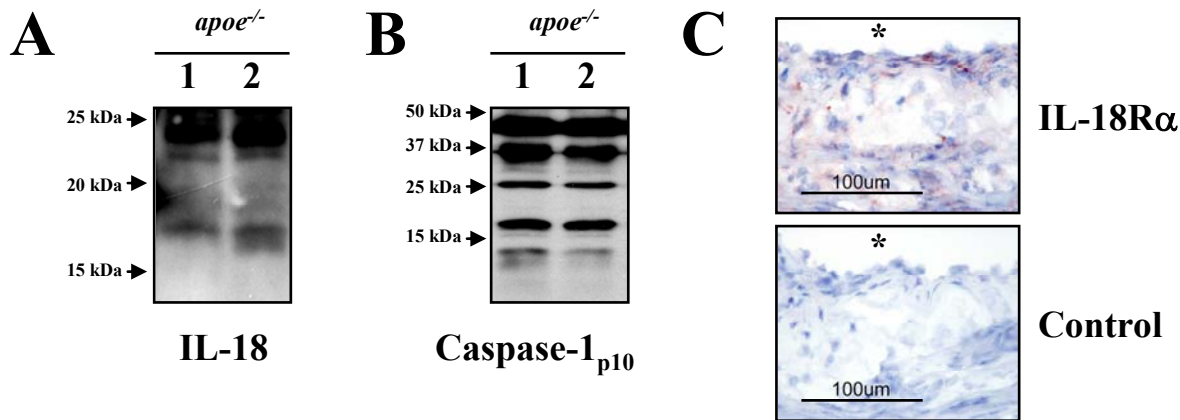


Figure 11: IL-18, IL-18R α , and Caspase-1 are expressed in murine atherosclerosis.

Protein extracts from aorta of two *apo $e^{-/-}$* mice fed a high-cholesterol diet for 8 weeks were subjected to SDS-PAGE and subsequent Western blot analysis for (A) IL-18 or (B) Caspase-1 (p10-subunit). Approximate molecular weights are indicated by the arrows on the left. (C) Immunohistochemical analysis employing an antibody for IL-18R α (*top*) or control IgG (*bottom*) on sections of atheroma from an *apo $e^{-/-}$* mouse fed a high-cholesterol diet for 8 weeks were analyzed. The asterisk indicates the lumen of the vessel. Similar results were obtained in three experiments employing tissue from 5 different mice.

monomer (~10 kDa) of Caspase-1. Moreover, immunohistochemical analysis revealed expression of IL-18R α in murine atherosclerosis (Figure 11C), which localized with most parts of the plaque, including endothelium and macrophage-rich areas, corroborating previous findings in human atheroma (Figure 3 in *Introduction*). Thus, these initial experiments assured the presence of these key components of the IL-18 signaling cascade supporting the rationale for the subsequent experiments aimed to test the effect of the respective gene-deficiency on murine atherosclerosis.

3.2.2. Deficiency of IL-18 delays development of atherosclerosis in hyperlipidemic mice

To assess directly the role of IL-18 in atherogenesis, we compared atherosclerotic lesion formation in the inner curvature of the aortic arch of *il18*^{+/+}*apoe*^{-/-} and *il18*^{-/-}*apoe*^{-/-} mice. To avoid subjective selection of areas of interest, we did not distinguish between media and intima, but rather analyzed the total wall area in longitudinal sections of a defined

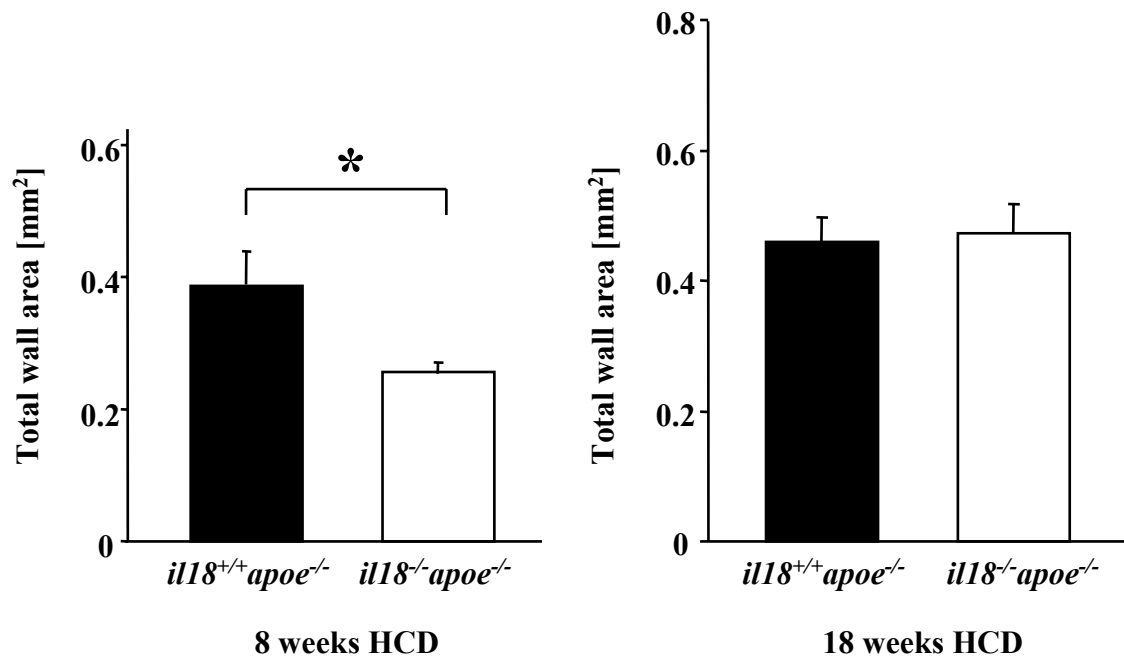


Figure 12: IL-18 deficiency delays atherosclerotic lesion formation in hyperlipidemic mice
Quantification of total wall area in the aortic arches of male *il18*^{+/+}*apoe*^{-/-} (black) and *il18*^{-/-}*apoe*^{-/-} (open) mice fed a high-cholesterol diet (HCD) for either 8 (left panel, n=7 or 9, respectively) or 18 weeks (right, n=10). Data are presented as mean ± SEM. The asterisk indicates a p-value <0.05.

segment of the inner curvature (see *Methods*). Aortic arches of *il18^{-/-}apoe^{-/-}* mice fed HCD for 8 weeks displayed significantly less atheroma than those of *il18^{+/+}apoe^{-/-}* mice (-35 %; $p<0.05$; Figure 12, left). Interestingly, the degree of atherosclerosis did not differ between the *il18^{+/+}apoe^{-/-}* and *il18^{-/-}apoe^{-/-}* mice after more prolonged (18 week) hypercholesterolemia (Figure 12, right). These results indicate a role for IL-18 in early rather than advanced lesion development. To test this hypothesis further, we fed *il18^{+/+}apoe^{-/-}* and *il18^{-/-}apoe^{-/-}* mice a low-cholesterol (chow) diet, which slowed the onset of atherosclerosis. After 8 weeks of chow diet, we observed little or no lesion development in either strain of mice (Figure 13, left).

However, following 18 weeks of chow diet, the aortic arches of *il18^{+/+}apoe^{-/-}* mice displayed early atheromata, resembling those observed following 8 weeks of HCD (Figure 13, right). In contrast, *il18^{-/-}apoe^{-/-}* mice still did not show any evident lesion burden after 18 weeks of HCD, corroborating the role of IL-18 in early lesion development. Furthermore, these data demonstrate that IL-18 mediates its pro-atherogenic function under both moderate and extreme hyperlipidemic conditions.

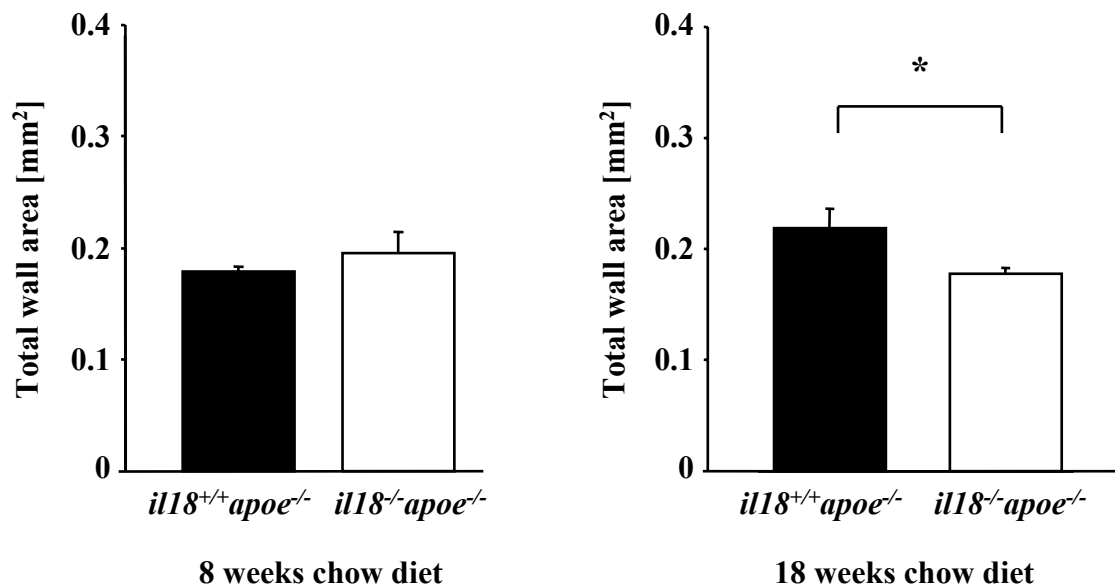


Figure 13: Diminished atherosclerosis in IL-18^{-/-} mice consuming a chow diet

Quantification of total wall in the aortic arches of male *il18^{+/+}apoe^{-/-}* (black) and *il18^{-/-}apoe^{-/-}* (open) mice fed a normal chow diet for either 8 (*left panel*, n=7 or 9, respectively) or 18 weeks (*right*, n=10). Data are presented as mean \pm SEM. The asterisk indicates a p -value <0.05 .

3.2.3. IL-18-deficiency attenuates early atherogenesis in mice of both genders

In view of a report by Whitman et al., demonstrating reduced atherosclerosis in male but not female IFN γ -deficient mice,⁷² published during the time of this thesis, I also analyzed the effect of IL-18 deficiency on lesion development in female mice. Comparable to the findings in male mice, lack of IL-18 led to smaller total wall areas in female mice after 8 weeks of HCD (-24 %; n=5, P<0.05; Figure 14, top). Also in accord with the findings in male mice, we observed no difference in lesion size between female *il18^{+/+}apoe^{-/-}* and *il18^{-/-}apoe^{-/-}* mice following either 18 weeks of HCD or 8 weeks of chow diet. However, following

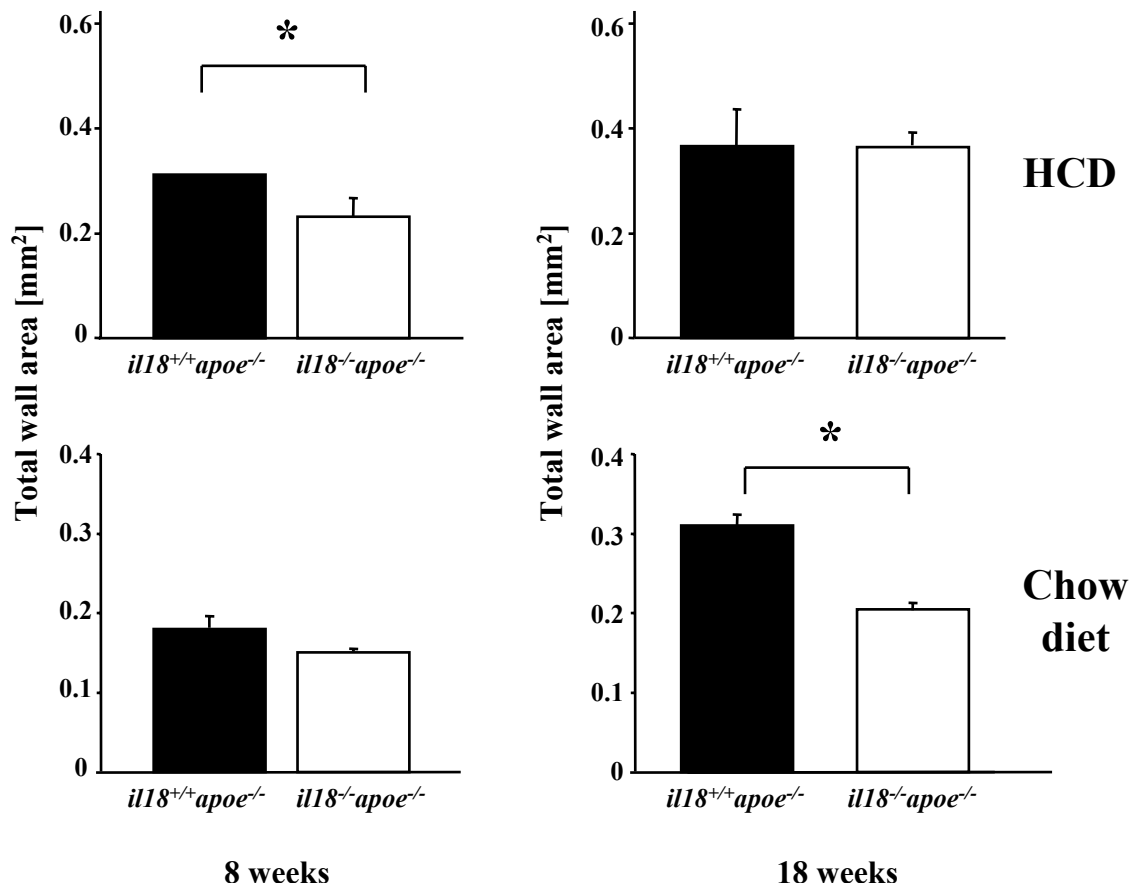


Figure 14: Reduction of atherosclerosis in IL-18 deficient mice is not gender-specific

Quantification of total wall in the aortic arches of female *il18^{+/+}apoe^{-/-}* (black) and *il18^{-/-}apoe^{-/-}* (open) mice fed a high-cholesterol diet (HCD; top panels, n=7) or a normal chow diet (chow; bottom panels, n=6 or 5, respectively) for either 8 (left panels) or 18 weeks (right panels). Data are presented as mean ± SEM. The asterisk indicates a p-value <0.05.

18 weeks of chow diet, total wall area in *il18^{-/-}apoe^{-/-}* mice was smaller compared to the control group, corroborating the findings in male mice and suggesting a gender-independent role of IL-18 in atherogenesis.

Table 7: Total plasma cholesterol, plasma triglyceride, and body weight of *il18^{+/+}apoe^{-/-}* and *il18^{-/-}apoe^{-/-}* mice at the end of the study

Duration of diet		8 weeks				18 weeks			
Type of diet		Chow		High-cholesterol		Chow		High-cholesterol	
IL-18 genotype		+/-	-/-	+/-	-/-	+/-	-/-	+/-	-/-
Male									
Number of animals		N = 9	N = 8	N = 9	N = 8	N = 10	N = 10	N = 10	N = 10
Total cholesterol [mg/dL]		546.5 ± 41.7	582.5 ± 38.8	732.9 ± 46.7	1197.3 ± 75.1*	402.5 ± 24.4	591.9 ± 61.5*	761.4 ± 70.6	913.1 ± 63.3
Triglycerides [mg/dL]		128.6 ± 9.9	184.0 ± 18.8	84.7 ± 8.9	137.5 ± 14.4*	58.3 ± 5.7	124.5 ± 14.3*	129.9 ± 21.2	167.4 ± 22.1
Body weight [g]		25.6 ± 0.5	26.1 ± 0.9	26.2 ± 0.7	27.5 ± 0.9	27.1 ± 0.8	27.9 ± 0.9	30.7 ± 0.5	32.1 ± 1.1
Female									
Number of animals		N = 5	N = 5	N = 5	N = 5	N = 5	N = 5	N = 4	N = 4
Total cholesterol [mg/dL]		342.4 ± 30.6	511.3 ± 28.6	653.1 ± 86.7	984.0 ± 66.3*	377.1 ± 24.8	459.0 ± 41.3	806.6 ± 69.4	918.4 ± 42.6
Triglycerides [mg/dL]		65.1 ± 8.9	105.5 ± 10.9	81.6 ± 7.0	158.3 ± 31.2*	63.0 ± 8.0	101.9 ± 7.9*	79.1 ± 7.1	110.4 ± 6.9*
Body weight [g]		20.2 ± 1.1	18.8 ± 0.7	19.7 ± 0.8	22.4 ± 0.7	23.5 ± 1.3	21.3 ± 0.5	24.7 ± 0.4	25.4 ± 1.1
Concentrations were measured following ≥ 8 hours starvation; Values represent mean ± SEM;									
* p ≤ 0.05 vs. control; +/− = <i>il18^{+/+}apoe^{-/-}</i> ; −/− = <i>il18^{-/-}apoe^{-/-}</i>									

3.2.4. IL-18 deficiency increases plasma total cholesterol and triglycerides

Elevated plasma lipid concentrations promote atherosclerotic lesion development in mice. Therefore it is necessary to determine whether alteration of a certain gene, e.g., IL-18, might lead to decreased plasma lipid levels, thereby potentially limiting atherogenesis. Our

data show that the delay of atherosclerotic lesion formation in the absence of IL-18 did not result from diminished plasma cholesterol levels. Rather, IL-18 deficiency delayed atherogenesis despite increased total plasma cholesterol and triglyceride concentrations (Table 7). Following 8 weeks of HCD, the time point with the greatest reduction of lesion development, IL-18 deficiency led to profoundly increased plasma cholesterol and triglyceride levels. This remarkable trend was observed regardless of either gender or durations of both HCD and chow diet, although statistical significance was not reached in some groups, probably due to the limited number of data points (e.g., in most groups of female mice). Furthermore, there was a trend towards elevated body weight in *il18*^{-/-}*apoE*^{-/-} mice compared to control mice following either diet regimen (Table 7). Nonetheless, a statistical significance for this trend could not be established. In sum, the elevated lipid levels further emphasize the role of IL-18 in atherogenesis.

3.2.5. IL-18 deficiency promotes a more stable plaque phenotype

Changes in lesion size upon genetic or pharmacologic inhibition of a certain gene allow only for limited conclusions regarding the pro- or anti-atherogenic role of this particular mediator. Therefore, analysis of plaque composition (e.g., leukocyte infiltration, lipid deposition, or content of SMC) is commonly employed to gain further insight into the functional relevance of deficiency or inhibition of a particular protein.

Notably, atheroma of IL-18-deficient mice (n=7) contained significantly fewer macrophages (-48 %; $p<0.05$) following 8 weeks of HCD compared to controls (n=9), as determined by immunohistochemical staining for Mac-3 (Figure 15). We observed no difference in macrophage content in mice consuming HCD for 18 weeks, corroborating the role of IL-18 in early rather than advanced atherogenesis. However, in this study, *il18*^{+/+}*apoE*^{-/-} and *il18*^{-/-}*apoE*^{-/-} mice displayed no difference in the amount of lipid deposition within the arterial wall following consumption of HCD (Figure 16) or chow diet (data not shown) for 8 or 18 weeks, as determined by Oil Red O staining. These data corroborate the previous finding that the cellular composition of the lesion was modified even under elevated levels of plasma lipids.

To further characterize the lesional composition and in particular to investigate the role of IL-18 in modulating plaque stability, we analyzed the number of SMCs and the content of collagen, both features commonly associated with a more stable plaque phenotype. Indeed, male *il18^{+/+}apoel^{-/-}* mice had a 32 % ($p<0.05$) higher content of SMC than did *il18^{+/+}apoel^{-/-}* following 8 weeks of HCD (Figure 17A and B, left). After prolonged

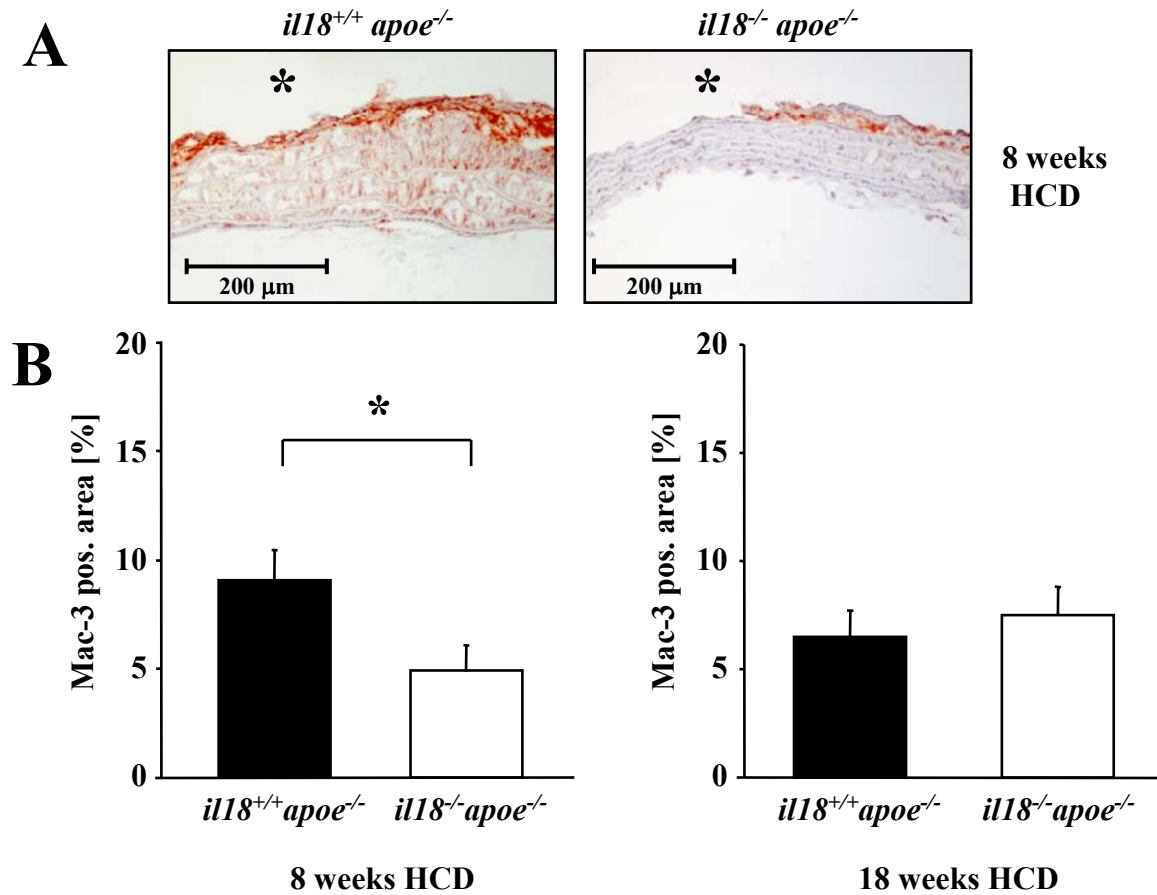


Figure 15: IL-18 deficiency reduces macrophage infiltration in atherosclerotic lesions

- (A) Immunohistochemical staining for macrophages, using a Mac-3-specific antibody, on longitudinal sections of representative aortic arches from male *il18^{+/+}apoel^{-/-}* (left) and *il18^{-/-}apoel^{-/-}* (right) mice fed an atherogenic diet for 8 weeks. The asterisk indicates the lumen of the vessel.
- (B) Quantitative analysis of immunohistochemical staining for macrophages of male *il18^{+/+}apoel^{-/-}* (black) and *il18^{-/-}apoel^{-/-}* (open) mice fed an atherogenic diet for either 8 (left panel, n=7 or 9, respectively) or 18 weeks (right panel, n=10). Data are presented as mean \pm SEM. The asterisk indicates a p -value <0.05 .

hypercholesterolemia for 18 weeks, however, SMC content did not differ between the two genotypes, in agreement with the comparable atherosclerotic lesion size and the presumed role of IL-18 in early atherogenesis (Figure 17B, right). Although both groups of mice showed comparable SMC-positive areas after 18 weeks of high cholesterol diet, the overall content of SMC was markedly less compared to the earlier time point, indicating evolution towards advanced SMC-depleted lesions following prolonged hypercholesterolemia (Figure 17B).

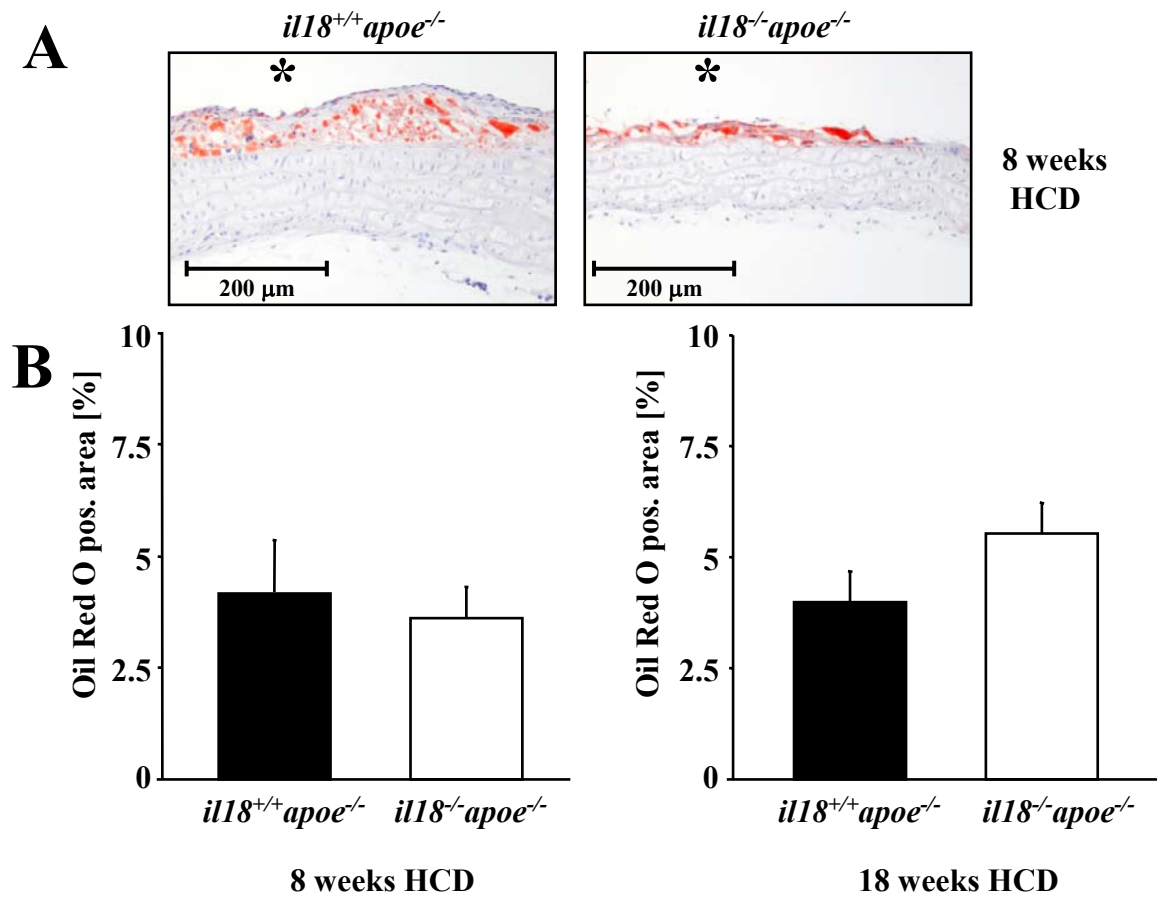


Figure 16: IL-18 deficiency does not change lipid deposition within the arterial wall

(A) Oil Red O staining on longitudinal sections of representative aortic arches of male *il18^{+/+}apoe^{-/-}* and *il18^{-/-}apoe^{-/-}* mice fed an atherogenic diet for 8 weeks. The asterisk indicates the lumen of the vessel. (B) Quantitative analysis of Oil Red O staining of male *il18^{+/+}apoe^{-/-}* (black) and *il18^{-/-}apoe^{-/-}* (open) mice fed an atherogenic diet for either 8 (left panel, n=7 or 9, respectively) or 18 weeks (right panel, n=10). Data are presented as mean ± SEM.

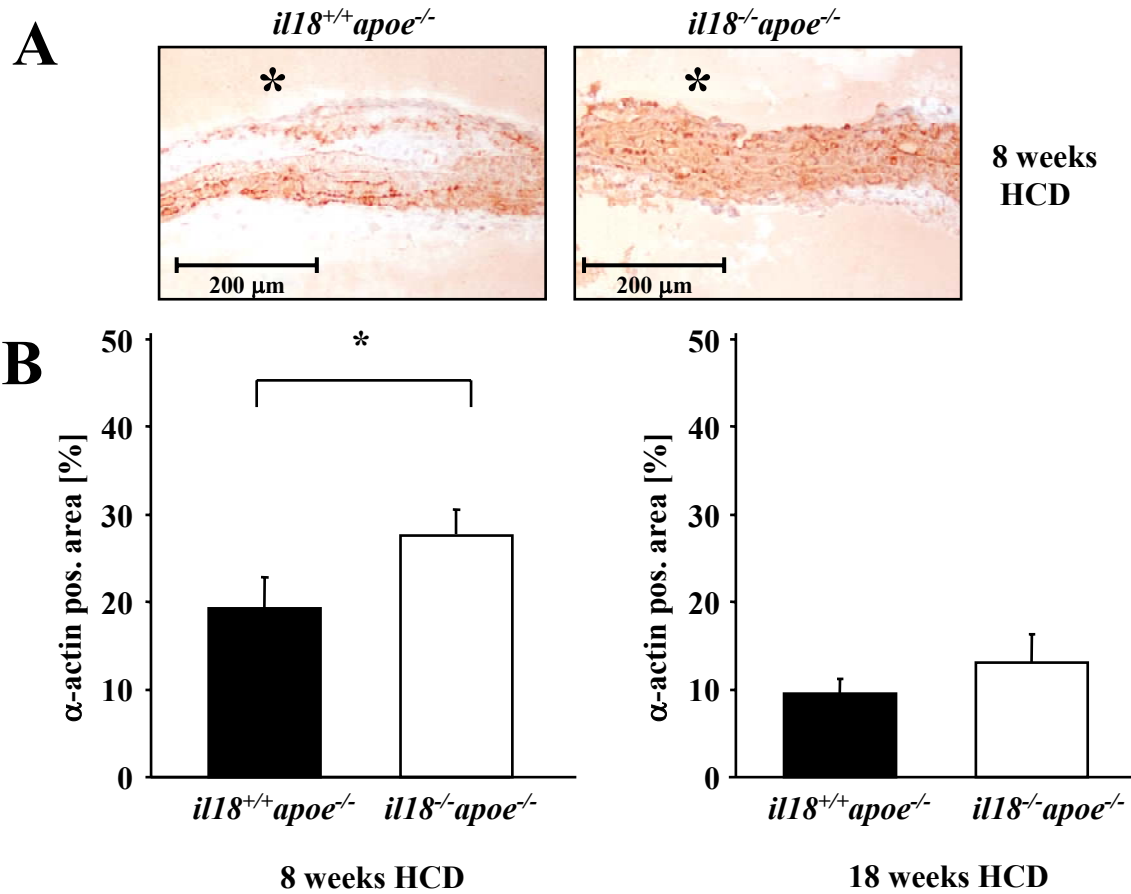


Figure 17: IL-18 deficiency increases the number of smooth muscle cells within the arterial wall.

(A) Immunohistochemical staining for smooth muscle cells, using an α -actin-specific antibody, on longitudinal sections of representative aortic arches of male *il18^{+/+}apoe^{-/-}* and *il18^{-/-}apoe^{-/-}* mice fed an atherogenic diet for 8 weeks. The asterisk indicates the lumen of the vessel. (B) Quantitative analysis of immunohistochemical staining for smooth muscle cells in male *il18^{+/+}apoe^{-/-}* (black) and *il18^{-/-}apoe^{-/-}* (open) mice fed an atherogenic diet for either 8 (left panel, n=7 or 9, respectively) or 18 weeks (right panel, n=10). Data are presented as mean \pm SEM. The asterisk indicates a *p*-value <0.05 .

This depletion of SMC indicates the functionality of the experimental model and, repeatedly highlights the relevance of IL-18 for early rather than advanced stages of plaque progression.

In contrast to the enhanced numbers of SMC, atherosclerotic lesions in *il18^{-/-}apoe^{-/-}* mice following 8 weeks of HCD displayed less collagen compared to *il18^{+/+}apoe^{-/-}* mice, as

determined by Picosirius Red staining (Figure 18). This trend, however, did not yield statistical significance (no difference was observed when HCD was continued for 18 weeks). Analysis of macrophage and SMC content as well as lipid and collagen deposition in atherosclerotic lesions revealed comparable results in female mice (data not shown), corroborating the findings in male mice and supporting the gender-independent role of IL-18 in atherogenesis.

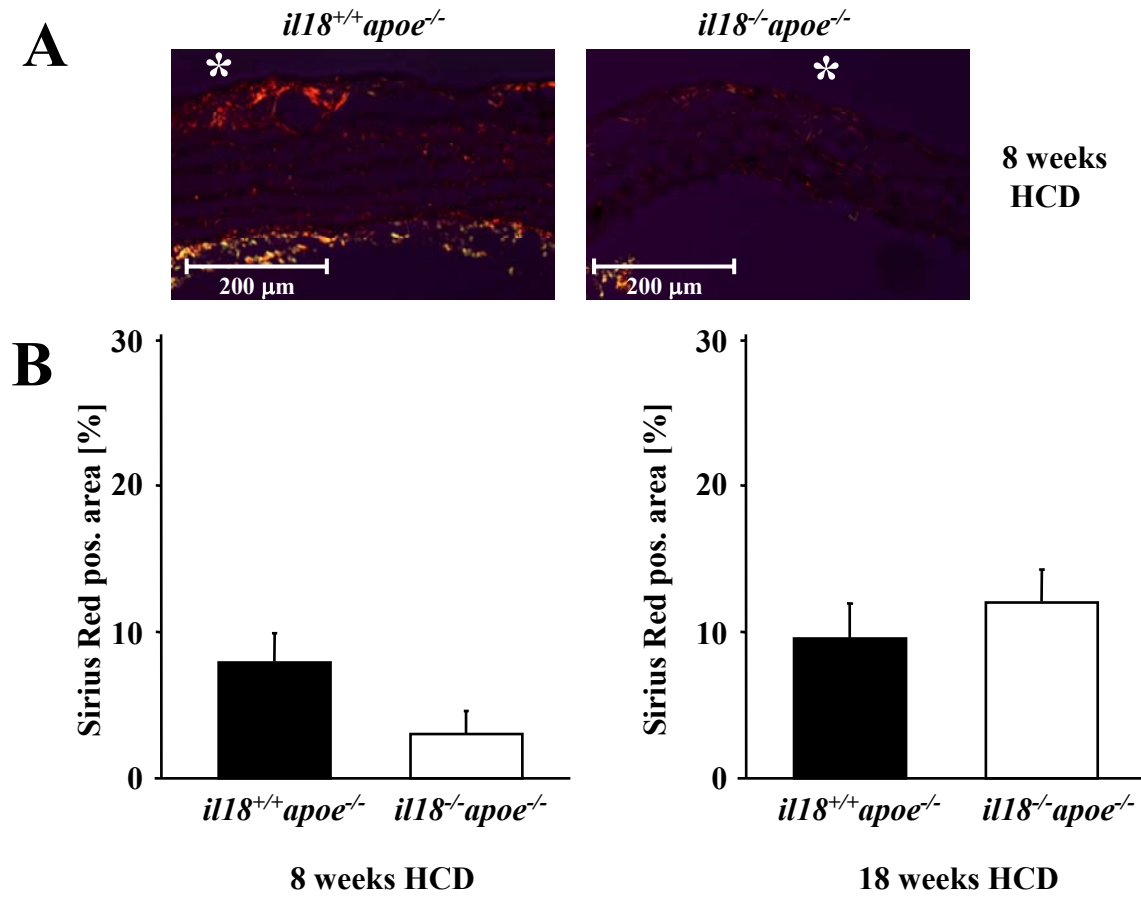


Figure 18: IL-18 deficiency does not change collagen content within the arterial wall.

(A) Picosirius Red staining for collagen on longitudinal sections of representative aortic arches from male *il18^{+/+}apoe^{-/-}* and *il18^{-/-}apoe^{-/-}* mice fed an atherogenic diet for 8 weeks. The asterisk indicates the lumen of the vessel. (B) Quantitative analysis of Picosirius Red staining of male *il18^{+/+}apoe^{-/-}* (black) and *il18^{-/-}apoe^{-/-}* (open) mice fed an atherogenic diet for either 8 (left panel, n=7 or 9, respectively) or 18 weeks (right panel, n=10). Data are presented as mean ± SEM.

3.2.6. IL-18 deficiency differentially modulates atherosclerosis in the aortic sinus or descending aorta

Several reports demonstrated considerable variability in the extent and chronology of atherosclerotic lesion development between distinct vascular locations in murine experimental models. Indeed, the earliest manifestations of lesion development, such as lipid deposition or macrophage infiltration, are usually observed in the aortic sinus of hyperlipidemic mice, whereas emergence of atherosclerosis in the distal aorta requires

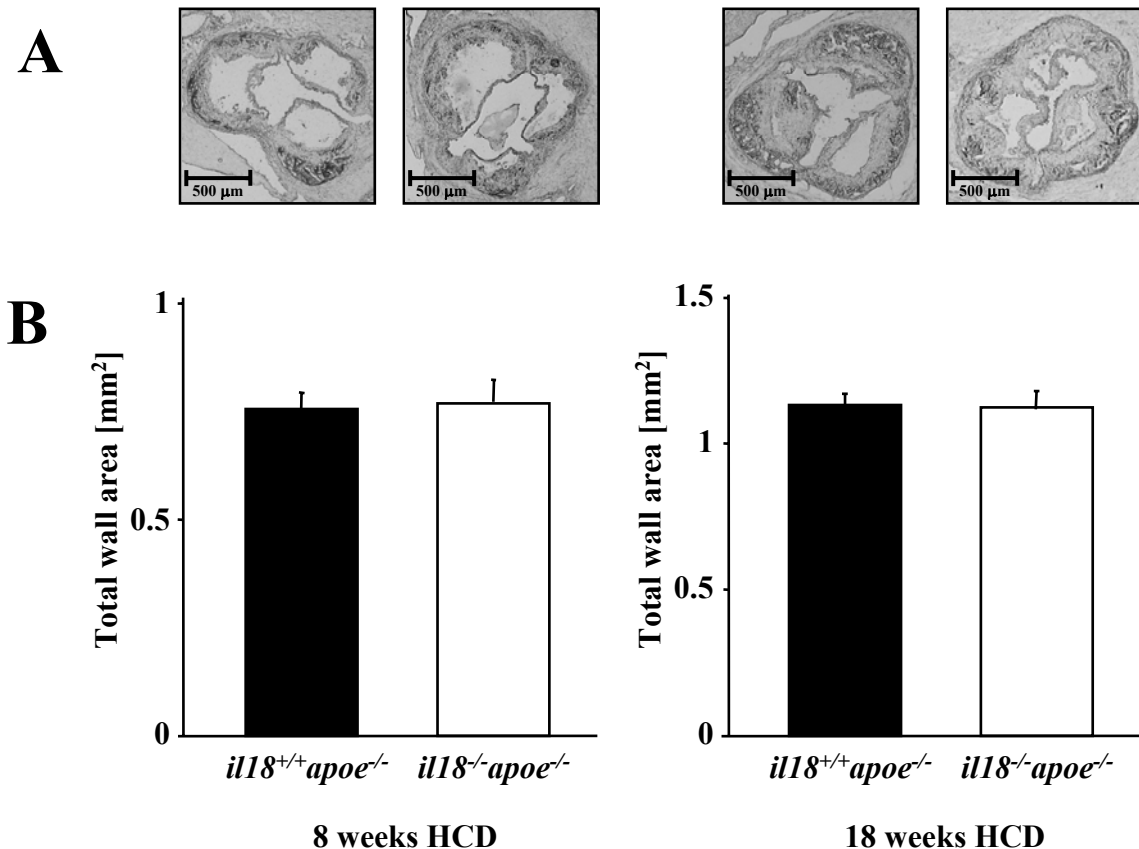


Figure 19: IL-18 deficiency does not reduce atherosclerosis in the aortic sinus.

(A) Representative section of the aortic sinus of male *il18^{+/+}apoe^{-/-}* and *il18^{-/-}apoe^{-/-}* mice fed an atherogenic diet for 8 (left) or 18 (right) weeks. (B) Quantification of total wall in the aortic sinus of male *il18^{+/+}apoe^{-/-}* (black) and *il18^{-/-}apoe^{-/-}* (open) mice fed a high-cholesterol diet (HCD) for either 8 (left panel, n=5) or 18 weeks (right, n=5). Data are presented as mean ± SEM.

prolonged hypercholesterolemia. To account for these potential differences and further validate the presumed role of IL-18 in early atherogenesis, lesion progression in these vascular locations was quantified. Notably, atherosclerotic lesion development in the aortic sinus of male $il18^{+/+}apoe^{-/-}$ and $il18^{-/-}apoe^{-/-}$ mice following 8 or 18 weeks of HCD did not differ significantly (Figure 19). Considering that these lesions are already at an advanced stage after only 8 weeks of hypercholesterolemia, these data are in agreement with the hypothesized role of IL-18 as a modulator of early atherogenesis.

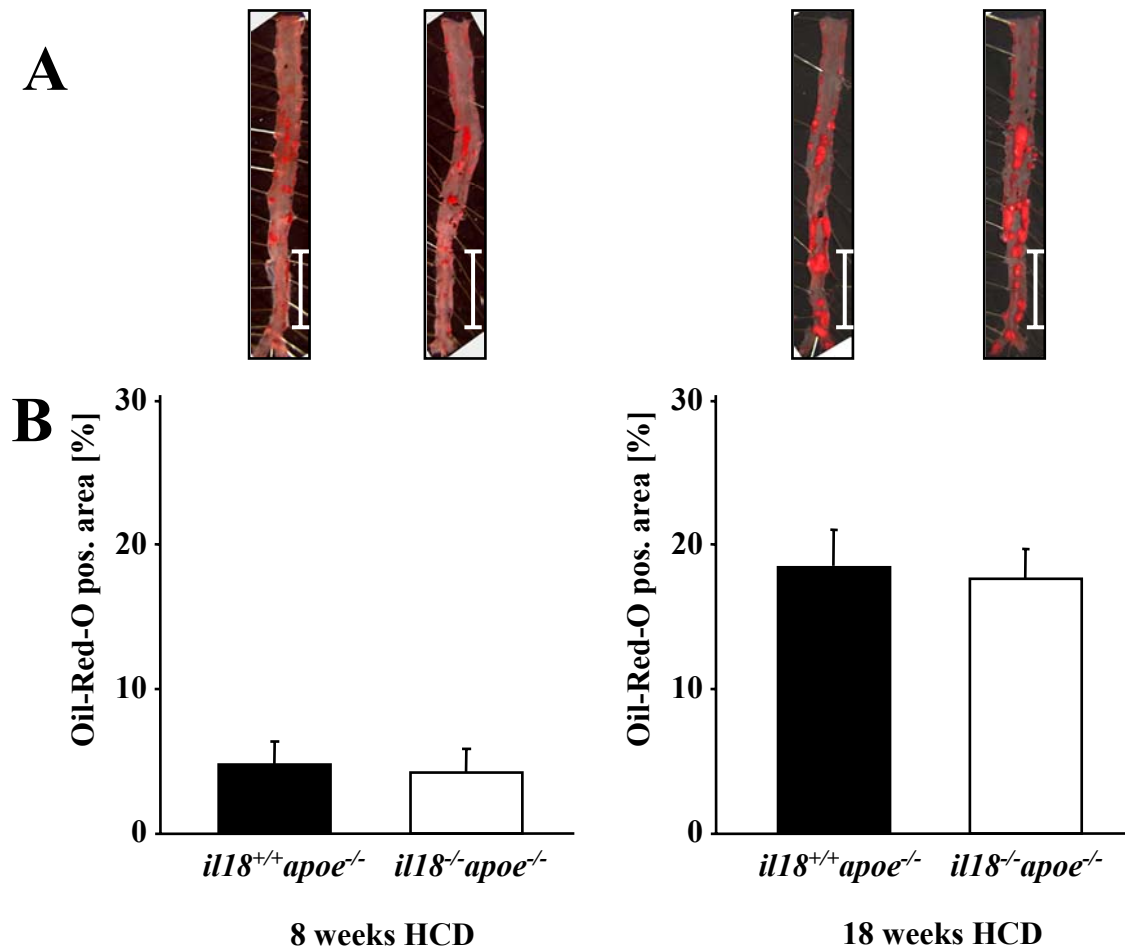


Figure 20: IL-18 deficiency does not affect lesion development in the thoracic/abdominal aorta.

(A) Representative Oil Red O-stained *en face*-preparations of thoracic/abdominal aortae of male $il18^{+/+}apoe^{-/-}$ and $il18^{-/-}apoe^{-/-}$ mice fed an high-cholesterol diet (HCD) for 8 (*left*) or 18 (*right*) weeks. The bars represent 0.5 cm. (B) Quantitative analysis of Oil-red O staining on aortae of male $il18^{+/+}apoe^{-/-}$ (black) and $il18^{-/-}apoe^{-/-}$ (open) fed a HCD for either 8 (*left panel*, n=5) or 18 weeks (*right*, n=5). Data are presented as mean \pm SEM.

Furthermore, *en face* analysis of Oil Red O-stained aortae revealed that IL-18 does not affect fatty streak development within the thoracic/abdominal aorta. Of note, Oil Red O-stained area, though minimal in this vascular bed following 8 weeks of HCD, was markedly increased following 18 weeks of this diet regimen independent of the genotype (Figure 20). Since the *en face* analysis of aortae employs Oil Red O staining and, thus primarily determines lipid deposition, these data are in accord with findings of unchanged lipid retention in lesions of the aortic arch. Indeed, the markedly elevated plasma lipid concentrations in IL-18 deficient mice likely account for the enhanced lipid deposition despite overall reduced lesion development (see *Discussion*).

3.2.7. The pro-atherogenic function of IL-18 is potentially independent of IFN γ

As discussed above, the original function of IL-18 has been described as the ability to induce IFN γ from T- and NK-cells.⁷⁵ Since IFN γ has been described as a potent agonist of atherogenesis,^{65-67,71,72} it appeared likely that IL-18 mediates its pro-atherogenic function via this traditional pathway. However, the lack of gender-specificity observed in our studies suggested a potential IFN γ -independent role for IL-18 signaling in atherosclerosis, since a recent report demonstrated a strong gender-dependent role for IFN γ in the development of atherosclerosis.⁷² To ascertain whether diminished atherosclerosis in IL-18-deficient mice results from the attenuation of IL-18's traditional downstream effector we analyzed expression of IFN γ and MHC II, which is strongly dependent on IFN γ .⁶⁹ Surprisingly, however, we observed no difference in the expression of IFN γ within atherosclerotic lesions of the aortic arch between *il18*^{+/+}*apoe*^{-/-} and *il18*^{-/-}*apoe*^{-/-} mice following 8 weeks of HCD, at which time lesion development differed significantly (Figure 21A; compare to Figure 12). Corroborating these findings, analysis of the IFN γ -regulated MHC II antigens within adjacent sections revealed no significant change of expression levels in mice of both genotypes following 8 weeks of HCD (Figure 21B). These data support the hypothesis that IL-18 mediates its atherogenic functions independent of IFN γ .

The observation that IL-18 deficiency modulates early lesion development suggests that IL-18 might promote the expression of mediators involved in the initiation of atherosclerosis. As discussed in the Introduction, expression of adhesion molecules and subsequent

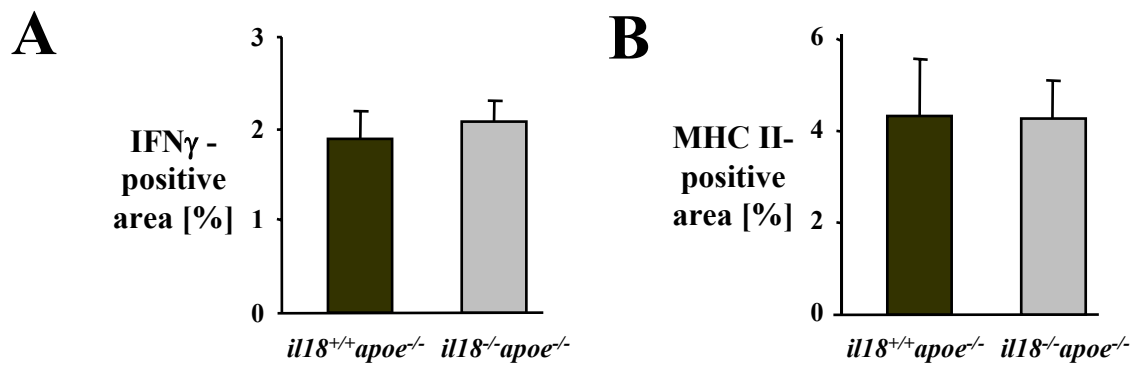


Figure 21: Reduction of atherosclerosis in IL-18 deficiency is independent of IFN γ expression and function.

Quantitative analysis of immunohistochemical staining for (A) IFN γ and (B) MHC II on sections of aortic arches from male *il18^{+/+}apoe^{-/-}* (black bars) and *il18^{-/-}apoe^{-/-}* (grey bars) mice fed an atherogenic diet for 8 weeks. n = 7 for each group. The bars represent the mean \pm SEM.

infiltration of leukocytes is one of the early mechanisms in lesion evolution. In addition, *in vitro* studies have recently demonstrated expression of adhesion molecules upon stimulation with IL-18,¹⁶⁷ suggesting that IL-18 might contribute to lesion development via this prominent pro-atherogenic pathway. To test this hypothesis, sections of atheroma in the aortic arch of *il18^{+/+}apoe^{-/-}* and *il18^{-/-}apoe^{-/-}* mice were analyzed for expression of VCAM-1, the most prominent adhesion molecule figuring in atherosclerosis. Indeed, IL-18 deficiency associated with diminished expression of the adhesion molecule VCAM-1 (-29 %) within atherosclerotic lesions following 8 weeks of HCD (data not shown), suggesting reduced leukocyte adhesion, and thus infiltration, as a possible mechanism by which IL-18 deficiency might, at least in part, alleviate atherogenesis.

3.3. The role of IL-18R in atherogenesis

3.3.1. Generation of chimeric mice lacking IL-18 receptor on either hematopoietic or somatic cells

After establishing that IL-18 deficiency alleviates atherogenesis, I aimed to investigate whether the ligation of IL-18R α on hematopoietic or somatic cells mediates the pro-atherogenic function of IL-18. Chimeric mice that expressed IL-18R α only either on the somatic/vascular or on the hematopoietic cells were generated employing bone marrow reconstitution experiments in hyperlipidemic mice. In control experiments homologue BMT yielded mice either completely deficient for IL-18R α or globally competent for IL-18R α (see also Figure 5 in *Methods*).

To verify successful reconstitution, we also generated mice deficient for ApoE and homozygous for allele 1 of the common leukocyte antigen CD45 ($cd45^{1/1}apoe^{-/-}$). Mice of the C57/Bl6 background commonly carry the CD45.2 allele. Employing mice with allelic variations of CD45 as donors and recipients in BMT allows for rapid discrimination of the origin of circulating cells by flow cytometry.¹⁶⁸ This method was used to establish successful reconstitution of bone marrow following three (not shown) and six weeks (Figure 22) of recovery. Indeed, lethal irradiation (14 Gy) and subsequent bone marrow engraftment led to >90 % leukocyte reconstitution. Notably, detailed analysis of leukocyte subpopulations revealed that monocytes (CD11b $^+$) and B-cells (CD19 $^+$) were more than 95 % of donor origin (Figure 22C,F, left and middle panels). T-cell reconstitution ranged between 85 % and 97 % (Figure 22C,F, right panels).

These experiments employed $cd45^{2/2}apoe^{-/-}il18r1^{+/+}$ or $cd45^{2/2}apoe^{-/-}il18r1^{-/-}$ donor bone marrow and $cd45^{1/1}apoe^{-/-}il18r1^{+/+}$ recipient mice as well as $cd45^{1/1}apoe^{-/-}il18r1^{+/+}$ donor bone marrow and $cd45^{2/2}apoe^{-/-}il18r1^{+/+}$ or $cd45^{2/2}apoe^{-/-}il18r1^{-/-}$ recipient mice (n=4 for each of the 4 combinations). We observed no difference in reconstitution efficiency, suggesting that IL-18 signaling does not influence the engraftment process. Furthermore, the total number of circulating leukocytes determined following recovery as well as at the end of the study, did not differ between the experimental groups. These control experiments demonstrated that bone marrow reconstitution successfully yielded chimeric mice, expressing

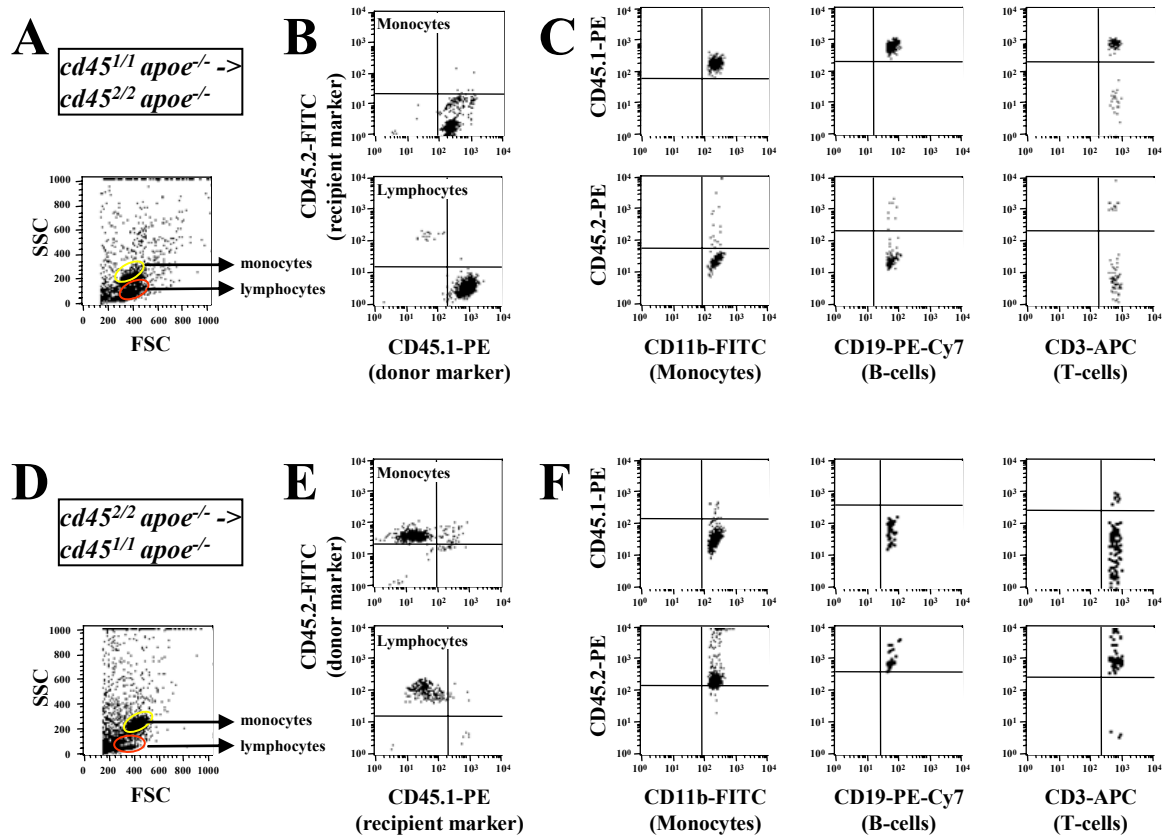


Figure 22: Successful bone marrow reconstitution in hyperlipidemic mice.

Lethally irradiated (14 Gy) male mice were reconstituted with bone marrow cells (2×10^6 cells/mouse) and blood was analyzed following 6 weeks of recovery by flow cytometry discriminating the common leukocyte antigen CD45. Bone marrow from donor $cd45^{1/1}apoe^{-/-}$ mice was transplanted into $cd45^{2/2}apoe^{-/-}$ recipient mice (**A-C**) or *vice versa* (**D-F**). Cell distribution in size (FSC) and optical refraction (SSC) is depicted (**A,D**). Monocyte- and lymphocyte population gated from the respective areas in **A** and **D**, respectively, were analyzed for distribution of the CD45 allele (**B,E**). Detailed analysis of the distribution of the CD45 allele in monocytes (*left*, $CD11b^+$), B-cells (*middle*, $CD19^+$), and T-cells (*right*, $CD3^+$) employing four color flow cytometry (**C,F**). Note, that donor and recipient marker are reciprocal in **B-C** vs. **E-F**. Similar results were obtained for $cd45^{2/2}apoe^{-/-}il18rl^{-/-}$ mice employed as either donors or recipients. Shown are representative data from total of 4 mice for each group.

Table 8: Total plasma cholesterol, plasma triglyceride, and body weight before and after 8 weeks of high cholesterol diet in IL-18R α -competent, -deficient, and -chimeric mice

Experimental procedure	Feeding			Bone-marrow transplantation		
Genotype	<i>wt</i>	<i>ko</i>	<i>wt</i> → <i>wt</i>	<i>ko</i> → <i>wt</i>	<i>ko</i> → <i>ko</i>	<i>wt</i> → <i>ko</i>
Number of animals	N = 12	N = 11	N=14	N = 11	N = 13	N = 12
Baseline (Start of HCD)						
Total cholesterol [mg/dL]	531 ± 42	489 ± 27	982 ± 126	501 ± 27	638 ± 43	617 ± 45
Triglycerides [mg/dL]	107.5 ± 15.6	96.5 ± 7.1	169.0 ± 35.5	82.0 ± 8.8	72.2 ± 7.3	80.1 ± 7.0
Body weight [g]	20.5 ± 0.6	22.7 ± 0.6	23.0 ± 0.6	22.8 ± 0.9	24.2 ± 0.6	23.5 ± 0.4
End of study (after 8 weeks of HCD)						
Total cholesterol [mg/dL]	1111 ± 74	1241 ± 72	1238 ± 74	993 ± 103	983 ± 88	1140 ± 79
Triglycerides [mg/dL]	76.5 ± 9.6	81.4 ± 7.8	404.6 ± 66.6	261.0 ± 55.0	141.5 ± 44.7**	104.5 ± 9.9*
Body weight [g]	26.9 ± 0.9	29.3 ± 1.0	25.0 ± 0.3	25.5 ± 0.5	26.3 ± 0.4	25.4 ± 0.4

Concentrations were measured following ≥ 8 hours starvation; Values represent mean ± SEM;

* = p ≤ 0.01 vs. *wt* → *wt*; ** = p ≤ 0.05 vs. *ko* → *wt*,

wt = *il18r1*^{+/+}*apoe*^{-/-}; *ko* = *il18r1*^{-/-}*apoe*^{-/-}; donor → recipient

IL-18R α either on hematopoietic or vascular cells. Furthermore, IL-18R α -deficiency apparently does not affect the engraftment process and, thus, the number of leukocytes.

Upon successful generation of chimeric mice and following a 6 week recovery period, these animals consumed HCD for an additional 8 weeks of HCD. Plasma cholesterol and triglyceride as well as body weight were determined before the start of the diet and at the end of the study (Table 8). Interestingly, plasma lipid levels, in particular triglycerides, were

elevated in bone marrow-transplanted mice globally competent for IL-18R α ($wt \rightarrow wt$), the exact cause for this difference, however, remains undetermined. Total body weight did not vary between the groups of animals before or after 8 weeks of HCD.

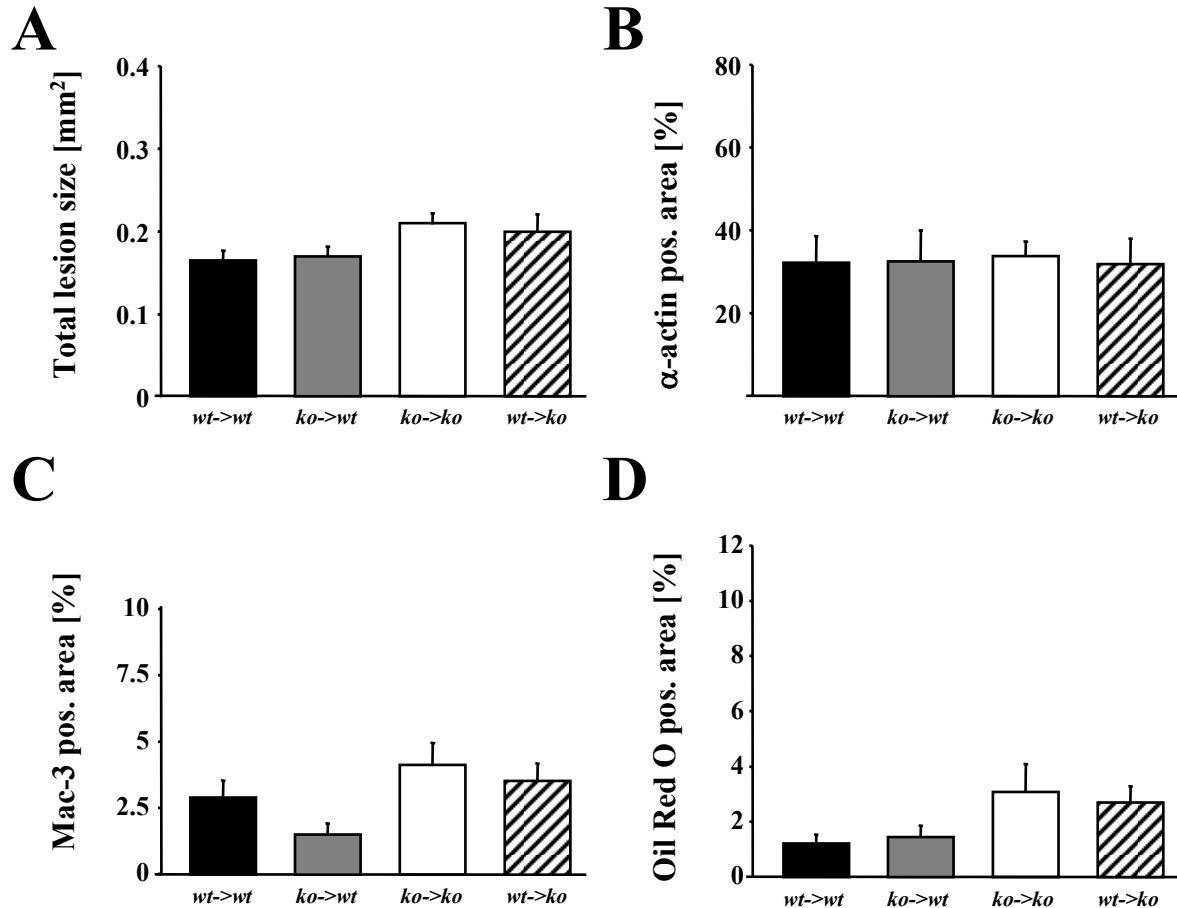


Figure 23: Lack of IL-18R α on either hematopoietic or vascular cells does not affect atherosclerotic lesion development in the aortic arch of hyperlipidemic mice.

Male mice were subjected to bone marrow transplantation (BMT), followed by a 6 week recovery period and additional 8 weeks consumption of high-cholesterol diet. BMT employed 6-8 weeks old mice as donors and recipients ($wt = il18r1^{+/+}apoe^{-/-}$ and $ko = il18r1^{-/-}apoe^{-/-}$; donor \rightarrow recipient). (A) Total wall area in longitudinal sections of the aortic arch was determined. Quantification of immunohistochemical staining for (B) smooth muscle cells, using an α -actin-specific antibody and for (C) macrophages, using a Mac-3-specific antibody on adjacent section of the aortic arch. (D) Quantification of Oil Red O staining for lipid deposition on adjacent sections. The bars represent the mean \pm SEM.

3.3.2. Absence of IL-18R α on either hematopoietic or somatic cells does not change atherogenesis in mice

Following the identification of IL-18 as a pro-atherogenic mediator, experiments employing chimeric mice lacking IL-18R α on either hematopoietic or vascular cells aimed to clarify which cell type play the predominant role in pro-atherogenic IL-18 signaling. Surprisingly, however, lesion size in the aortic arch of mice from all four groups of chimeric mice did not differ following 8 weeks of HCD (Figure 23A). Furthermore, when IL-18R α was absent on vascular cells, hematopoietic or both cells, plaque composition such as SMC- and macrophage content or lipid deposition was not affected (Figure 23B-D).

In sum, the failure of partial or complete deficiency of IL-18R α to reduce atherogenesis is unexpected and contrasts the reduced lesion development previously observed in IL-18-deficient mice.

3.3.3. Lack of IL-18R α does not affect atherosclerosis

Comparable atherogenesis in mice competent or deficient for IL-18R α on either hematopoietic or non-hematopoietic cell types suggested a potential receptor-independent function of IL-18. Due to the relevance of this conclusion additional experiments employing mice globally lacking IL-18R α were performed. Interestingly, analysis of atherosclerotic lesions in the aortic arch revealed no difference in lesion development between *il18r1^{+/+} apoe^{-/-}* and *il18r1^{-/-} apoe^{-/-}* mice following 8 weeks of HCD (Figure 24A). Furthermore, measures of plaque composition, namely macrophage and SMC content as well as lipid deposition did not differ between mice lacking IL-18R α and their controls, supporting the findings in the chimeric mice.

These data support the observation obtained in the BMT study: considering that deficiency of the ligand IL-18 in this model yielded marked reduction in lesion size and modulated plaque composition (Figures 12 and 15-17), these data strongly suggest that IL-18 mediates its pro-atherogenic function in mice via a receptor(s) other than IL-18R α .

Of note, plasma cholesterol and triglyceride levels did not differ between *il18r1^{+/+} apoe^{-/-}* and *il18r1^{-/-} apoe^{-/-}* mice, contrasting the previous finding of elevated lipid levels in IL-18-deficient mice and, thus, further supporting the hypothesis that IL-18 mediates pro-atherogenic functions independent of its classical receptor (Table 8).

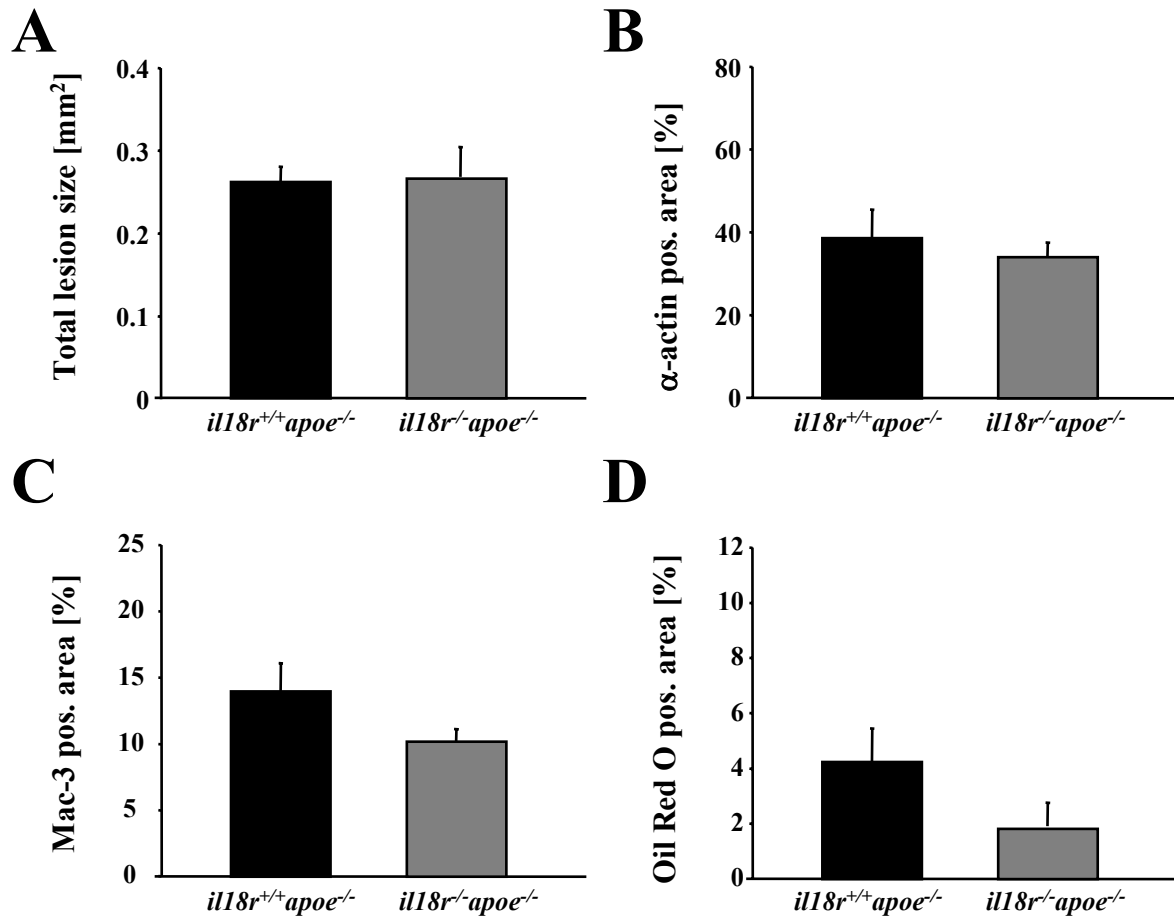


Figure 24: IL-18R α deficiency does not affect atherosclerotic lesion development in the aortic arch of hyperlipidemic mice

(A) Quantification of total wall area in the aortic arches of male *il18r*^{+/+}*apoe*^{-/-} (black) and *il18r*^{-/-}*apoe*^{-/-} (grey) mice fed a high-cholesterol diet (HCD) for 8 weeks. Quantification of immunohistochemical staining for (B) smooth muscle cells, using an α -actin-specific antibody and for (C) macrophages, using a Mac-3-specific antibody on adjacent section of the aortic arch. (D) Quantification of Oil Red O staining for lipid deposition on adjacent sections. The bars represent the mean \pm SEM.

3.4. Caspase-1 deficiency does not limit atherogenesis in hyperlipidemic mice

After successfully establishing the crucial role of IL-18 signaling in experimental atherosclerosis, we aimed to clarify whether lack of Caspase-1, the traditional processing enzyme for IL-18, would also lead to diminished atherosclerosis. During the time this study was designed, Kirii *et al.* reported markedly reduced atherosclerosis in IL-1 β deficient mice.¹⁶⁹ Thus, considering that both substrates of Caspase-1, IL-18 and IL-1 β , proved pro-atherogenic, we hypothesized that lack of Caspase-1 leads to a cumulative reduction of atherosclerotic lesion development.

To test the pro-atherogenic role of IL-1 signaling in our model of atherogenesis we applied mice compound-deficient for IL-1R type I and ApoE (*il1rI*^{-/-}*apoe*^{-/-}) to a study regimen similar to the one described above for IL-18 and IL-18R α . Employing mice deficient for the receptor rather than the ligand would also address the question whether IL-1 β also would signal independent of its receptor. Analysis of atherosclerosis in *il1rI*^{-/-}*apoe*^{-/-} mice revealed a marked reduction of lesion development in both genders following 8 but not 18 weeks of HCD, corroborating the previous findings in IL-1 β -deficient mice (Figure 25).¹⁶⁹ Furthermore, the reduced atherosclerosis in *il1rI*^{-/-}*apoe*^{-/-} mice following short-term but not prolonged hyperlipidemia implicates IL-1 signaling similar to IL-18 in promotion of early atherogenesis. However, in contrast to *il18*^{-/-}*apoe*^{-/-} mice, *il1rI*^{-/-}*apoe*^{-/-} mice did not display altered content of α -actin positive cells indicating that the IL-1 and IL-18 pathways differentially influence SMC proliferation and/or apoptosis (Figure 26). In contrast, when analyzing features of plaque destabilization, IL-1R1-deficiency provoked results closely resembling those obtained in IL-18-deficient mice. Although *il1rI*^{-/-}*apoe*^{-/-} mice displayed reduced infiltration of macrophages in aortic lesions of the aortic arch compared to control animals, lipid deposition, as determined by Oil Red O staining, was unchanged (Figure 27).

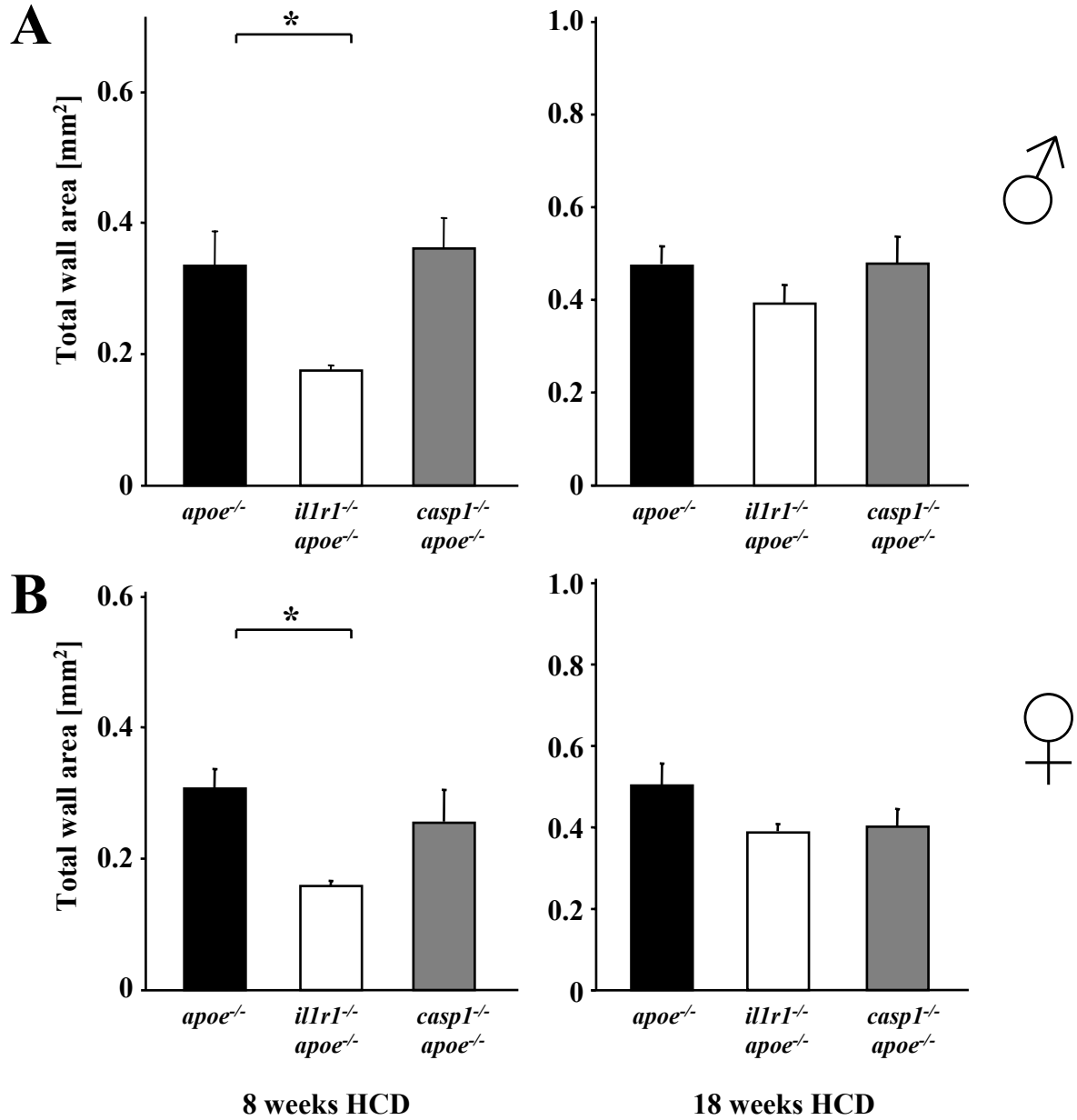


Figure 25: Caspase-1 deficiency does not attenuate atherosclerosis in hyperlipidemic mice.

Quantification of total wall area in the aortic arch of (A) male or (B) female *illr1*^{-/-} *apoe*^{-/-} (open) and *casp1*^{-/-} *apoe*^{-/-} (grey) vs. *apoe*^{-/-} (black) mice fed a high-cholesterol diet for either 8 (left panels) or 18 weeks (right panels). The squares represent the mean \pm SEM. The asterisk indicates a *p*-value <0.05 .

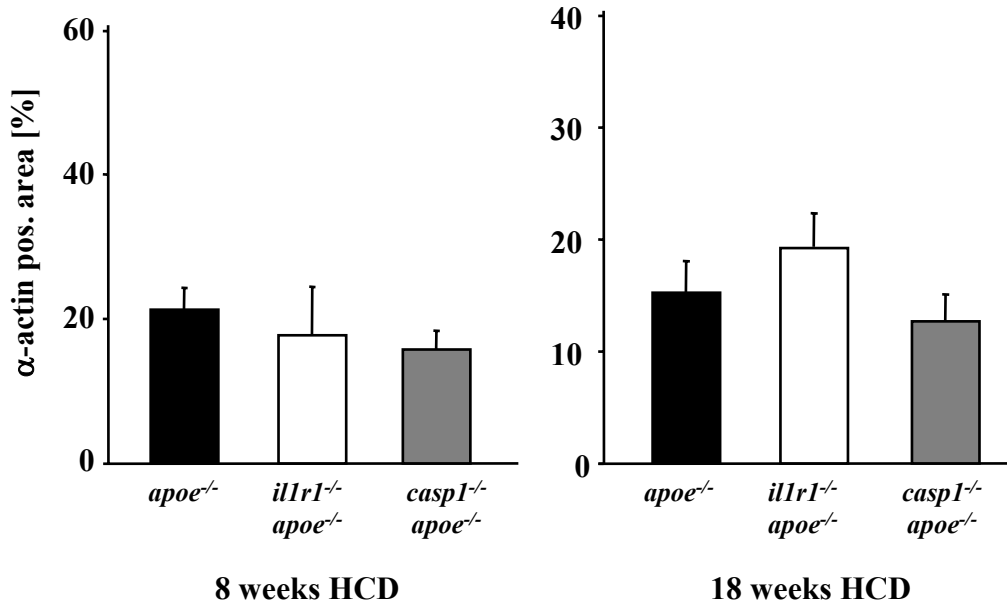


Figure 26: Deficiency in Caspase-1 or IL-1R1 do not alter smooth muscle cell content in atherosclerotic lesions of hyperlipidemic mice

Quantification of immunohistochemical staining for smooth muscle cells, using an α -actin-specific antibody, on longitudinal sections of representative aortic arches of male *apoe*^{-/-} (black), *il1rl*^{-/-}*apoe*^{-/-} (open), and *casp1*^{-/-}*apoe*^{-/-} (grey) mice fed an atherogenic diet for either 8 (left) or 18 weeks (right). The squares represent the mean \pm SEM.

Surprisingly, Caspase-1 deficiency did not affect atherogenesis, as demonstrated by comparable total wall area in the aortic arch of male and female *casp1*^{+/+}*apoe*^{-/-} and *casp1*^{-/-}*apoe*^{-/-} mice following 8 or 18 weeks of HCD (Figure 25). Moreover, Caspase-1 deficiency did not cause significant changes in lesion composition, e.g., SMC content (Figure 26), contrasting the findings in *il18*^{-/-}*apoe*^{-/-} and *il1rl*^{-/-}*apoe*^{-/-} mice described above. Similarly, Caspase-1 deficiency did not affect macrophage- or lipid content, suggesting differential atherogenic functions of the substrates IL-1 β and IL-18 versus the processing enzyme Caspase-1. As expected and previously observed, overall content of macrophages and lipids in atherosclerotic lesions did increase after prolonged (18 weeks) hyperlipidemia independent of the genotype (Figure 25, compare left and right panels). To verify the differential role of

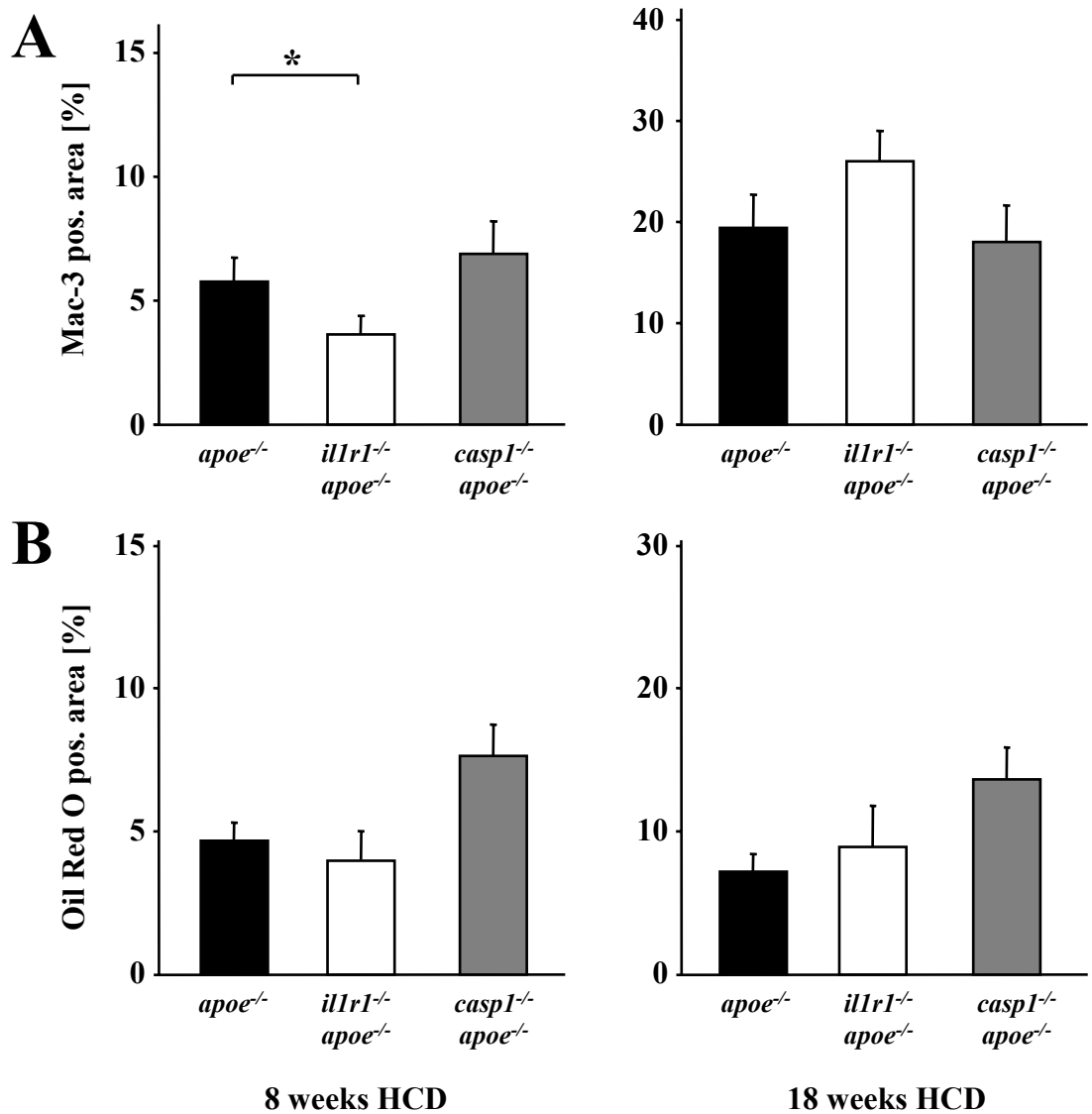


Figure 27: Deficiency in IL-1R1 but not in Caspase-1 reduces macrophage infiltration in atherosclerotic lesions of hyperlipidemic mice

Quantitative analysis of (A) immunohistochemical staining for macrophages, using a Mac-3-specific antibody, or (B) Oil Red O staining on longitudinal sections of representative aortic arches of male *apo*e^{-/-} (black), *il1rl*^{-/-}*apo*e^{-/-} (open), and *casp1*^{-/-}*apo*e^{-/-} mice (grey) fed an atherogenic diet for either 8 (left panels) or 18 weeks (right panels). The squares represent the mean \pm SEM. The asterisk indicates a p -value <0.05 .

the processing enzyme versus the substrate in a different vascular location, we analyzed lesion progression in the descending aorta. Again, although *il1rl^{-/-}apo^{e-/-}* mice featured reduced lesion development in the abdominal aorta similar to that observed in *il18^{-/-}apo^{e-/-}* mice (Figure 20), Oil Red O staining on *en face* preparation of aortae revealed that atherosclerosis of this vascular bed was unchanged in *casp1^{-/-}apo^{e-/-}* mice compared with the control group (Figure 28).

Analysis of plasma lipids and body weight revealed that the elevated total plasma cholesterol and triglyceride concentration previously observed in *il18^{-/-}apo^{e-/-}* mice extends further to *il1rl^{-/-}apo^{e-/-}* mice (Table 9). Interestingly, levels of plasma total cholesterol and triglycerides in *casp1^{-/-}apo^{e-/-}* mice markedly exceeded those in IL-1R1- and IL-18- deficient

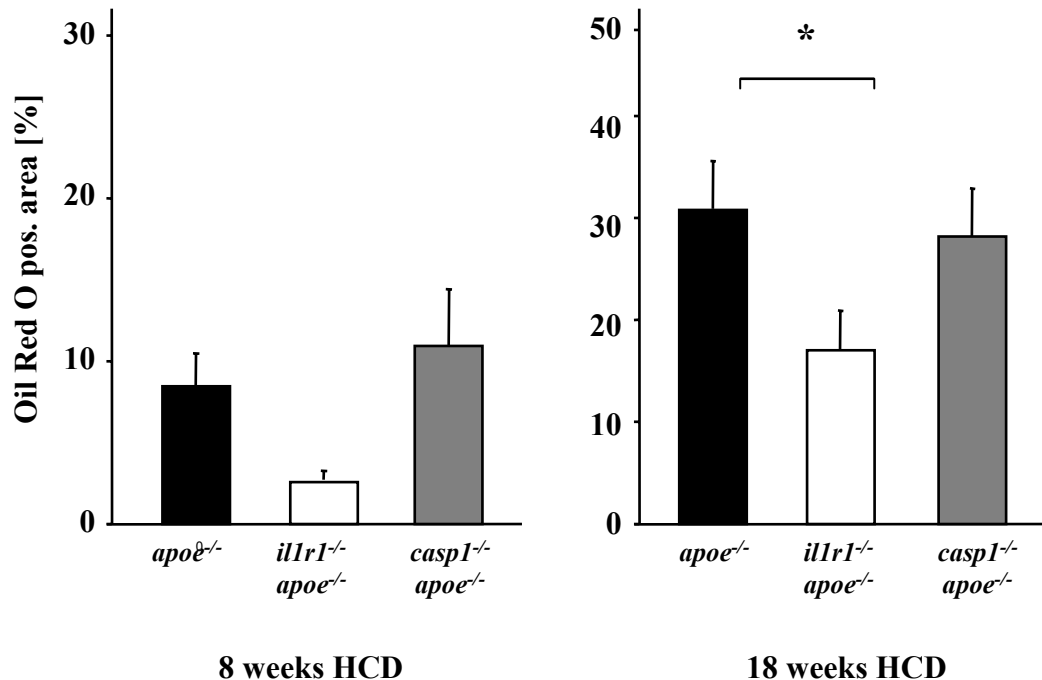


Figure 28: Caspase-1 deficiency does not reduce lesion development in the descending aorta.

Quantification of Oil Red O-stained *en face*-preparations of thoracic/abdominal aortae of male *apo e^{-/-}* (black), *il1rl^{-/-}apo e^{-/-}* (open), and *casp1^{-/-}apo e^{-/-}* mice (grey) fed an high-cholesterol diet for 8 (left) or 18 (right) weeks. The squares represent the mean \pm SEM. The asterisk indicates a *p*-value <0.05 .

animals, which were already elevated compared to controls. Male mice displayed significantly higher levels than those observed in female *apoε*^{-/-} mice following HCD for 8 and 18 weeks (Table 9). At the end of the study, body weight of *casp1*^{-/-}*apoε*^{-/-} mice was significantly higher than that of the controls (Table 9).

Table 9: Total plasma cholesterol, plasma triglyceride, and body weight at the end of the study in *il1rl1*^{-/-}*apoε*^{-/-} and *casp1*^{-/-}*apoε*^{-/-} mice vs. *apoε*^{-/-} mice

Duration of diet	8 weeks			18 weeks		
	Genotype	<i>apoε</i> ^{-/-}	<i>il1rl1</i> ^{-/-} <i>apoε</i> ^{-/-}	<i>casp1</i> ^{-/-} <i>apoε</i> ^{-/-}	<i>apoε</i> ^{-/-}	<i>il1rl1</i> ^{-/-} <i>apoε</i> ^{-/-}
Male						
Number of animals	N = 14	N = 14	N = 15	N = 14	N = 15	N = 14
Total cholesterol [mg/dL]	1350 ± 77	1488 ± 146	2267 ± 155*	340 ± 31	494 ± 52	1033 ± 129*
Triglycerides [mg/dL]	77.8 ± 15.2	143.8 ± 13.7*	108.8 ± 13.5*	133.8 ± 10.3	172.9 ± 19.4	311.7 ± 22.7*
Body weight [g]	26.2 ± 0.4	28.0 ± 0.5	29.0 ± 0.8*	30.7 ± 0.6	32.1 ± 1.1	37.2 ± 1.6*
Female						
Number of animals	N = 15	N = 15	N = 16	N = 15	N = 12	N = 16
Total cholesterol [mg/dL]	1265 ± 75	878 ± 129*	1267 ± 153	512 ± 28	682 ± 69	827 ± 40*
Triglycerides [mg/dL]	78.0 ± 13.5	93.0 ± 11.6	41.3 ± 3.5	101.6 ± 9.7	135.6 ± 27.9	124.3 ± 14.8
Body weight [g]	21.9 ± 0.4	23.0 ± 0.8*	26.8 ± 0.6*	23.6 ± 0.6	27.7 ± 0.6*	28.4 ± 0.7*

Concentrations were measured following ≥ 8 hours starvation; Values represent mean ± SEM;

* = p ≤ 0.05 vs. control

In sum, lack of an effect of Caspase-1 deficiency on atherosclerotic lesion development is sharply contrasted by the lesion reduction in *il1rl1*^{-/-}*apoε*^{-/-} mice and *il1rl1*^{-/-}*apoε*^{-/-} mice reported here and in IL-1β-deficient mice, as reported previously. This apparent paradox, displayed again in Figure 29, leads to the hypothesis that Caspase-1 does not represent the

exclusive IL-18- and IL-1 β -activating enzyme in inflammatory conditions such as atherosclerosis. Instead, these findings raise the feasibility of alternative mechanisms that may regulate the activity of these prominent pro-inflammatory cytokines.

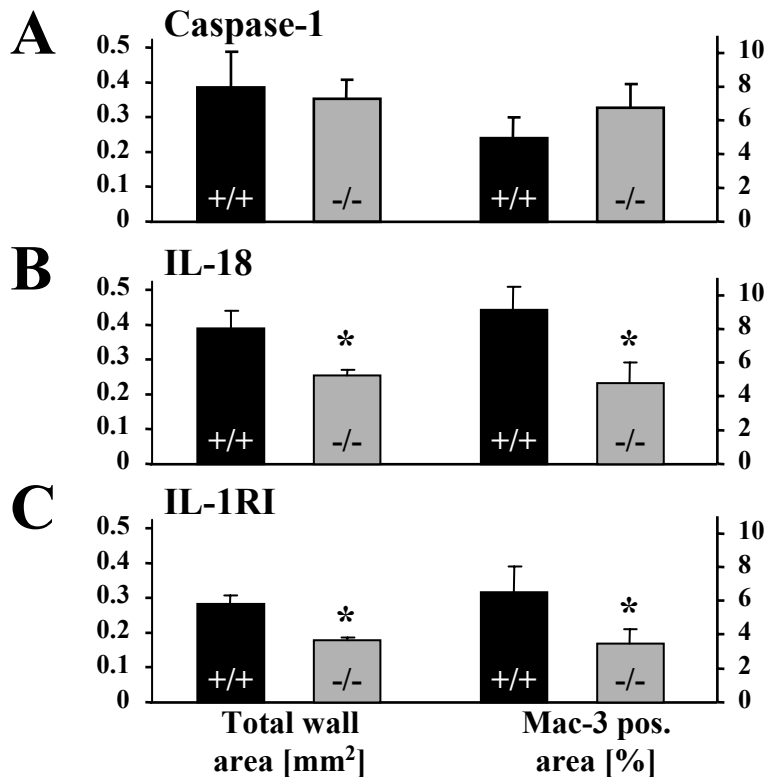


Figure 29: Deficiency in IL-18 but not in Caspase-1 diminishes atherosclerotic lesion formation in hyperlipidemic mice

Total wall area (*left*) and macrophage content (*right*) within the aortic arch of mice either deficient (grey bars) for Caspase-1 (*casp1*^{-/-}*apoe*^{-/-}, **A**), IL-18 (*il18*^{-/-}*apoe*^{-/-}, **B**), or IL-1 receptor type 1 (*il1rl*^{-/-}*apoe*^{-/-}, **C**) are shown in comparison to the respective control groups (*apoe*^{-/-}, black bars). 6-8 week old mice consumed a high cholesterol diet for an additional 8 weeks. Lesion size or macrophage content, as determined by positive immunohistochemical staining for the macrophage-specific marker Mac-3 was quantified on longitudinal sections of aortic arches employing computer-assisted analysis of. The bars represent the mean \pm SEM of $n \geq 8$. The asterisk indicates a p -value <0.05 .

3.5. Caspase-1 independent processing of proIL-18

3.5.1. MMPs process precursor IL-18

The lack of an effect of Caspase-1-deficiency on murine atherosclerosis compared to the potent reduction in IL-18-deficient mice creates an obvious paradox and challenges the accepted notion that IL-18 activation requires Caspase-1, thereby implicating alternative modes of IL-18 activation.

Seeking an explanation for these conflicting results, we hypothesized that MMPs might mediate a potential alternative, Caspase-1-independent mechanism of IL-18-activation. In fact, our group has previously reported that MMPs can produce active forms of IL-1 β ,¹⁷⁰ Furthermore, MMPs were reported to process the chemokine MCP-1, generating antagonists and thus inhibiting function of the native molecule.¹⁷¹ Notably, MMPs are highly expressed at sites of inflammation, including atherosclerotic lesions. Thus, the long-standing interest of our group in this class of enzymes and their role in atherogenesis led us to test the hypothesis that MMPs provide likely candidates for Caspase-1-independent IL-18 regulation.

To determine whether MMPs process the IL-18 precursor, an *in vitro* IL-18-processing assay was established employing recombinant MMPs and recombinant pro-IL-18. MMP-mediated processing of proIL-18 was examined by co-incubation of activated MMPs with proIL-18, followed by SDS-PAGE and Western blot analysis employing an IL-18-specific polyclonal antibody. The tested MMPs, namely gelatinases (MMP-2 and -9; Figure 30), collagenases (MMP-1, -8, and -13; Figure 31), stromelysins (MMP-3 and -10; Figure 32A+B), matrilysin (MMP-7; Figure 32C), and macrophage elastase (MMP-12; Figure 32D), concentration-dependently processed proIL-18 and yielded distinct processing products. Of note, processing efficacies varied among the different MMPs. Furthermore, some MMPs yielded multiple products, which appeared generated successively (e.g., MMP-8, MMP-13; Figure 31). As expected, processing progressed comparing 1 h and 24 h of co-incubation. Although some MMPs at high concentrations and after prolonged incubation (e.g., MMP-12, Figure 32 and MMP-13, Figure 31) resulted in complete degradation of IL-18, others yielded

more stable products upon co-incubation with proIL-18 (e.g., MMP-2 and -9, Figure 30 and MMP-8, Figure 31).

Interestingly, all MMPs yielded one product closely co-migrating on SDS-PAGE with the 18 kDa mature form cleaved by Caspase-1. A correlation of the characteristics of proIL-18 processing and the functional relationship among the MMPs (i.e., gelatinases vs. collagenases) was not recognizable. All tested MMPs also exhibited clear time-dependent processing of pro-IL-18. MMP-1, -2, -3, -7, -9, -10, -12 (data not shown) as well as MMP-8, and MMP-13 (Figure 33A) displayed processing products similar to those observed in their respective concentration-dependent assays. As expected, the non-activated MMP zymogens (no APMA treatment) yielded virtually no processing (Figure 33A, right lane).

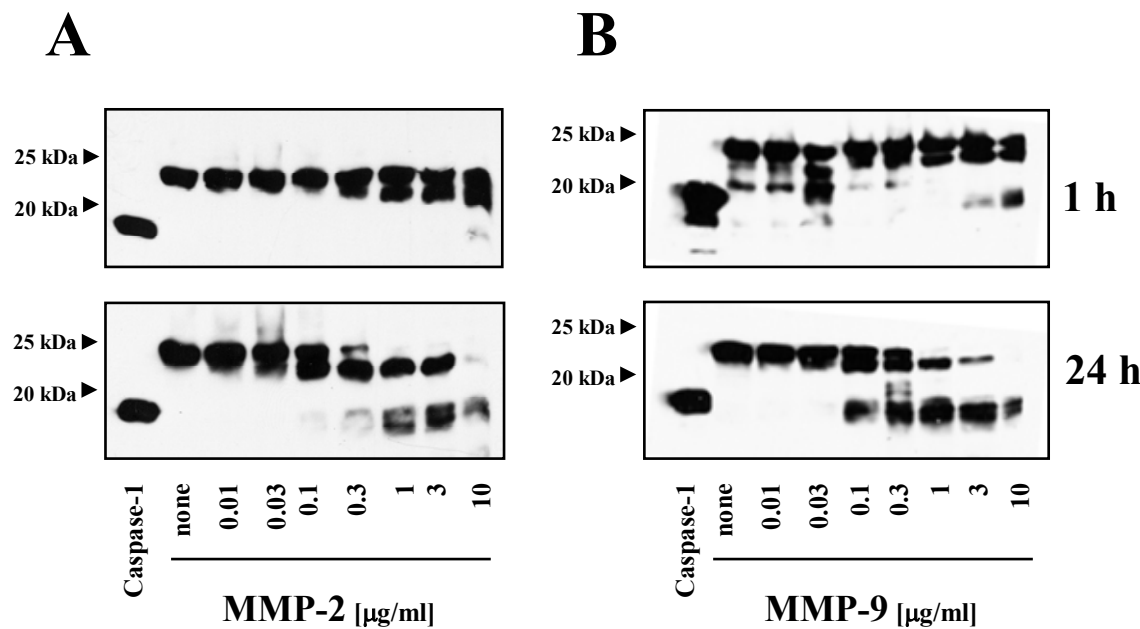


Figure 30: The Gelatinases MMP-2 and MMP-9 process pro-IL-18.

Increasing concentrations of (A) MMP-2 and (B) MMP-9 were incubated with pro-IL-18 (2.5 $\mu\text{g}/\text{ml}$) for 1 h and 24 h. Caspase-1 (0.5 $\mu\text{g}/\text{ml}$) was incubated with pro-IL-18 as a positive control. The equivalent of 100 ng of pro-IL-18 was analyzed by Western blotting employing a polyclonal anti-human IL-18 antibody. Arrows on the left indicate approximate molecular weight. Shown are representative blots from a minimum of three independent experiments.

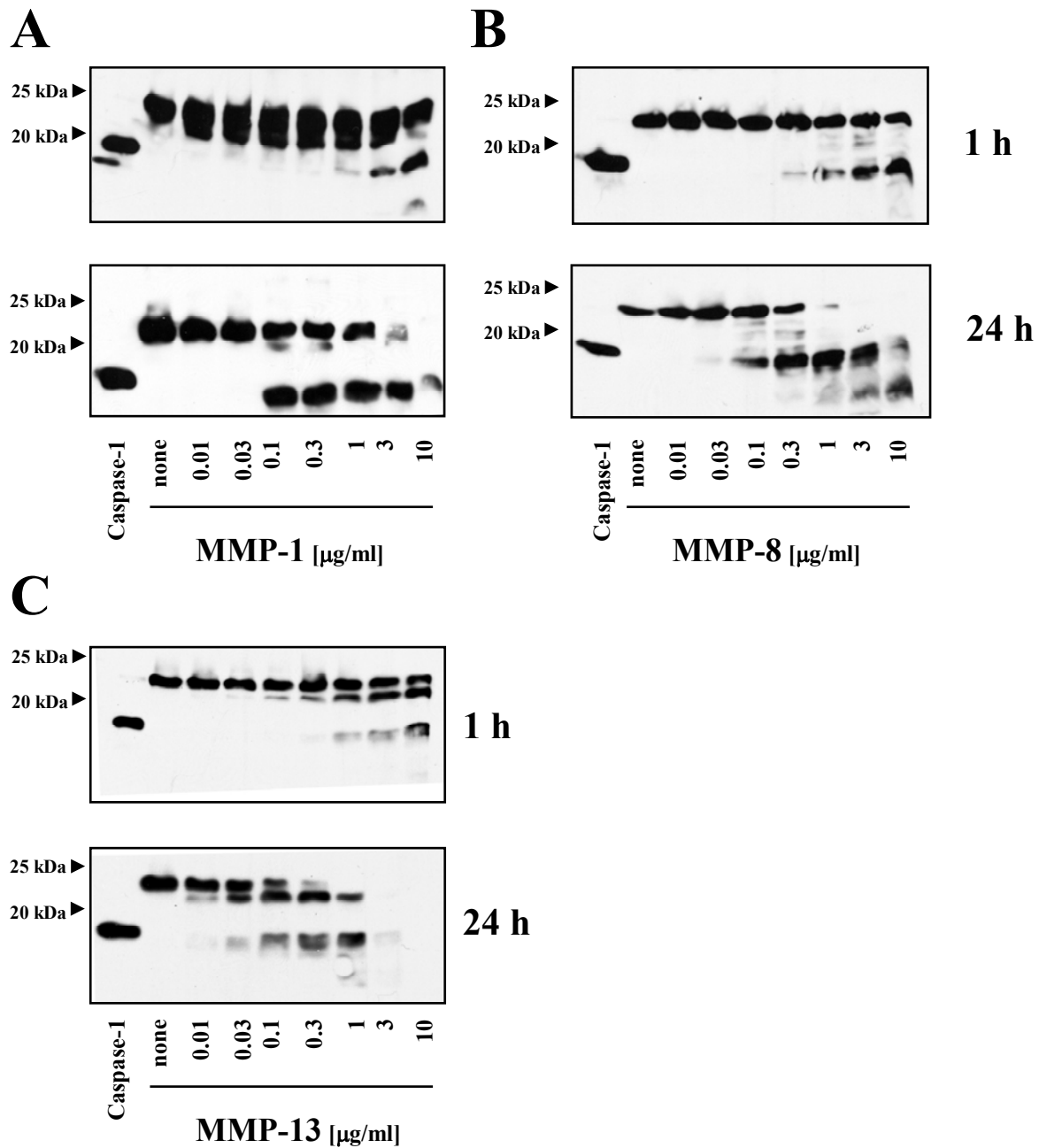


Figure 31: The Collagenases MMP-1, MMP-8, and MMP-13 process pro-IL-18.

Increasing concentrations of (A) MMP-1, (B) MMP-8, and (C) MMP-13 were incubated with pro-IL-18 (2.5 μg/ml) for 1 h and 24 h. Caspase-1 (0.5 μg/ml) was incubated with pro-IL-18 as a positive control. The equivalent of 100 ng of pro-IL-18 was analyzed by Western blot employing a polyclonal anti-human IL-18 antibody. Arrows on the left indicate approximate molecular weight. Shown are representative blots from a minimum of three independent experiments.

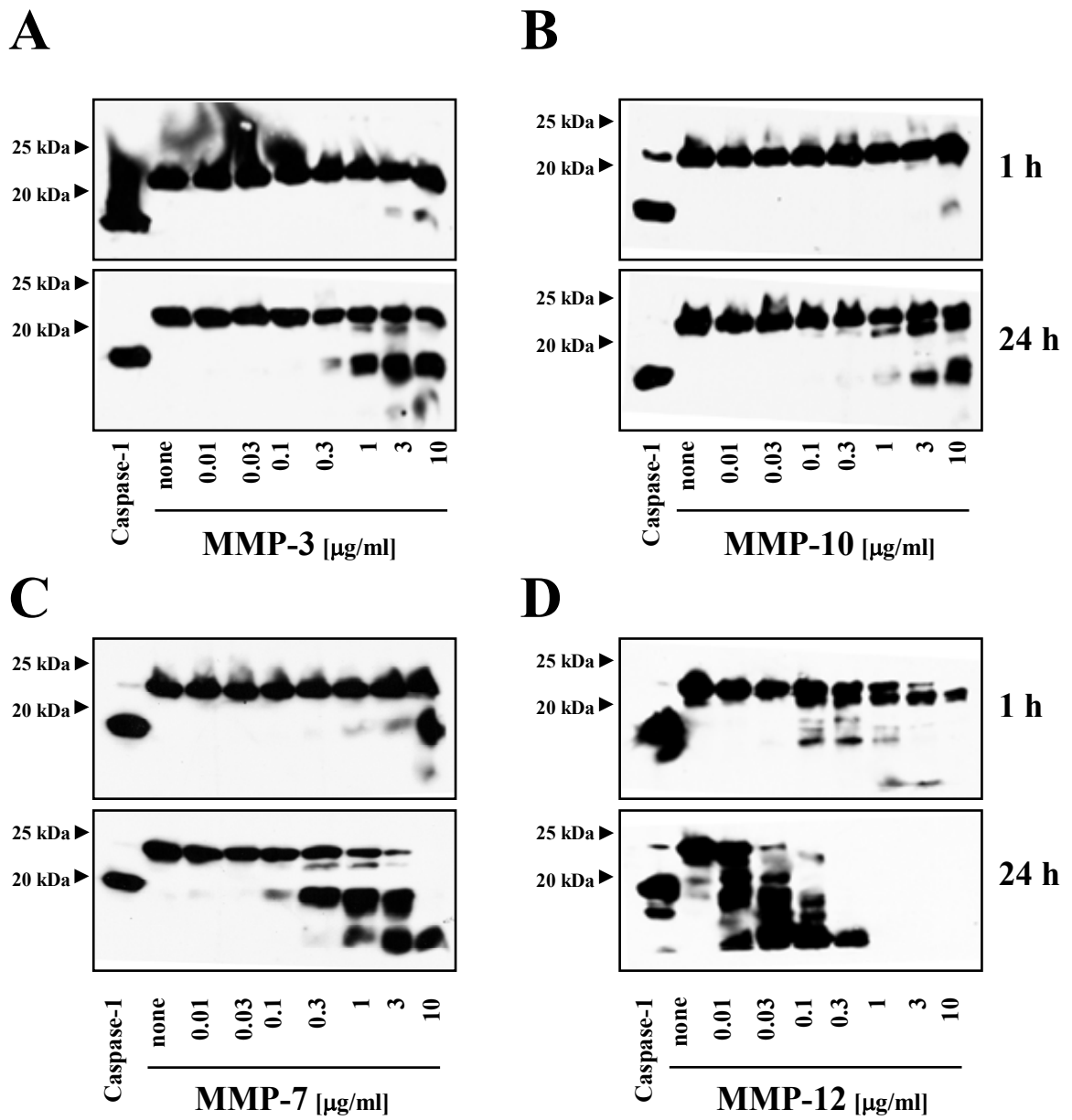


Figure 32: Stromelysins (MMP-3 and MMP-10), Matrilysin (MMP-7), and Macrophage Elastase (MMP-12) concentration-dependently process pro-IL-18.

Increasing concentrations of (A) MMP-3, (B) MMP-10, (C) MMP-7, and (D) MMP-12 were incubated with pro-IL-18 (2.5 µg/ml) for 1 h and 24 h. Caspase-1 (0.5 µg/ml) was incubated with pro-IL-18 as a positive control. The equivalent of 100 ng of pro-IL-18 was analyzed by Western blot employing a polyclonal anti-human IL-18 antibody. Arrows on the left indicate approximate molecular weight. Shown are representative blots from a minimum of three independent experiments.

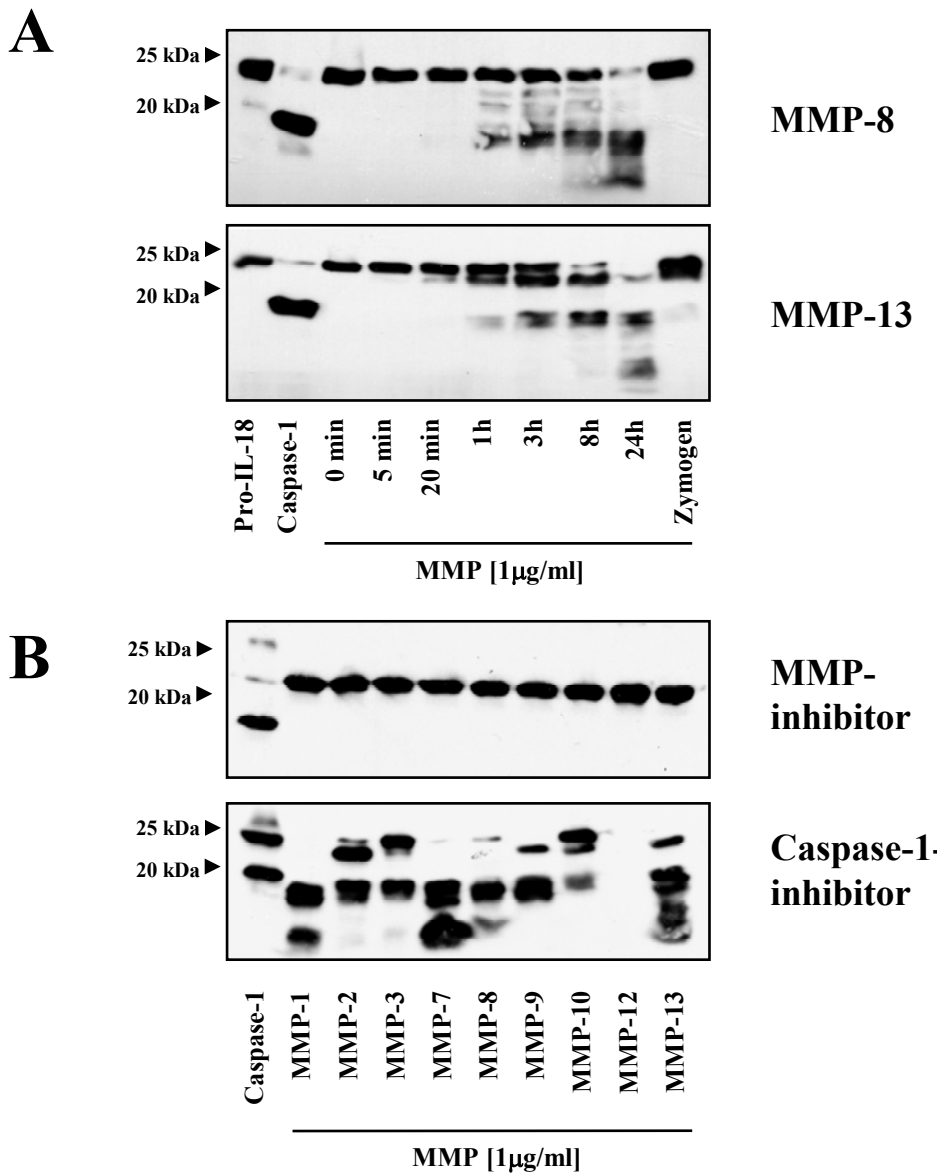


Figure 33: MMP-mediated processing of pro-IL-18 is time-dependent and abolished by MMP-inhibitor but not Caspase-1-inhibitor.

(A) MMP-8 and MMP-13 (both at 1 μ g/ml) or Caspase-1 (0.5 μ g/ml) were incubated with pro-IL-18 (2.5 μ g/ml) for a range of time points (0 min-24 h). The non-APMA-treated MMP zymogen was co-incubated with pro-IL-18 for 8 h in each assay. Pro-IL-18 was incubated alone for 1 h as a negative control. (B) MMPs (1 μ g/ml) or Caspase-1 (0.5 μ g/ml) were added to pro-IL-18 (2.5 μ g/ml) and incubated for 24 h in the presence of MMP-inhibitor (GM6001; *top panel*) or Caspase-1 inhibitor (Ac-YVAD-CHO); *bottom panel*. The equivalent of 100 ng of pro-IL-18 was analyzed by Western blotting. Arrows indicate approximate molecular weight. Shown are representative blots from at least three independent experiments.

To verify that the observed processing indeed resulted from the action of MMPs and not from potential contamination with other proteolytic enzymes, two separate control assays were performed, one in the presence of the generic MMP-inhibitor GM6001 and the other in the presence of the reversible Caspase-1-inhibitor Ac-YVAD-CHO (YVAD). In the presence of GM6001, no MMP-mediated processing of proIL-18 was observed (Figure 33B, top). However, Caspase-1 processed proIL-18 to its mature, 18 kDa form, demonstrating that Caspase-1-function is not impaired by GM6001 and, more importantly, that cleavage in the preceding assays was MMP-specific.

In contrast, in the presence of YVAD, MMPs did process proIL-18 in a manner consistent with previous experiments, whereas function of Caspase-1 was limited, supporting the specificity of the MMP-mediated processing (Figure 33B, bottom). Of note, Ac-YVAD-CHO is a reversible inhibitor, potentially explaining the incomplete inhibition of Caspase-1 function observed in these experiments (Figure 33B, bottom).

3.5.2. MMP-2 and MMP-8 cleave precursor IL-18 into biologically active forms

Although some of the MMP-processed products co-migrate with Caspase-1-cleaved mature IL-18, the processing experiments and subsequent Western blot analysis does not allow any conclusion regarding their biological activity. Thus, I established a bioactivity assay to test the functionality of the MMP-processed proIL-18 products, employing the monocytic cell line KG-1, which secretes IFN γ upon incubation with active IL-18.¹⁷² These cells were pre-stimulated with TNF α for 24 h to up-regulate expression of IL-18R, rendering them more responsive to IL-18.¹⁷²

ProIL-18 samples processed by MMPs for 1 h or 24 h were applied in parallel to the bioactivity assay, to test for potential functionality, and to Western blot analysis, to visualize the processed products (Figure 34). As shown earlier, MMPs yielded a ~18 kDa form of IL-18 following 1 h of processing. While proIL-18 processed by Caspase-1 induced high levels of IFN γ in KG-1 cells, only proIL-18 cleaved by MMP-2, -8, and -12 exhibited elevated levels of bioactivity. After 24 h of processing, a greater amount of precursor was processed to a ~18 kDa form, and some MMP-mediated degradation was observed. Interestingly, the bioactivities of MMP-2- and MMP-8-processed proIL-18 were comparable to those of

Caspase-1-processed pro-IL-18. However, all other MMPs failed to generate bio-active products. Interestingly, proIL-18 processed by MMP-12 exhibited a loss of bioactivity, an observation consistent with the complete degradation of IL-18 by the enzyme after 24 h, as demonstrated in the Western blot analysis.

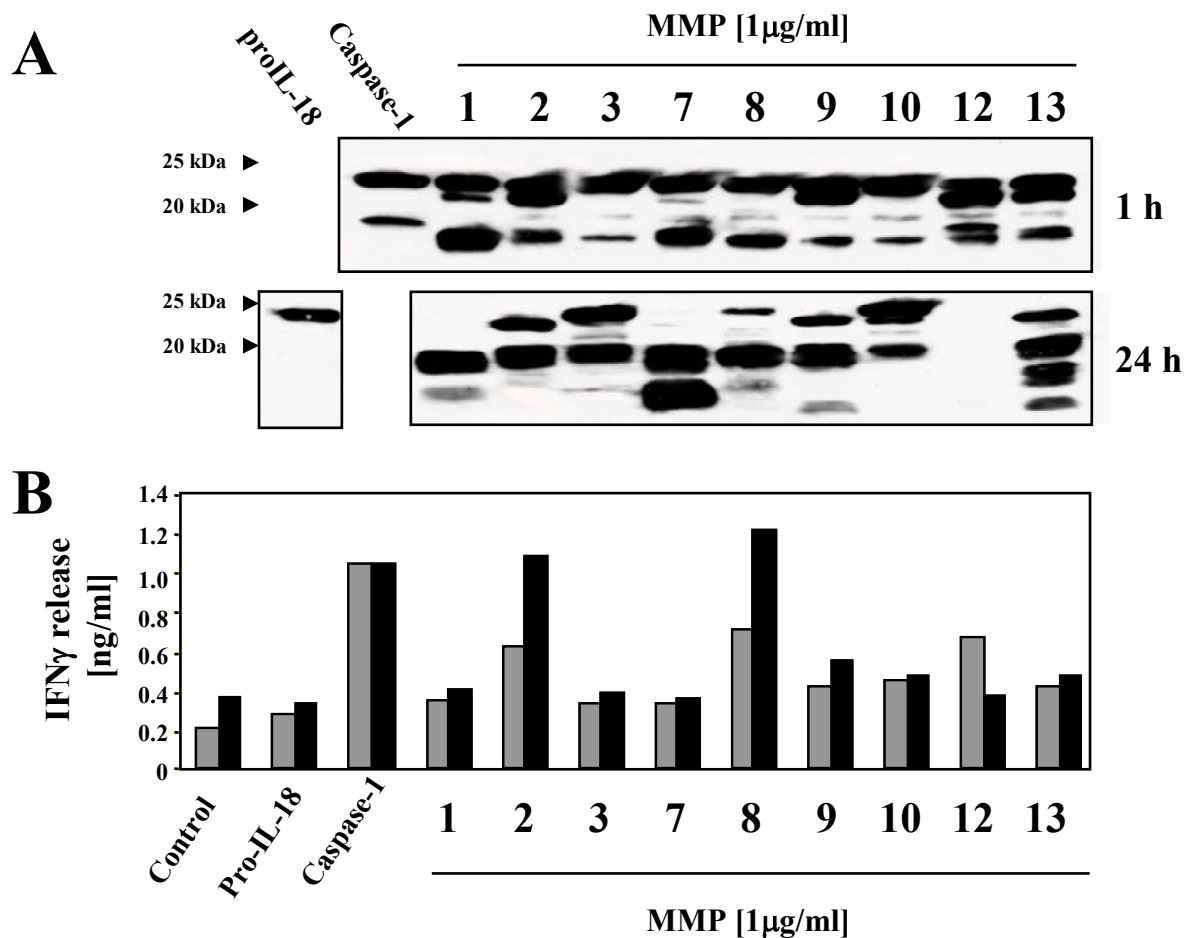


Figure 34: Pro-IL-18 processed by MMP-2 and MMP-8 displays biological activity.

Pro-IL-18 (2.5 μ g/ml) and MMPs (1 μ g/ml) were incubated for 1 h and 24 h. Pro-IL-18 incubated with Caspase-1 (0.5 μ g/ml; 1 h) or alone (24 h) as positive and negative controls, respectively. Reaction mixtures were added, in equal parts, to (A) Western blot analysis for IL-18 or to (B) KG-1 cell suspensions (500,000 cells/ml). Following 24 h of co-incubation, supernatants were removed and assayed for IFN γ by ELISA. The amount of IFN γ correlates with the IL-18 activity contained in the mixtures obtained from 1 h (gray bars) and 24 h (black bars) processing. Samples were assayed in duplicates on ELISA and the mean result of each reading is reported. Shown are representative data from three independent experiments. Blots are aligned with the corresponding bioactivity data. Approximate molecular weight markers are indicated on the left.

3.5.3. Sequence analysis of active IL-18 fragments and MMP-cleavage site identification

To further characterize the MMP-processed IL-18 products that demonstrate biological activity and test whether these products differ from Caspase-1-processed IL-18, additional experiments aimed to determine the exact cleavage site of MMP-2 and MMP-8 on the IL-18 precursor. Aliquots of the MMP-2/proIL-18 and MMP-8/proIL-18 processing mixtures were separated by SDS-PAGE on separate lanes of the gel and subjected to either Coomassie Brilliant Blue staining, Silver staining, or Western blot analysis (Figure 35). Blots were aligned with the aid of molecular weight markers, allowing for identification of bands of

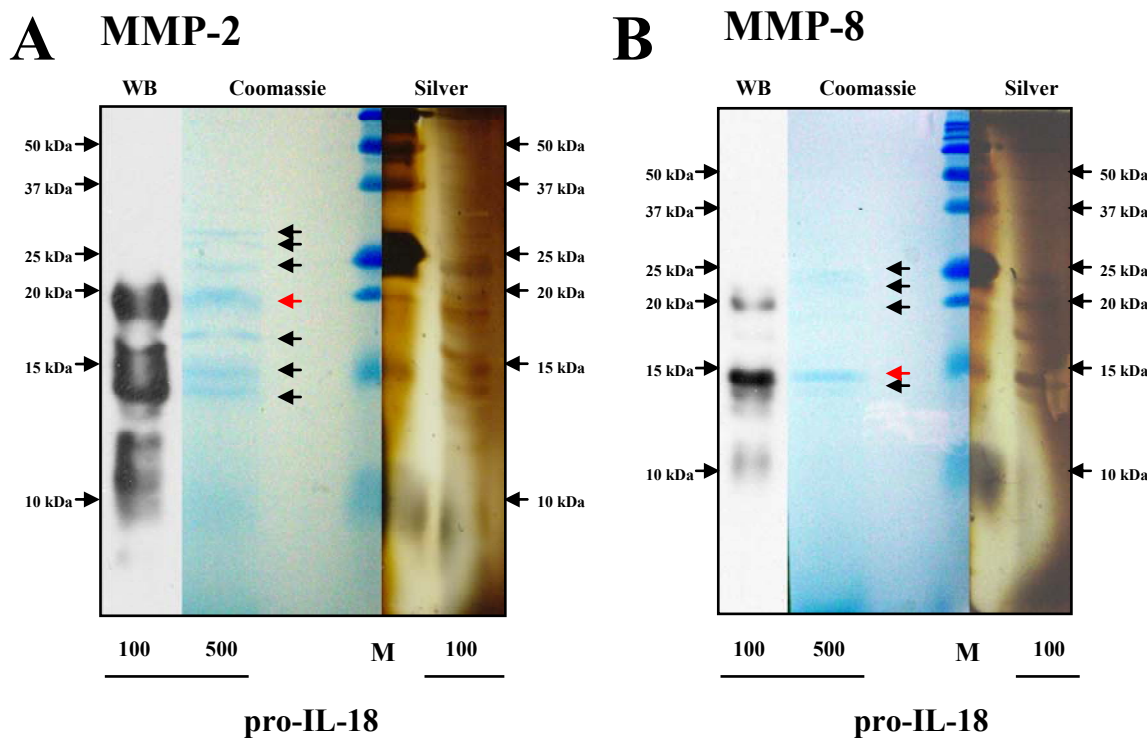


Figure 35: SDS-PAGE of MMP-2 and MMP-8-cleaved pro-IL-18 fragments for sequence analysis

Pro-IL-18 co-incubated for 24 h with either MMP-2 (**A**) or MMP-8 (**B**) was separated by SDS-PAGE and subsequently applied to Western blot analysis employing a polyclonal anti-human IL-18 antibody (WB; 100 ng pro-IL-18). Additional lanes of the same gel were visualized by either Silver staining (Silver; 100 ng pro-IL-18) or Coomassie Brilliant Blue staining (Coomassie; 500 ng pro-IL-18). Arrows indicate approximate molecular weight. Red arrows indicate bands applied to further sequence analysis. M indicates molecular weight marker.

interest, which were subsequently excised from the Coomassie blue-stained gel. The protein bands were subjected to trypsin digestion, eluted from the gel, and reduced and alkylated. Finally, the samples were applied to LC-MS/MS analysis. Peptide analysis identified an N-terminal cleavage site for MMP-2 as Tyr²⁴-Phe²⁵, 12 amino acids N-terminal of the prototypical Caspase-1 cleavage site of proIL-18 (Table 10). Processing at this MMP-2 cleavage site yielded an IL-18 fragment with a calculated molecular weight of approximately 19.8 kDa, correlating to the ~19-20 kDa predominant band of the MMP-2/proIL-18 reaction mixture observed on the Coomassie gel and the Western blots (Figure 35A). Insufficient sequence coverage hampered determination of the MMP-8 cleavage site on proIL-18 through a similar peptide analysis. Instead, reverse sequence search calculating hypothetical molecular weights for particular peptide fragments and searching the MS database for matching molecular weights was performed to detail the cleavage site. By determining the presence and relative abundance of these fragments in the mass spectra, we identified two putative cleavage sites for MMP-8 at Asp⁵⁹-Gln⁶⁰ and Gly⁶¹-Arg⁶², which would yield 15.8 and 15.6 kDa IL-18 fragments, respectively (Table 10), again correlating with the most abundant fragment on the gel (Figure 35B).

3.5.4. Atheromatous lesions of Caspase-1-deficient mice contain mature IL-18 and IL-1 β

To determine the *in vivo* relevance of alternative Caspase-1-independent mechanisms of IL-18 and IL-1 β activation, we compared the expression of different forms of these two pro-inflammatory cytokines in the atherosclerotic tissue of mice either competent or deficient for Caspase-1.

Interestingly, both *apoe*^{-/-} as well as *casp1*^{-/-}*apoe*^{-/-} mice readily expressed mature IL-1 β (~17 kDa) in atherosclerotic aortae following 8 and 18 weeks of high-cholesterol diet (HCD). Furthermore, the amount of processed IL-1 β appeared greater in *casp1*^{-/-}*apoe*^{-/-} mice than in *apoe*^{-/-} mice after 18 weeks of HCD. Expression of the precursor (~33 kDa) and intermediate forms (~28 kDa) of IL-1 β remained comparable (Figure 36, middle panels). These findings indicate that alternative IL-18 processing pathways may accelerate inflammatory conditions more potently than Caspase-1.

Table 10: Mass ions identified in MMP-processed proIL-18

MMP-2

1 MAAEPVEDNC INFVAMKFID NTLY FIAEDD ENLESDYFGK LESKLSVIRN				
51 LNDQVLFIDQ GNRPLFEDMT DSDCRDNAPR TIFIISMYKD SQPRGMAVTI				
101 SVKCEKISTL SCENKIISFK EMNPPDNIKD TKSDIIFQQR SVPGHDNKMQ				
151 FESSSYEGYF LACEKERDLF KLILKKEDEL GDRSSIMFTVQ NED				
Observed	Mr(expt)	Mr(calc)	Delta	Sequence
946.36	1890.71	1890.82	-0.10	²⁵ FIAEDDENLESDYFGK ⁴⁰
928.46	1854.91	1854.96	-0.05	⁵⁰ NLNDQVLFIDQGNRPL ⁶⁵
1043.41	3127.21	3127.40	-0.18	⁵⁰ NLNDQVLFIDQGNRPLFEDMTDSDCR ⁷⁵ Oxidation (M)
921.12	3680.44	3680.66	-0.22	⁵⁰ NLNDQVLFIDQGNRPLFEDMTDSDCRNAPR ⁸⁰ Oxidation (M)
566.29	1130.56	1130.60	-0.04	⁸¹ TIFIISMYK ⁸⁹ Oxidation (M)
572.29	1713.86	1713.88	-0.01	⁸¹ TIFIISMYKDSQPR ⁹⁴ Oxidation (M)
461.25	920.48	920.50	-0.02	⁹⁵ GMAVTISVK ¹⁰³ Oxidation (M)
526.25	1050.49	1050.50	-0.01	¹⁰⁷ ISTLSCENK ¹¹⁵
701.30	1400.58	1400.66	-0.08	¹²¹ EMNPPDNIKDTK ¹³²
514.25	1026.48	1026.53	-0.05	¹²⁴ PPDNIKDTK ¹³²
513.26	1024.51	1024.53	-0.03	¹³³ SDIIFFFQR ¹⁴⁰
1046.39	2090.77	2090.86	-0.09	¹⁴⁹ MQFESSSYEGYFLACEK ¹⁶⁵ Oxidation (M)

MMP-8

1 MAAEPVEDNC INFVAMKFID NTLY FIAEDD ENLESDYFGK LESKLSVIRN				
51 LNDQVLFIDQ GNRPLFEDMT DSDCRDNAPR TIFIISMYKD SQPRGMAVTI				
101 SVKCEKISTL SCENKIISFK EMNPPDNIKD TKSDIIFQQR SVPGHDNKMQ				
151 FESSSYEGYF LACEKERDLF KLILKKEDEL GDRSSIMFTVQ NED				
Observed	Mr(expt)	Mr(calc)	Delta	Sequence
566.33	1130.64	1130.60	0.04	⁸¹ TIFIISMYK ⁸⁹ Oxidation (M)
461.28	920.54	920.50	0.04	⁹⁵ GMAVTISVK ¹⁰³ Oxidation (M)
Manual search:				
878.4438	1756.688	1755.743	0.94	⁶² NRPLFEDMTDSDCR ⁷⁵ Oxidation (M)
970.9923	1941.984	1940.823	1.16	⁶⁰ QGNRPLFEDMTDSDCR ⁷⁵ Oxidation (M)

Ions matching with the sequence of proIL-18 are shown in bold.

Peptides derived from manual search are underlined.

Observed = experimental m/z (mass/charge) value

Mr(expt) = experimental m/z value transformed to a relative molecular mass

Mr(calc) = Calculated relative molecular mass of the matched peptide

Delta = Difference between experimental and calculated mass

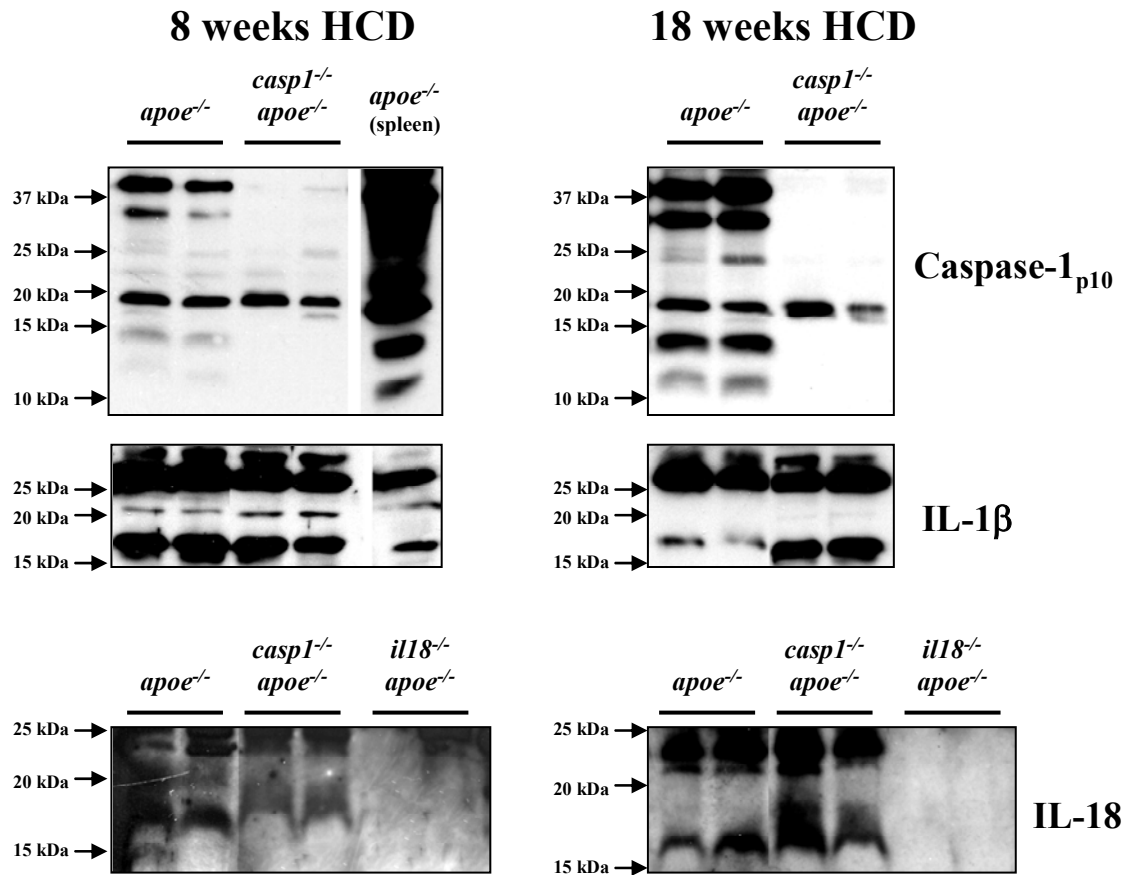


Figure 36: Atherosclerotic lesions from Caspase-1-deficient mice contain cleaved forms of IL-18 and IL-1 β .

Protein extracts from aorta of *apoe*^{-/-}, *casp1*^{-/-}*apoe*^{-/-}, and *il18*^{-/-}*apoe*^{-/-} mice fed an high-cholesterol diet (HCD) for 8 (left) or 18 weeks (right) were subjected to SDS-PAGE and subsequent Western blot analysis for Caspase-1 (top), IL-1 β (middle), or IL-18 (bottom). The spleen of an *apoe*^{-/-} mouse suffering from an acute skin infection served as a positive control for caspase-1 and IL-1 β . Approximate molecular weights are indicated by the arrows on the left.

A processed form of IL-18 was detected in aortas of *apoe*^{-/-} mice as well as in *casp1*^{-/-}*apoe*^{-/-} mice following 8 and 18 weeks of HCD in the absence of Caspase-1 expression (Figure 36, bottom panels). Similar to IL-1 β , the amount of processed IL-18 in *casp1*^{-/-}*apoe*^{-/-} mice appeared equal to if not greater than that in *apoe*^{-/-} mice, despite similar levels of proIL-18 expression. Notably, the molecular weight of the processed IL-18 in *casp1*^{-/-}*apoe*^{-/-}

mice appeared marginally greater than in *apoe*^{-/-} mice, further supporting the presence of a Caspase-1-independent IL-18 processing mechanism similar to the one described above for by MMPs.

As expected, *il18*^{-/-}*apoe*^{-/-} mice did not express any forms of IL-18 within their aortae, thereby strengthening the validity of the above data. Additional Western blot analysis employing an antibody for Caspase-1 verified that expression of this protease is indeed absent in *casp1*^{-/-}*apoe*^{-/-} mice. Following 8 and 18 weeks of HCD, *apoe*^{-/-} mice expressed amounts of Caspase-1 within their aortic walls (Figure 36, top panels). The band migrating at ~20 kDa appears unspecific, since it is also observed in protein extract in *casp1*^{-/-}*apoe*^{-/-} mice. Other bands include the 45 kDa precursor, the 10 kDa p10-subunit, and the 30 kDa p10/p20-heterodimer.

In sum, these data demonstrating immunoreactive species of IL-18 and IL-1 β in atherosclerotic tissue of mice lacking functional Caspase-1 provide evidence for the presence of processing mechanisms independent of the classical activating enzyme. In agreement with previous reports, these findings further highlight the potential relevance of the MMP-mediated activation of these cytokines under pro-inflammatory conditions *in vivo*.

4. Discussion

Recent research points to a prominent role of immunity and inflammation in the pathogenesis of atherosclerosis and increasing data support the hypothesis that the network of cytokines orchestrate many of the complex processes underlying this prevalent human disease.^{16,17,32,68} During my diploma thesis I demonstrated expression and *in vitro* pro-inflammatory function of the cytokine IL-18,^{111,112} giving rise to a steady growing field of IL-18 biology in cardiovascular disease. Although the elevated expression of IL-18 and its receptor in atherosclerotic tissue *in situ* in combination with the pro-inflammatory function on atheroma-associated cells *in vitro* suggests a prominent atherogenic role of this molecule, direct evidence for the crucial involvement of IL-18 and factors associated with the IL-18 pathway in atherogenesis *in vivo* remained elusive. This doctoral thesis thus aimed to evaluate the *in vivo* contribution of IL-18- and IL-1-signaling as well as Caspase-1 to experimental atherosclerosis in murine models of atherosclerosis and hence to explore their potential value as targets for therapeutic intervention.

IFN γ expression in smooth muscle cells

This thesis started in direct continuation of my diploma thesis extending the findings of IL-18's pro-atherogenic functions and identifying non-lymphatic cells, namely macrophages and, surprisingly, SMC as potent producers of IFN γ expression mediated by IL-18.

Several studies implicated IFN γ in various pro-atherogenic processes, including loss of fibrillar collagen and modulation of inflammatory processes, demonstrating its aggravating role in atherogenesis *in vivo*.^{65,67,173-175} However, the proximal inducers remained elusive.

Notably, IFN γ expression by T-cells and NK cells, comprising a minimal fraction of lesional cells, was identified as the traditional function of IL-18.⁷³⁻⁷⁵ However, expression and function of IFN γ showed only limited localization with these cells. Therefore, this thesis examined whether other atheroma-associated cell types, such as macrophages, but also non-hematopoietic cells, namely EC and SMC, can produce this pro-atherogenic mediator.

Indeed, freshly isolated monocytes, but not differentiated macrophages secreted IFN γ upon stimulation with IL-18. This finding addresses the previously raised controversy around expression of IFN γ in monocytes and macrophages,^{116,176,177} adding this cell type to the list of IFN γ producers in atherosclerotic lesions.

Interestingly, SMC also expressed IFN γ when stimulated with IL-18 and even more potently in synergism with IL-12, representing a finding previously not reported and not anticipated due to the non-hematopoietic origin of these cells. The lack of appropriate antibodies hampered experiments aimed to verify the presence of the protein and to localize it with SMC *in situ*. Immunohistochemical analysis of IFN γ expression *in situ* is known to be problematic and a report published around the time of my findings has called into question the specificity of various (13 different) anti-IFN γ antibodies.¹⁷⁸ However, the detection of IFN γ mRNA in SMC-enriched areas of human atheroma *in situ* supports the validity of this observation. Further highlighting the IFN γ production from sources other than T-cells, Tenger *et al.* showed that injection of recombinant IL-18 did evoke atherosclerotic lesion development and raised plasma levels of IFN γ even in the absence of lymphocytes.¹⁷⁹ These findings imply that IL-18 promotes its functions, including the induction of IFN γ , at least in part by other cell types associated with atherosclerosis, namely macrophages or SMC.

The secretion of IFN γ by SMC might have broad implications considering the abundance of this cell type in the vasculature compared to immune cells, such as T-lymphocytes.¹⁶ Notably, this mechanism may constitute part of a feedback loop modulating the proliferation of SMC in the vessel wall, as IFN γ is a potent anti-mitogenic mediator,¹⁷³ thus limiting plaque growth and inflammatory conditions.

The present observation also contributes to our understanding of the predominant T_H1 response during atherogenesis.^{16,17,60} IFN γ enhances the expression of both IL-18 receptor chains in combination with IL-1 β or TNF α , two prominent pro-inflammatory cytokines also found in plaques.¹¹² The elicitation of IL-18R α/β by IFN γ in an inflammatory setting combined with the induction of IFN γ expression via IL-18 signaling in T-cell and macrophages, but also SMC, suggests a positive feedback loop in the vasculature, which might contribute to the dysregulated inflammatory response characterizing atheroma.

In sum, my previous *in vitro* studies and the continuation thereof detailed in this thesis strongly implicated the IL-18 ligand/receptor dyad in atherogenesis and add considerably to the burgeoning evidence of a locally self-sustaining immune and inflammatory response within the atheromatous plaque. Nonetheless, the contribution of IL-18 and related mediators to atherosclerotic lesion development *in vivo* remained undefined, demanding direct evaluation. In light of the pro-atherogenic functions, detailed in this thesis and my previous diploma thesis, it remains to be elucidated whether a potential pro-atherogenic role of IL-18 *in vivo* is mediated via its classical downstream effector IFN γ or independently thereof.

The role of IL-18 in experimental atherosclerosis

Following successful generation of *il18^{-/-}apo $e^{-/-}$* mice, comparison of atherosclerotic lesion development in the aortic arch to that of *il18^{+/+}apo $e^{-/-}$* mice definitively demonstrated a role for IL-18 in early atherogenesis. Of note, IL-18 appears not to affect later stages of lesion development following prolonged hypercholesterolemia. These data also provide new insight into the mechanisms by which IL-18 contributes to early atherogenesis and suggest that IL-18 acts, at least in part, independently of IFN γ .

Supporting this hypothesis, the expression of IFN γ and MHC II antigens (highly regulated by IFN γ) was similar in *il18^{+/+}apo $e^{-/-}$* and *il18^{-/-}apo $e^{-/-}$* mice despite significantly diminished lesion size. The fact that levels of IFN γ remained high despite diminished numbers of macrophages and unaltered T-cell content in *il18^{-/-}apo $e^{-/-}$* mice attributed *in vivo* relevance to our observation of IFN γ expression by vascular SMC *in vitro* and in human atherosclerotic plaques *in situ*.¹¹² Alternative triggers for IFN γ induction obviously compensate for the lack of IL-18. Of note, oxidized LDL potently induces the expression of IFN γ in T-cells.¹⁸⁰ Moreover, oxidized LDL also induces IL-12, an established co-factor of IFN γ expression, in leukocytes.¹⁸¹ Hence, elevated lipid levels in the circulation might compensate, directly and/or via induction of IL-12, the lack of IL-18 as the IFN γ -inducing factor. In accord, we found elevated levels of lipid deposition in *il18^{-/-}apo $e^{-/-}$* compared to *il18^{+/+}apo $e^{-/-}$* mice.

The fact that IL-18 deficiency led to significantly reduced atherogenesis despite unaffected IFN γ expression renders IFN γ -independent functions of IL-18 prominent in atherosclerosis. Among potential direct pro-atherogenic functions this study identified induction of the adhesion molecule VCAM-1, expression of which is diminished in mice lacking IL-18. Considering the crucial role of adhesion molecules in the initial stage of lesion development, these data are in agreement with IL-18's accelerating effect in early rather than late atherogenesis. In addition, the modulation of this and other adhesion molecules has been confirmed by us and others as a prominent function of IL-18 *in vitro*.^{112,182-184} Another potential avenue of IL-18 function contributing to early stages of atherosclerosis is thought to be the enhanced attraction of leukocytes to developing atherosclerotic lesions by chemokines. Indeed, enhanced production of these pro-atherogenic mediators has been attributed to IL-18.^{78,112,118} More importantly, IL-18 itself was recently identified as a potent chemoattractant,^{112,185,186} strongly supporting the hypothesis developed in this work.

Remarkably, IL-18 deficiency did result in elevated plasma lipid concentration, yet reduced atherosclerosis. Thus, the pro-atherogenic function of IL-18 in this study might actually be underestimated. Interestingly, enhanced inflammation has been reported as responsible for a variety of changes in lipid metabolism.¹⁸⁷ Since this trend was also observed in mice lacking Caspase-1 and IL-1R1, it might be speculated that it is caused by a systemic, probably hepatic, alteration of lipid metabolism rather than local changes in the lesions. These findings support a developing understanding that not only dyslipidemia propagates inflammation, but also *vice versa* inflammatory mechanisms mediate profound changes in lipid metabolism.¹⁸⁷ Although, this interesting observation deserves further attention, the complexity of both, the immune system and lipid metabolism, would easily expand an investigation of the underlying mechanisms far beyond the scope of this thesis.

Indeed, the elevated plasma lipid levels likely explain the observed unchanged lipid deposition in the vessel wall despite diminished macrophage content. Considering that macrophage infiltration and lipid content of atheromatous lesions commonly correlate in experimental studies in mice or clinical pathological samples,^{152,153,188,189} the overwhelming circulating lipid levels likely account for enhanced lipid deposition in the vessel wall.

In accord with the findings of this thesis, a recent report demonstrated that intraperitoneal treatment of *apoε*^{-/-} mice with exogenous recombinant IL-18 enhanced

lesional lipid- and diminished collagen content.¹⁹⁰ Furthermore, electrotransfer of an expression plasmid encoding IL-18 binding protein (IL-18BP), an endogenous inhibitor of IL-18, diminished lipid deposition in the vessel wall.¹⁹¹ Noteworthy, mice in these studies did not display altered plasma lipid levels, suggesting that complete absence of IL-18 by targeted gene disruption, as used in our model, affects systemic lipid metabolism, whereas transient inhibition or overexpression does not.

Further supporting the hypothesis of IFN γ -independent atherogenic functions of IL-18, is the finding that reduction in lesion formation did not depend on gender. A study by Whitman *et al.* showed that IFN γ deficiency i) decreased atherosclerosis in male but not female in *apoE*^{-/-} mice and ii) did not alter total plasma cholesterol.⁷² Our data obtained with IL-18 deficient mice differ in both points. First, no gender specific influence of IL-18 deficiency on the extent of atherosclerotic lesions formation was observed. Furthermore, total plasma cholesterol and triglyceride concentrations did differ between *il18*^{+/+} *apoE*^{-/-} and *il18*^{-/-} *apoE*^{-/-} mice, as outlined above. Thus, the present findings detailing comparable reduction in atherosclerotic lesion formation in male and female mice disagree with the observation by Whitman *et al.* and, thus, support the hypothesis that IL-18 promotes atherosclerosis independent of IFN γ .

Several studies in mice have now corroborated the pro-atherogenic role of IL-18 *in vivo*. Enhanced atherosclerosis was observed in hypercholesterolemic mice receiving recombinant IL-18.¹⁹⁰ Furthermore, in a separate study overexpression of the endogenous inhibitor IL-18BP, limited plaque development in *apoE*^{-/-} mice, including a decrease in the numbers of macrophages and T-cells, apoptotic cells, lipid content, and an increase in smooth muscle cell and collagen content, suggesting a more stable plaque.¹⁹¹ Besides corroborating the findings of our current study Elhage *et al.* observed in *il18*^{-/-} *apoE*^{-/-} mice a shift from a T_H1-predominant immune response to one that features a T_H2, thus, rather atheroprotective profile.¹⁹² Of note, the involvement of IL-18 in this basic immunologic mechanism is supported by previous reports,^{78,131} although was not yet applied to atherosclerosis.

The present thesis also provides evidence that IL-18 not only affects lesion size but also composition, which is critical for plaque stability and, thus, propensity to cause clinical complications. In fact, the enhanced SMC- and diminished macrophage content in mice lacking IL-18 indicating stabilized lesions is corroborated by a recent report displaying

decreased collagen content and enhanced proteolytic activity following overexpression of IL-18 in a model of mechanically induced atherosclerosis.¹⁹³

In conclusion, this thesis identifies IL-18 as a crucial mediator of early but probably not advanced atherogenesis, supporting a proximal role in the cytokine cascade underlying this disease.^{194,195} Furthermore, it furnishes evidence that IL-18 promotes chronic inflammatory diseases, such as atherosclerosis, at least in part via IFN γ -independent pathways. Future studies investigating IL-18 as a potential therapeutic target of inflammatory diseases should therefore take into account the present observation that abrogation of IL-18 signaling delays but does not prevent experimental atherosclerosis.

Atherosclerosis in IL-18R deficient mice

The present finding that selective absence of IL-18R α on either hematopoietic or vascular cells does not affect atherogenesis, although in agreement with the data obtained in mice globally deficient for IL-18R α , was unexpected. The paradoxical outcome for these studies testing the lack of the ligand and receptor, respectively, exposes the intriguing possibility that IL-18 mediates its pro-atherogenic function via a pathway independent of IL-18R α .

It is unlikely, that IL-18 directly interacts with IL-18R β subunit, since this receptor chain is not implicated in ligand binding but is rather considered to facilitate the downstream signaling upon formation of the IL-18R α /IL-18 β /IL-18 complex.⁷⁸

The IL-1 family consist of 10 known ligands as well as 10 closely related receptors.^{196,197} However, only a minority of these, including IL-1 and IL-18, as well as their respective receptors, have been described in more detail. Amid some orphan ligands and receptors among these mediators the existence of additional, yet unidentified family members has been proposed.^{196,197} Thus, it may be speculated that IL-18 mediates its atherogenic function, at least in part, through alternative, potentially yet undiscovered members of this receptor family. Indeed, signaling independent of the classical receptor has been previously suggested for the related IL-1 β in a model of traumatic injury-induced neuronal cell death and ischemic brain injury.^{198,199} In view of the growing redundancy of the IL-1 family of receptors and ligands, it was proposed that alternative IL-1 signaling mechanisms are

relevant in these pathophysiologic conditions.²⁰⁰ However, so far no alternative receptor for IL-1 or IL-18 has been identified. Considering the similarities between the IL-1 and IL-18 receptors and ligands,¹⁹⁷ the existence of alternative pathways for IL-18 action appears entirely reasonable.²⁰⁰ Interestingly, two new members of the IL-1 family were recently identified and shown to bind to IL-18R α albeit without classical IL-18-related functions, highlighting the potential for crossreactivity in this receptor/ligand system.^{201,202} Moreover, a recent report showed that absence of IL-18R α does not affect progression of an experimental model of lupus erythematosus, although IL-18 itself has been implicated in the disease.^{203,204}

In sum, the studies investigating atherogenesis in *il18r1^{-/-}apoe^{-/-}* mice yielded the novel insight that IL-18R α might not be required for IL-18 function in atherosclerosis. In accordance, IL-18 signaling independent of the classical IL-18R pathway, may provide an explanation for the divergent results observed in the two *in vivo* studies employing IL-18 or IL-18R α -deficient mice. Thus, the present work has opened a new field of research critical with respect to potential therapeutic intervention and future studies should elucidate the growing field of the IL-1/IL-18 system, including potential crosstalk between members of the IL-1 and IL-18 signaling pathways.¹⁹⁷

Atherosclerosis in IL-1R- and Caspase-1 deficient mice

In contrast to the differential findings discussed above for deficiency in IL-18 and IL18R α , respectively, lack of either IL-1 β or IL-1R1 displayed a similar effect on atherogenesis. Lesion development in mice deficient for IL-1R1 was markedly limited, in agreement with a study by Kirii *et al.*, demonstrating reduced atherogenesis in mice lacking the ligand IL-1 β .¹⁶⁹

Notably, IL-1R1 deficiency led to reduction of lesion development and macrophage infiltration following 8 but not 18 weeks of HCD, reflecting the results observed with *il18^{-/-}apoe^{-/-}* mice. However, in contrast to IL-18 deficiency lack of IL-1R1 did not lead to an increase of SMC content in the lesions. This observation might result from a differential effect of IL-1 and IL-18 signaling on expression of IFN γ , a crucial negative modulator of SMC proliferation.

Following the implication of IL-18 and IL-1 signaling in atherogenesis and the reduced severity of disease in the respective deficient mice, the failure of Caspase-1 deficiency to reduce lesion progression was indeed surprising. Since the experimental study and blinded analysis of *il1rl^{-/-}apoel^{-/-}* (yielding a difference in atherogenesis) and *casp1^{-/-}apoel^{-/-}* mice was performed at the same time, methodological pitfalls accounting for these unexpected results can be excluded. This apparently paradoxical observation that IL-18 (and probably IL-1 β) contributes more to development of atherosclerosis than the proposed processing enzyme Caspase-1, fostered the search for a mechanistic explanation.

Caspase-1-independent activation of proIL-18

The growing implication of IL-18 and IL-1 β in chronic inflammatory disorders has fostered much interest in Caspase-1, the enzyme reported to mediate the proteolytic activation of these two pro-inflammatory cytokines. Seeking a mechanistic explanation for the apparently paradoxical results in mice lacking IL-18 on one hand and Caspase-1 on the other, this thesis identified MMPs as potent alternative activators of IL-18 *in vitro*, and provides *in vivo* evidence for the presence of Caspase-1-independent IL-18 cleavage mechanisms.

Until this present work, alternative IL-18 activation mechanisms remained poorly characterized and only the serine protease proteinase-3 (PR-3) had been identified as a potential Caspase-1-independent activator of IL-18.²⁰⁵ However, expression of PR-3 was restricted to oral epithelium and no reports of PR-3 in atheromatous tissue limit the implication of this alternative IL-18 activating pathway in atherogenesis.

Fantuzzi et al. recently demonstrated that wild-type and Caspase-1-deficient mice show a similar response to turpentine-induced tissue damage, which leads to IL-1 β -dependent increase of serum IL-6 and symptoms, such as fever, anorexia, and weight loss.²⁰⁶ However, IL-1 β -deficient mice display none of these inflammatory reactions, suggesting that turpentine-induced local inflammation produces a biologically active form of IL-1 β even in the absence of Caspase-1. Corroborating the findings of my work, this and other studies have established the generation of immunoreactive mature IL-1 β in Caspase-1-deficient mice or by Caspase-1-independent mechanisms.^{206,207} Moreover, our group previously reported that

MMPs can produce active forms of IL-1 β ,¹⁷⁰ thereby expanding the generally accepted role of MMPs in the pathogenesis of atherosclerosis.

While MMPs prominently localize and act extracellularly, IL-1 β and IL-18 are typically processed and activated intracellularly prior to their secretion,⁹³ potentially raising concern regarding the relevance of the proposed mechanism. However, the precursors of IL-18 and IL-1 β can be secreted in certain circumstances, such as Caspase-1 inhibition, which might occur under both physiological and pathological situations.^{97,110} Furthermore, intracellular proteins can be released from the cytosol or organelles upon apoptosis or necrotic cell death,²⁰⁸ both events frequently observed in atheroma.^{18,38} Thus, processing of proIL-18 by MMPs, which generally localize to the extracellular matrix,⁵⁴ represents a plausible mechanism for IL-18 activation in atherosclerosis and other chronic inflammatory diseases.

While assessing the physiological relevance of the proposed cytokine activation mechanism, two key elements must be addressed: the specific activity of the resulting processed cytokine and the local concentrations of both enzyme and substrate at sites of inflammation. Pro-IL-18 processed by MMP-2 and MMP-8 exhibited biological activity comparable to that of the Caspase-1-processed, mature form of IL-18, proving that these MMP-processed products can induce IL-18-specific function in the absence of Caspase-1. As discussed above, IL-18 is constitutively expressed and can be secreted as a precursor.^{110,209} MMPs are highly expressed and active within chronic inflammatory diseases, including atherosclerosis.^{51,53,210} Although not determined in atherosclerotic tissue, their concentrations can locally reach up to 350 $\mu\text{g}/\text{ml}$ (e.g., in synovial fluid of patients suffering from rheumatoid arthritis),²¹¹⁻²¹⁶ rendering the MMP concentrations employed in the proIL-18 processing assay (0.5 - 10 $\mu\text{g}/\text{ml}$) well within physiological range. Thus, the well-documented expression of the substrate proIL-18 and the enzyme in atherosclerotic tissue adds to the likelihood of this alternative proIL-18 processing pathway indeed figuring in atherogenesis.

Originally characterized as exclusively matrix-degrading enzymes, MMPs have been implicated in the processes of vascular remodeling and atherosclerotic plaque destabilization.⁵⁴ However, the present finding that MMPs potently process and activate IL-18, along with their previously established role in IL-1 β activation,¹⁷⁰ add further complexity

to the already intricate role of MMPs in atherosclerosis and other inflammatory diseases, such as rheumatoid arthritis, osteoarthritis, and tumor metastasis.^{48,217-219}

In atherosclerosis, MMPs mediate collagenolysis within the plaque, one of two distinct mechanisms responsible for collagen loss along with IFN γ -mediated inhibition of collagen production by SMC.²²⁰ Considering the present findings, however, activation of IL-18 by MMPs might augment the expression of IFN γ , a prominent function of IL-18. IFN γ , in turn, directly inhibits SMC proliferation and collagen synthesis. Thus, MMPs may contribute to plaque destabilization not only through direct breakdown of collagen but also by indirectly promoting IFN γ production and subsequent inhibition of collagen synthesis.

Moreover, the proteolytic functions of MMPs may extend beyond ECM catabolism and pro-inflammatory cytokine activation to the degradation and hence, inactivation of various inflammatory mediators. In addition to the previously reported degradation of IL-1 β by MMP-3,¹⁷⁰ McQuibban *et al.* recently demonstrated that several MMPs degrade prominent chemokines, such as MCP-1, -2, -3, and -4, yielding functionally inactive products.¹⁷¹ Of note, the present study indicates similar MMP-mediated degradation of IL-18, as observed upon extended co-incubation of MMPs (e.g., MMP-12 and MMP-13) with proIL-18. Of note, processing by MMP-12 yielded diminished bioactivity coinciding with complete degradation of the IL-18 protein in Western blot analysis. Such potential anti-inflammatory actions of MMPs might hold physiological relevance by providing a feedback system to limit the otherwise deleterious pro-inflammatory and matrix-deteriorating effects of MMPs within the atherosclerotic plaque.

While MMPs are generally characterized as an entire family or by their subgroups, accruing data prompt analysis of individual MMP functions. In the present study, only two of the nine tested MMPs produced biologically active forms of IL-18 despite apparent proIL18 processing and formation of ~18 kDa products by all tested MMPs. Interestingly, the two activating MMPs are members of two separate classes. MMP-2 is a gelatinase (gelatinase B), while MMP-8 is a member of the collagenase family (neutrophil collagenase). Our preliminary findings suggest that these MMPs activate proIL-18 through cleavage at unique sites, different from the traditional Caspase-1 cleavage site (Figure 37). Furthermore, it illustrates that IL-18 activation is not limited to one particular family of MMPs. In fact, MMPs from the same class yield proIL-18 products that either contain or lack biological

activity. Therefore, it might be instructive not only to identify the cleavage sites of biologically active IL-18 fragments, but also of inactive processing products. Besides providing information about the sequence specificity of individual MMPs, this approach could lend further explanation as to why fragments of similar molecular weight exhibit markedly differing activities. Nonetheless, the determination of the cleavage sites of MMP-2 and MMP-8 still requires verification. In fact, during preparation of the samples for mass-spectrometric analysis, the protein is subjected to a tryptic digestion. To ensure, that MMPs do not utilize a cleavage site identical to that of trypsin, future experiments will employ an alternative proteolytic enzyme, such as chymotrypsin, which features a distinct sequence preference.

The putative cleavage sites identified for MMP-2 and MMP-8 would result in IL-18 species of distinct molecular weight. While MMP-2 cleaves N-terminal of the traditional Caspase-1 cleavage site, the suggested cleavage sites of MMP-8 are more than 20 amino acids towards the C-terminus relative to it. Accordingly, the proteolytic processing by MMP-2 results in a fragment, which is larger than the Caspase-1-cleaved mature IL-18. In contrast, MMP-8 processing yields a fragment of smaller molecular weight, in agreement with the ~ 15 kDa band observed. Of note, the MMP-8 cleavage sites localizes to an exposed loop region on the exterior surface of the protein (Figure 37B), thus rendering proteolytic cleavage more feasible.

The broad implication of IL-18 and IL-1 β in a variety of human inflammatory diseases has promoted extensive research to uncover and characterize novel pharmacological and endogenous inhibitors of Caspase-1, the prototypical activator of these pro-inflammatory cytokines.²²¹ In fact, newly developed Caspase-1 inhibitors are currently under clinical investigation for use as anti-inflammatory drugs in the treatment of rheumatoid arthritis.⁹⁹ Moreover, such treatment has been discussed for its potential benefit in other chronic inflammatory diseases, including atherosclerosis. However, the results of this thesis challenge the proposed effectiveness of Caspase-1-inhibitors in the treatment of atherosclerosis. The present data suggest that targeted inhibition of either IL-1 β or IL-18 through novel therapeutic agents might provide more effective and/or more selective suppression of inflammation than the envisioned interruption of both IL-1 β and IL-18 pathways through inhibition of their traditional upstream activator.

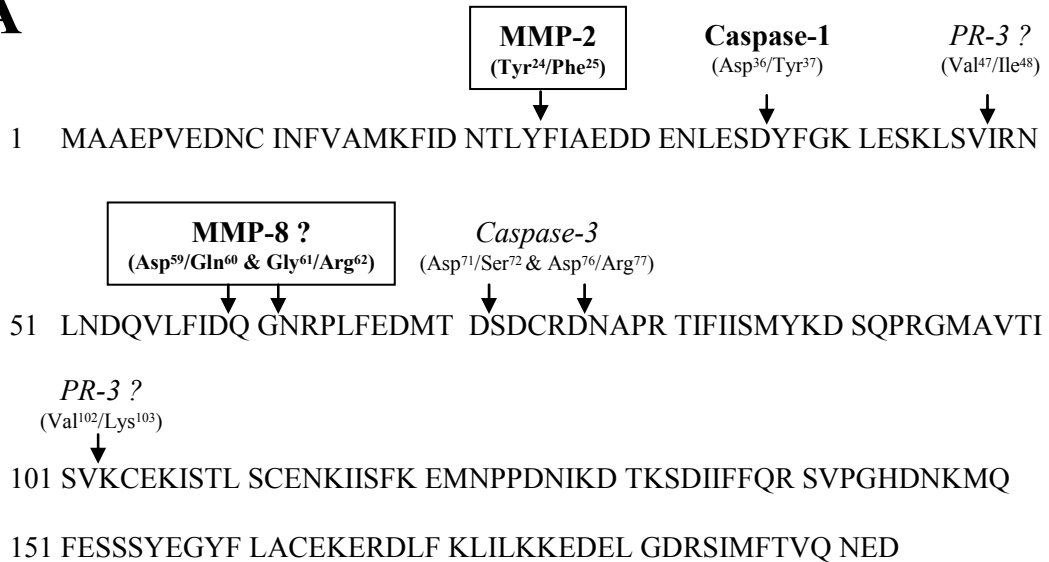
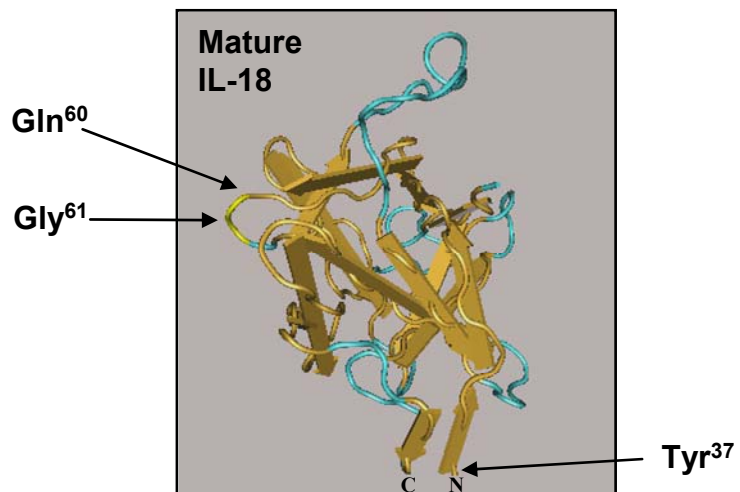
A**B**

Figure 37: Identification of putative MMP-2 and MMP-8 cleavage sites within the pro-IL-18 sequence

(A) Putative cleavage sites of MMP-2 and MMP-8, as identified by mass-spectrometric analysis. In addition, previously described cleavage sites for Caspase-1, Caspase-3, and Proteinase-3 are shown (B) The region of the putative MMP-8 cleavage site is indicated on a illustration of the three-dimensional structure of human mature IL-18. Of note, the putative MMP-2 cleavage site is not displayed, since it is 12 amino acids N-terminal of the Caspase-1 cleavage site, which yield Tyr³⁷ on the N-terminus. Structural data for proIL-18 are not available.

Furthermore, while aiming to ameliorate the pro-atherogenic function of IL-18, the unchanged severity of atherosclerosis in *il18r1^{-/-}apoe^{-/-}* mice strongly suggests to focus efforts towards inhibition of the ligand rather than the receptor IL-18R α . Accordingly, additional research should aim to unravel the underlying signaling of IL-18 in murine and human atherosclerosis, potentially leading to identification of alternative receptors. Hence, the findings of this thesis should stimulate new research to uncover alternative, Caspase-1-independent mechanisms for the activation of IL-18 and IL-1 β and incite renewed interest in the biology of MMPs in the context of atherosclerosis and other inflammatory diseases, beyond the classical scope of matrix degradation and vascular remodeling.

Overall, the previously simple world of Caspase-1 and its substrates, presumed to consist of one enzyme, two substrates, and their respective receptors, has turned out more complex than anticipated. Thus, this thesis, although it answered several imminent questions, proposes new avenues of IL-18 and its related biology asking researchers to dissect IL-18's signaling mechanisms in atherosclerosis and to detail molecular characterization of MMP-mediated cytokine activation.

5. References

1. Murray CJ, and Lopez AD. Global mortality, disability, and the contribution of risk factors: Global Burden of Disease Study. *Lancet* 1997;349:1436-42.
2. Lopez AD, and Murray CC. The global burden of disease, 1990-2020. *Nat Med* 1998;4:1241-3.
3. American Heart Association. Heart Disease and Stroke Statistics-2005 Update. Dallas; American Heart Association; 2005.
4. Petersen S, Peto V, Rayner M, Leal J, Luengo-Fernandez R, and Gray A. European cardiovascular disease statistics, 2005 edition. London; British Heart Foundation; 2005.
5. Levenson JW, Skerrett PJ, and Gaziano JM. Reducing the global burden of cardiovascular disease: the role of risk factors. *Prev Cardiol* 2002;5:188-99.
6. Pearson TA. Coronary arteriography in the study of the epidemiology of coronary artery disease. *Epidemiol Rev* 1984;6:140-66.
7. Ambrose JA, Tannenbaum MA, Alexopoulos D, Hjemdal-Monsen CE, Leavy J, Weiss M, Borrico S, Gorlin R, and Fuster V. Angiographic progression of coronary artery disease and the development of myocardial infarction. *Journal of the American College of Cardiology* 1988;12:56-62.
8. Little WC, Constantinescu M, Applegate RJ, Kutcher MA, Burrows MT, Kahl FR, and Santamore WP. Can coronary angiography predict the site of a subsequent myocardial infarction in patients with mild-to-moderate coronary artery disease? *Circulation* 1988;78:1157-66.
9. Giroud D, Li JM, Urban P, Meier B, and Rutishauser W. Relation of the site of acute myocardial infarction to the most severe coronary arterial stenosis at prior angiography. *American Journal of Cardiology* 1992;69:729-32.
10. Fuster V, Stein B, Ambrose JA, Badimon L, Badimon JJ, and Chesebro JH. Atherosclerotic plaque rupture and thrombosis. Evolving concepts. *Circulation* 1990.
11. Ambrose JA. Plaque disruption and the acute coronary syndromes of unstable angina and myocardial infarction: if the substrate is similar, why is the clinical presentation different? *Journal of the American College of Cardiology* 1992;19:1653-8.
12. Jonasson L, Holm J, Skalli O, Bondjers G, and Hansson GK. Regional accumulations of T cells, macrophages, and smooth muscle cells in the human atherosclerotic plaque. *Arteriosclerosis* 1986;6:131-8.
13. Libby P, Sukhova G, Lee RT, and Liao JK. Molecular biology of atherosclerosis. *Int J Cardiol* 1997;62 Suppl 2:S23-9.
14. Ross R. Atherosclerosis--an inflammatory disease. *N Engl J Med* 1999;340:115-26.
15. Glass CK, and Witztum JL. Atherosclerosis: The road ahead. *Cell* 2001;104:503-16.
16. Libby P. Inflammation in atherosclerosis. *Nature* 2002;420:868-74.
17. Hansson GK. Inflammation, atherosclerosis, and coronary artery disease. *N Engl J Med* 2005;352:1685-95.
18. Lee RT, and Libby P. The unstable atheroma. *Arterioscler Thromb Vasc Biol* 1997;17:1859-67.

19. Shah PK. Pathophysiology of coronary thrombosis: role of plaque rupture and plaque erosion. *Prog Cardiovasc Dis* 2002;44:357-68.
20. Taubman MB, Fallon JT, Schechter AD, Giesen P, Mendlowitz M, Fyfe BS, Marmor JD, and Nemerson Y. Tissue factor in the pathogenesis of atherosclerosis. *Thromb Haemost* 1997;78:200-4.
21. Stary HC, Chandler AB, Glagov S, Guyton JR, Insull W, Jr., Rosenfeld ME, Schaffer SA, Schwartz CJ, Wagner WD, and Wissler RW. A definition of initial, fatty streak, and intermediate lesions of atherosclerosis. A report from the Committee on Vascular Lesions of the Council on Arteriosclerosis, American Heart Association. *Circulation* 1994;89:2462-78.
22. Stary HC. Evolution and progression of atherosclerotic lesions in coronary arteries of children and young adults. *Arteriosclerosis* 1989;9:I-19 - I-32.
23. Fernandez-Brito JE, Wong R, Contreras D, Nordet P, and Sternby NH. Pathomorphometrical characteristics of atherosclerosis in youth. A multinational investigation of WHO/World Heart Federation (1986-1996), using atherometric system. *Nutr Metab Cardiovasc Dis* 1999;9:210-9.
24. Strong JP, Malcom GT, McMahan CA, Tracy RE, Newman WP, 3rd, Herderick EE, and Cornhill JF. Prevalence and extent of atherosclerosis in adolescents and young adults: implications for prevention from the Pathobiological Determinants of Atherosclerosis in Youth Study. *Jama* 1999;281:727-35.
25. Miyake Y, Tajima S, Yamamura T, and Yamamoto A. Homozygous familial hypercholesterolemia mutant with a defect in internalization of low density lipoprotein. *Proc Natl Acad Sci U S A* 1981;78:5151-5.
26. Thompson GR, Soutar AK, Spengel FA, Jadhav A, Gavigan SJ, and Myant NB. Defects of receptor-mediated low density lipoprotein catabolism in homozygous familial hypercholesterolemia and hypothyroidism in vivo. *Proc Natl Acad Sci U S A* 1981;78:2591-5.
27. Libby P, Aikawa M, and Schonbeck U. Cholesterol and atherosclerosis. *Biochim Biophys Acta* 2000;1529:299-309.
28. Skalen K, Gustafsson M, Rydberg EK, Hulten LM, Wiklund O, Innerarity TL, and Boren J. Subendothelial retention of atherogenic lipoproteins in early atherosclerosis. *Nature* 2002;417:750-4.
29. Leitinger N. Oxidized phospholipids as modulators of inflammation in atherosclerosis. *Curr Opin Lipidol* 2003;14:421-30.
30. Gimbrone MA, Jr., Topper JN, Nagel T, Anderson KR, and Garcia-Cardena G. Endothelial dysfunction, hemodynamic forces, and atherogenesis. *Ann N Y Acad Sci* 2000;902:230-9; discussion 39-40.
31. Topper JN, and Gimbrone MA, Jr. Blood flow and vascular gene expression: fluid shear stress as a modulator of endothelial phenotype. *Mol Med Today* 1999;5:40-6.
32. Hansson GK, and Berne GP. Atherosclerosis and the immune system. *Acta Paediatr Suppl* 2004;93:63-9.
33. Zhou X, Caligiuri G, Hamsten A, Lefvert AK, and Hansson GK. LDL immunization induces T-cell-dependent antibody formation and protection against atherosclerosis. *Arterioscler Thromb Vasc Biol* 2001;21:108-14.

34. Libby P, Geng YJ, Aikawa M, Schönbeck U, Mach F, Clinton SK, Sukhova GK, and Lee RT. Macrophages and atherosclerotic plaque stability. *Current Opinion in Lipidology* 1996;76:330 - 35.
35. Clinton S, Underwood R, Sherman M, Kufe D, and Libby P. Macrophage-colony stimulating factor gene expression in vascular cells and in experimental and human atherosclerosis. *Am J Pathol* 1992;140:301-16.
36. Hegyi L, Hardwick SJ, Mitchinson MJ, and Skepper JN. The presence of apoptotic cells in human atherosclerotic lesions. *Am J Pathol* 1997;150:371-3.
37. Cai W, Devaux B, Schaper W, and Schaper J. The role of Fas/APO 1 and apoptosis in the development of human atherosclerotic lesions. *Atherosclerosis* 1997;131:177-86.
38. Mallat Z, and Tedgui A. Apoptosis in the vasculature: mechanisms and functional importance. *Br J Pharmacol* 2000;130:947-62.
39. Newby AC, and Zaltsman AB. Fibrous cap formation or destruction--the critical importance of vascular smooth muscle cell proliferation, migration and matrix formation. *Cardiovasc Res* 1999;41:345-60.
40. Cheng GC, Loree HM, Kamm RD, Fishbein MC, and Lee RT. Distribution of circumferential stress in ruptured and stable atherosclerotic lesions. *Circulation* 1993;87:1179 - 87.
41. Loree HM, Kamm RD, Stringfellow RG, and Lee RT. Effects of fibrous cap thickness on peak circumferential stress in model atherosclerotic vessels. *Circulation Research* 1992;71:850-8.
42. McCarthy NJ, and Bennett MR. The regulation of vascular smooth muscle cell apoptosis. *Cardiovasc Res* 2000;45:747-55.
43. Pasterkamp G, Schoneveld AH, van der Wal AC, Hijnen DJ, van Wolveken WJ, Plomp S, Teepen HL, and Borst C. Inflammation of the atherosclerotic cap and shoulder of the plaque is a common and locally observed feature in unruptured plaques of femoral and coronary arteries. *Arterioscler Thromb Vasc Biol* 1999;19:54-8.
44. Shah PK. Plaque disruption and thrombosis: potential role of inflammation and infection. *Cardiol Rev* 2000;8:31-9.
45. Yokoya K, Takatsu H, Suzuki T, Hosokawa H, Ojio S, Matsubara T, Tanaka T, Watanabe S, Morita N, Nishigaki K, Takemura G, Noda T, Minatoguchi S, and Fujiwara H. Process of progression of coronary artery lesions from mild or moderate stenosis to moderate or severe stenosis: A study based on four serial coronary arteriograms per year. *Circulation* 1999;100:903-9.
46. Visse R, and Nagase H. Matrix metalloproteinases and tissue inhibitors of metalloproteinases: structure, function, and biochemistry. *Circ Res* 2003;92:827-39.
47. Galis ZS, and Khatri JJ. Matrix metalloproteinases in vascular remodeling and atherogenesis: the good, the bad, and the ugly. *Circ Res* 2002;90:251-62.
48. Galis Z, Sukhova G, Lark M, and Libby P. Increased expression of matrix metalloproteinases and matrix degrading activity in vulnerable regions of human atherosclerotic plaques. *J Clin Invest* 1994;94:2493-503.
49. Nikkari ST, O'Brien KD, Ferguson M, Hatsukami T, Welgus HG, Alpers CE, and Clowes AW. Interstitial collagenase (MMP-1) expression in human carotid atherosclerosis. *Circulation* 1995;92:1393-8.

50. Brown DL, Hibbs MS, Kearney M, Loushin C, and Isner JM. Identification of 92-kD gelatinase in human coronary atherosclerotic lesions. Association of active enzyme synthesis with unstable angina. *Circulation* 1995;91:2125-31.
51. Herman MP, Sukhova GK, Libby P, Gerdes N, Tang N, Horton DB, Kilbride M, Breitbart RE, Chun M, and Schonbeck U. Expression of neutrophil collagenase (matrix metalloproteinase-8) in human atheroma: a novel collagenolytic pathway suggested by transcriptional profiling. *Circulation* 2001;104:1899-904.
52. Li Z, Li L, Zielke HR, Cheng L, Xiao R, Crow MT, Stetler-Stevenson WG, Froehlich J, and Lakatta EG. Increased expression of 72-kd type IV collagenase (MMP-2) in human aortic atherosclerotic lesions. *Am J Pathol* 1996;148:121-8.
53. Galis ZS, Sukhova GK, and Libby P. Microscopic localization of active proteases by in situ zymography: detection of matrix metalloproteinase activity in vascular tissue. *Faseb J* 1995;9:974-80.
54. Newby AC. Dual role of matrix metalloproteinases (matrixins) in intimal thickening and atherosclerotic plaque rupture. *Physiol Rev* 2005;85:1-31.
55. Jones CB, Sane DC, and Herrington DM. Matrix metalloproteinases: a review of their structure and role in acute coronary syndrome. *Cardiovasc Res* 2003;59:812-23.
56. Stary HC. The sequence of cell and matrix changes in atherosclerotic lesions of coronary arteries in the first forty years of life. *Eur Heart J* 1990;11 Suppl E:3-19.
57. Sukhova GK, Schonbeck U, Rabkin E, Schoen FJ, Poole AR, Billinghurst RC, and Libby P. Evidence for increased collagenolysis by interstitial collagenases-1 and -3 in vulnerable human atheromatous plaques. *Circulation* 1999;99:2503-9.
58. Fabunmi RP, Sukhova GK, Sugiyama S, and Libby P. Expression of tissue inhibitor of metalloproteinases-3 in human atheroma and regulation in lesion-associated cells: a potential protective mechanism in plaque stability. *Circ Res* 1998;83:270-8.
59. Herman MP, Sukhova GK, Kisiel W, Foster D, Kehry MR, Libby P, and Schonbeck U. Tissue factor pathway inhibitor-2 is a novel inhibitor of matrix metalloproteinases with implications for atherosclerosis. *J Clin Invest* 2001;107:1117-26.
60. Frostegard J, Ulfgren AK, Nyberg P, Hedin U, Swedenborg J, Andersson U, and Hansson GK. Cytokine expression in advanced human atherosclerotic plaques: dominance of pro-inflammatory (Th1) and macrophage-stimulating cytokines. *Atherosclerosis* 1999;145:33-43.
61. Pinderski Oslund LJ, Hedrick CC, Olvera T, Hagenbaugh A, Territo M, Berliner JA, and Fyfe AI. Interleukin-10 blocks atherosclerotic events in vitro and in vivo. *Arterioscler Thromb Vasc Biol* 1999;19:2847-53.
62. Morel PA, and Oriss TB. Crossregulation between Th1 and Th2 cells. *Crit Rev Immunol* 1998;18:275-303.
63. Szabo SJ, Sullivan BM, Peng SL, and Glimcher LH. Molecular mechanisms regulating Th1 immune responses. *Annu Rev Immunol* 2003;21:713-58.
64. Uyemura K, Demer LL, Castle SC, Jullien D, Berliner JA, Gately MK, Warrier RR, Pham N, Fogelman AM, and Modlin RL. Cross-regulatory roles of interleukin (IL)-12 and IL-10 in atherosclerosis. *J Clin Invest* 1996;97:2130-8.
65. Gupta S, Pablo AM, Jiang X, Wang N, Tall AR, and Schindler C. IFN-gamma potentiates atherosclerosis in ApoE knock-out mice. *J Clin Invest* 1997;99:2752-61.

66. Tellides G, Tereb DA, Kirkiles-Smith NC, Kim RW, Wilson JH, Schechner JS, Lorber MI, and Pober JS. Interferon-gamma elicits arteriosclerosis in the absence of leukocytes. *Nature* 2000;403:207-11.
67. Buono C, Come CE, Stavrakis G, Maguire GF, Connelly PW, and Lichtman AH. Influence of interferon-gamma on the extent and phenotype of diet-induced atherosclerosis in the LDLR-deficient mouse. *Arterioscler Thromb Vasc Biol* 2003;23:454-60.
68. Young JL, Libby P, and Schonbeck U. Cytokines in the pathogenesis of atherosclerosis. *Thromb Haemost* 2002;88:554-67.
69. Boehm U, Klamp T, Groot M, and Howard JC. Cellular responses to interferon-gamma. *Annu Rev Immunol* 1997;15:749-95.
70. Amento EP, Ehsani N, Palmer H, and Libby P. Cytokines and growth factors positively and negatively regulate interstitial collagen gene expression in human vascular smooth muscle cells. *Arterioscler Thromb* 1991;11:1223-30.
71. Whitman SC, Ravisankar P, Elam H, and Daugherty A. Exogenous interferon-gamma enhances atherosclerosis in apolipoprotein E-/- mice. *Am J Pathol* 2000;157:1819-24.
72. Whitman SC, Ravisankar P, and Daugherty A. IFN-gamma deficiency exerts gender-specific effects on atherogenesis in apolipoprotein E-/- mice. *J Interferon Cytokine Res* 2002;22:661-70.
73. Micallef MJ, Ohtsuki T, Kohno K, Tanabe F, Ushio S, Namba M, Tanimoto T, Torigoe K, Fujii M, Ikeda M, Fukuda S, and Kurimoto M. Interferon-gamma-inducing factor enhances T helper 1 cytokine production by stimulated human T cells: synergism with interleukin-12 for interferon-gamma production. *Eur J Immunol* 1996;26:1647-51.
74. Ushio S, Namba M, Okura T, Hattori K, Nukada Y, Akita K, Tanabe F, Konishi K, Micallef M, Fujii M, Torigoe K, Tanimoto T, Fukuda S, Ikeda M, Okamura H, and Kurimoto M. Cloning of the cDNA for human IFN-gamma-inducing factor, expression in Escherichia coli, and studies on the biologic activities of the protein. *J Immunol* 1996;156:4274-9.
75. Okamura H, Tsutsi H, Komatsu T, Yutsudo M, Hakura A, Tanimoto T, Torigoe K, Okura T, Nukada Y, Hattori K, Akita K, Namba M, Tanabe F, Konishi K, Fukuda S, and Kurimoto M. Cloning of a new cytokine that induces IFN-gamma production by T cells. *Nature* 1995;378:88-91.
76. Kalina U, Ballas K, Koyama N, Kauschat D, Miethling C, Arnemann J, Martin H, Hoelzer D, and Ottmann OG. Genomic organization and regulation of the human interleukin-18 gene. *Scand J Immunol* 2000;52:525-30.
77. Pirhonen J. Regulation of IL-18 expression in virus infection. *Scand J Immunol* 2001;53:533-9.
78. Nakanishi K, Yoshimoto T, Tsutsui H, and Okamura H. Interleukin-18 regulates both th1 and th2 responses. *Annu Rev Immunol* 2001;19:423-74.
79. Gracie JA, Forsey RJ, Chan WL, Gilmour A, Leung BP, Greer MR, Kennedy K, Carter R, Wei XQ, Xu D, Field M, Foulis A, Liew FY, and McInnes IB. A proinflammatory role for IL-18 in rheumatoid arthritis. *J Clin Invest* 1999;104:1393-401.

80. Udagawa N, Horwood NJ, Elliott J, Mackay A, Owens J, Okamura H, Kurimoto M, Chambers TJ, Martin TJ, and Gillespie MT. Interleukin-18 (interferon-gamma-inducing factor) is produced by osteoblasts and acts via granulocyte/macrophage colony-stimulating factor and not via interferon-gamma to inhibit osteoclast formation. *J Exp Med* 1997;185:1005-12.
81. Olee T, Hashimoto S, Quach J, and Lotz M. IL-18 is produced by articular chondrocytes and induces proinflammatory and catabolic responses. *J Immunol* 1999;162:1096-100.
82. Stoll S, Muller G, Kurimoto M, Saloga J, Tanimoto T, Yamauchi H, Okamura H, Knop J, and Enk AH. Production of IL-18 (IFN-gamma-inducing factor) messenger RNA and functional protein by murine keratinocytes. *J Immunol* 1997;159:298-302.
83. Stoll S, Jonuleit H, Schmitt E, Muller G, Yamauchi H, Kurimoto M, Knop J, and Enk AH. Production of functional IL-18 by different subtypes of murine and human dendritic cells (DC): DC-derived IL-18 enhances IL-12-dependent Th1 development. *Eur J Immunol* 1998;28:3231-9.
84. Takeuchi M, Nishizaki Y, Sano O, Ohta T, Ikeda M, and Kurimoto M. Immunohistochemical and immuno-electron-microscopic detection of interferon-gamma-inducing factor ("interleukin-18") in mouse intestinal epithelial cells. *Cell Tissue Res* 1997;289:499-503.
85. Cameron LA, Taha RA, Tsicopoulos A, Kurimoto M, Olivenstein R, Wallaert B, Minshall EM, and Hamid QA. Airway epithelium expresses interleukin-18. *Eur Respir J* 1999;14:553-9.
86. Kanai T, Watanabe M, Okazawa A, Nakamaru K, Okamoto M, Naganuma M, Ishii H, Ikeda M, Kurimoto M, and Hibi T. Interleukin 18 is a potent proliferative factor for intestinal mucosal lymphocytes in Crohn's disease. *Gastroenterology* 2000;119:1514-23.
87. Greene CM, Meachery G, Taggart CC, Rooney CP, Coakley R, O'Neill SJ, and McElvaney NG. Role of IL-18 in CD4+ T lymphocyte activation in sarcoidosis. *J Immunol* 2000;165:4718-24.
88. McInnes IB, Gracie JA, Leung BP, Wei XQ, and Liew FY. Interleukin 18: a pleiotropic participant in chronic inflammation. *Immunol Today* 2000;21:312-5.
89. Ohta Y, Hamada Y, and Katsuoka K. Expression of IL-18 in psoriasis. *Arch Dermatol Res* 2001;293:334-42.
90. Pages F, Berger A, Lebel-Binay S, Zinzindohoue F, Danel C, Piqueras B, Carriere O, Thiounn N, Cugnenc PH, and Fridman WH. Proinflammatory and antitumor properties of interleukin-18 in the gastrointestinal tract. *Immunol Lett* 2000;75:9-14.
91. Ghayur T, Banerjee S, Hugunin M, Butler D, Herzog L, Carter A, Quintal L, Sekut L, Talanian R, Paskind M, Wong W, Kamen R, Tracey D, and Allen H. Caspase-1 processes IFN-gamma-inducing factor and regulates LPS-induced IFN-gamma production. *Nature* 1997;386:619-23.
92. Gu Y, Kuida K, Tsutsui H, Ku G, Hsiao K, Fleming MA, Hayashi N, Higashino K, Okamura H, Nakanishi K, Kurimoto M, Tanimoto T, Flavell RA, Sato V, Harding MW, Livingston DJ, and Su MS. Activation of interferon-gamma inducing factor mediated by interleukin-1beta converting enzyme. *Science* 1997;275:206-9.
93. Fantuzzi G, and Dinarello CA. Interleukin-18 and interleukin-1 beta: two cytokine substrates for ICE (caspase-1). *J Clin Immunol* 1999;19:1-11.

94. Akita K, Ohtsuki T, Nukada Y, Tanimoto T, Namba M, Okura T, Takakura-Yamamoto R, Torigoe K, Gu Y, Su MS, Fujii M, Satoh-Itoh M, Yamamoto K, Kohno K, Ikeda M, and Kurimoto M. Involvement of caspase-1 and caspase-3 in the production and processing of mature human interleukin 18 in monocytic THP.1 cells. *J Biol Chem* 1997;272:26595-603.
95. Alnemri ES, Livingston DJ, Nicholson DW, Salvesen G, Thornberry NA, Wong WW, and Yuan J. Human ICE/CED-3 Protease nomenclature. *Cell* 1996;87:171.
96. Cerretti DP, Kozlosky CJ, Mosley B, Nelson N, Van Ness K, Greenstreet TA, March CJ, Kronheim SR, Druck T, Cannizzaro LA, and et al. Molecular cloning of the interleukin-1 beta converting enzyme. *Science* 1992;256:97-100.
97. Thornberry NA, Bull HG, Calaycay JR, Chapman KT, Howard AD, Kostura MJ, Miller DK, Molineaux SM, Weidner JR, Aunins J, and et al. A novel heterodimeric cysteine protease is required for interleukin-1 beta processing in monocytes. *Nature* 1992;356:768-74.
98. Livingston DJ. In vitro and in vivo studies of ICE inhibitors. *J Cell Biochem* 1997;64:19-26.
99. Randle JC, Harding MW, Ku G, Schonharting M, and Kurulle R. ICE/Caspase-1 inhibitors as novel anti-inflammatory drugs. *Expert Opin Investig Drugs* 2001;10:1207-9.
100. Schönbeck U, Herzberg M, Petersen A, Wohlenberg C, Gerdes J, Flad HD, and Loppnow H. Human vascular smooth muscle cells express interleukin-1beta-converting enzyme (ICE), but inhibit processing of the interleukin-1beta precursor by ICE. *J Exp Med* 1997;185:1287-94.
101. Wong ML, Bongiorno PB, Gold PW, and Licinio J. Localization of interleukin-1 beta converting enzyme mRNA in rat brain vasculature: evidence that the genes encoding the interleukin-1 system are constitutively expressed in brain blood vessels. Pathophysiological implications. *Neuroimmunomodulation* 1995;2:141-8.
102. Moyer CF, Sajuthi D, Tulli H, and Williams JK. Synthesis of IL-1 alpha and IL-1 beta by arterial cells in atherosclerosis. *Am J Pathol* 1991;138:951-60.
103. Ariizumi K, Kitajima T, Bergstresser OR, and Takashima A. Interleukin-1 beta converting enzyme in murine Langerhans cells and epidermal-derived dendritic cell lines. *Eur J Immunol* 1995;25:2137-41.
104. Martinon F, and Tschoopp J. Inflammatory caspases: linking an intracellular innate immune system to autoinflammatory diseases. *Cell* 2004;117:561-74.
105. Friedlander RM, Gagliardini V, Rotello RJ, and Yuan J. Functional role of interleukin 1 beta (IL-1 beta) in IL-1 beta- converting enzyme-mediated apoptosis. *J Exp Med* 1996;184:717-24.
106. Clark RS, Kochanek PM, Chen M, Watkins SC, Marion DW, Chen J, Hamilton RL, Loeffert JE, and Graham SH. Increases in Bcl-2 and cleavage of caspase-1 and caspase-3 in human brain after head injury. *Faseb J* 1999;13:813-21.
107. Wilson KP, Black JA, Thomson JA, Kim EE, Griffith JP, Navia MA, Murcko MA, Chambers SP, Aldape RA, Raybuck SA, and et al. Structure and mechanism of interleukin-1 beta converting enzyme. *Nature* 1994;370:270-5.
108. Boudreau N, Sympson CJ, Werb Z, and Bissell MJ. Suppression of ICE and apoptosis in mammary epithelial cells by extracellular matrix. *Science* 1995;267:891-3.

- 109.** Beuscher HU, Günther C, and Röllinghoff M. IL-1 β is secreted by activated murine macrophages as biologically inactive precursor. *J Immunol* 1990;144:2179 - 83.
- 110.** Puren AJ, Fantuzzi G, and Dinarello CA. Gene expression, synthesis, and secretion of interleukin 18 and interleukin 1beta are differentially regulated in human blood mononuclear cells and mouse spleen cells. *Proc Natl Acad Sci U S A* 1999;96:2256-61.
- 111.** Gerdes N, Sukhova GK, Libby P, and Schönbeck U. Human atheroma-associated cells express functional IL-18 and IL-18 receptor in vitro and in situ. *Circulation* 2000;102:Suppl. II-66.
- 112.** Gerdes N, Sukhova GK, Libby P, Reynolds RS, Young JL, and Schonbeck U. Expression of interleukin (IL)-18 and functional IL-18 receptor on human vascular endothelial cells, smooth muscle cells, and macrophages: implications for atherogenesis. *J Exp Med* 2002;195:245-57.
- 113.** Yoshimoto T, Nagase H, Ishida T, Inoue J, and Nariuchi H. Induction of interleukin-12 p40 transcript by CD40 ligation via activation of nuclear factor-kappaB. *Eur J Immunol* 1997;27:3461-70.
- 114.** Chang JT, Segal BM, Nakanishi K, Okamura H, and Shevach EM. The costimulatory effect of IL-18 on the induction of antigen-specific IFN-gamma production by resting T cells is IL-12 dependent and is mediated by up-regulation of the IL-12 receptor beta2 subunit. *Eur J Immunol* 2000;30:1113-9.
- 115.** Lawless VA, Zhang S, Ozes ON, Bruns HA, Oldham I, Hoey T, Grusby MJ, and Kaplan MH. Stat4 regulates multiple components of IFN-gamma-inducing signaling pathways. *J Immunol* 2000;165:6803-8.
- 116.** Schindler H, Lutz MB, Rollinghoff M, and Bogdan C. The production of IFN-gamma by IL-12/IL-18-activated macrophages requires STAT4 signaling and is inhibited by IL-4. *J Immunol* 2001;166:3075-82.
- 117.** Lebel-Binay S, Berger A, Zinzindohoue F, Cugnenc P, Thiounn N, Fridman WH, and Pages F. Interleukin-18: biological properties and clinical implications. *Eur Cytokine Netw* 2000;11:15-26.
- 118.** Puren AJ, Fantuzzi G, Gu Y, Su MS, and Dinarello CA. Interleukin-18 (IFNgamma-inducing factor) induces IL-8 and IL-1beta via TNFalpha production from non-CD14+ human blood mononuclear cells. *J Clin Invest* 1998;101:711-21.
- 119.** McInnes IB, Gracie JA, Leung BP, Wei XQ, and Liew FY. Interleukin 18: a pleiotropic participant in chronic inflammation. *Immunol Today* 2000;21:312-5.
- 120.** Tsutsui H, Nakanishi K, Matsui K, Higashino K, Okamura H, Miyazawa Y, and Kaneda K. IFN-gamma-inducing factor up-regulates Fas ligand-mediated cytotoxic activity of murine natural killer cell clones. *J Immunol* 1996;157:3967-73.
- 121.** Hyodo Y, Matsui K, Hayashi N, Tsutsui H, Kashiwamura S, Yamauchi H, Hiroishi K, Takeda K, Tagawa Y, Iwakura Y, Kayagaki N, Kurimoto M, Okamura H, Hada T, Yagita H, Akira S, Nakanishi K, and Higashino K. IL-18 up-regulates perforin-mediated NK activity without increasing perforin messenger RNA expression by binding to constitutively expressed IL-18 receptor. *J Immunol* 1999;162:1662-8.
- 122.** Parnet P, Garka KE, Bonnert TP, Dower SK, and Sims JE. IL-1Rrp is a novel receptor-like molecule similar to the type I interleukin-1 receptor and its homologues T1/ST2 and IL-1R AcP. *J Biol Chem* 1996;271:3967-70.

- 123.** Torigoe K, Ushio S, Okura T, Kobayashi S, Taniai M, Kunikata T, Murakami T, Sanou O, Kojima H, Fujii M, Ohta T, Ikeda M, Ikegami H, and Kurimoto M. Purification and characterization of the human interleukin-18 receptor. *J Biol Chem* 1997;272:25737-42.
- 124.** Born TL, Thomasson E, Bird TA, and Sims JE. Cloning of a novel receptor subunit, AcPL, required for IL-18 signaling. *J Biol Chem* 1998;273:29445-50.
- 125.** Kanakaraj P, Ngo K, Wu Y, Angulo A, Ghazal P, Harris CA, Siekierka JJ, Peterson PA, and Fung-Leung WP. Defective interleukin (IL)-18-mediated natural killer and T helper cell type 1 responses in IL-1 receptor-associated kinase (IRAK)-deficient mice. *J Exp Med* 1999;189:1129-38.
- 126.** Lomaga MA, Yeh WC, Sarosi I, Duncan GS, Furlonger C, Ho A, Morony S, Capparelli C, Van G, Kaufman S, van der Heiden A, Itie A, Wakeham A, Khoo W, Sasaki T, Cao Z, Penninger JM, Paige CJ, Lacey DL, Dunstan CR, Boyle WJ, Goeddel DV, and Mak TW. TRAF6 deficiency results in osteopetrosis and defective interleukin-1, CD40, and LPS signaling. *Genes Dev* 1999;13:1015-24.
- 127.** Cheung H, Chen NJ, Cao Z, Ono N, Ohashi PS, and Yeh WC. Accessory Protein-Like Is Essential for IL-18-Mediated Signaling. *J Immunol* 2005;174:5351-7.
- 128.** Adachi O, Kawai T, Takeda K, Matsumoto M, Tsutsui H, Sakagami M, Nakanishi K, and Akira S. Targeted disruption of the MyD88 gene results in loss of IL-1- and IL-18-mediated function. *Immunity* 1998;9:143-50.
- 129.** Thomas JA, Allen JL, Tsen M, Dubnicoff T, Danao J, Liao XC, Cao Z, and Wasserman SA. Impaired cytokine signaling in mice lacking the IL-1 receptor-associated kinase. *J Immunol* 1999;163:978-84.
- 130.** Nakamura S, Otani T, Okura R, Ijiri Y, Motoda R, Kurimoto M, and Orita K. Expression and responsiveness of human interleukin-18 receptor (IL-18R) on hematopoietic cell lines. *Leukemia* 2000;14:1052-9.
- 131.** Xu D, Chan WL, Leung BP, Hunter D, Schulz K, Carter RW, McInnes IB, Robinson JH, and Liew FY. Selective expression and functions of interleukin 18 receptor on T helper (Th) type 1 but not Th2 cells. *J Exp Med* 1998;188:1485-92.
- 132.** Blankenberg S, Luc G, Ducimetiere P, Arveiler D, Ferrieres J, Amouyel P, Evans A, Cambien F, and Tiret L. Interleukin-18 and the risk of coronary heart disease in European men: the Prospective Epidemiological Study of Myocardial Infarction (PRIME). *Circulation* 2003;108:2453-9.
- 133.** Rosso R, Roth A, Herz I, Miller H, Keren G, and George J. Serum levels of interleukin-18 in patients with stable and unstable angina pectoris. *Int J Cardiol* 2005;98:45-8.
- 134.** Yamaoka-Tojo M, Tojo T, Masuda T, Machida Y, Kitano Y, Kurosawa T, and Izumi T. C-reactive protein-induced production of interleukin-18 in human endothelial cells: a mechanism of orchestrating cytokine cascade in acute coronary syndrome. *Heart Vessels* 2003;18:183-7.
- 135.** Blankenberg S, Tiret L, Bickel C, Peetz D, Cambien F, Meyer J, and Rupprecht HJ. Interleukin-18 is a strong predictor of cardiovascular death in stable and unstable angina. *Circulation* 2002;106:24-30.
- 136.** Mallat Z, Henry P, Fressonnet R, Alouani S, Scoazec A, Beaufils P, Chvatchko Y, and Tedgui A. Increased plasma concentrations of interleukin-18 in acute coronary syndromes. *Heart* 2002;88:467-9.

137. Woldbaek PR, Tonnessen T, Henriksen UL, Florholmen G, Lunde PK, Lyberg T, and Christensen G. Increased cardiac IL-18 mRNA, pro-IL-18 and plasma IL-18 after myocardial infarction in the mouse; a potential role in cardiac dysfunction. *Cardiovasc Res* 2003;59:122-31.
138. Mallat Z, Heymes C, Corbaz A, Logeart D, Alouani S, Cohen-Solal A, Seidler T, Hasenfuss G, Chvatchko Y, Shah AM, and Tedgui A. Evidence for altered interleukin 18 (IL)-18 pathway in human heart failure. *Faseb J* 2004;18:1752-4.
139. Yamaoka-Tojo M, Tojo T, Inomata T, Machida Y, Osada K, and Izumi T. Circulating levels of interleukin 18 reflect etiologies of heart failure: Th1/Th2 cytokine imbalance exaggerates the pathophysiology of advanced heart failure. *J Card Fail* 2002;8:21-7.
140. Naito Y, Tsujino T, Fujioka Y, Ohyanagi M, Okamura H, and Iwasaki T. Increased circulating interleukin-18 in patients with congestive heart failure. *Heart* 2002;88:296-7.
141. Esposito K, Pontillo A, Ciotola M, Di Palo C, Grella E, Nicoletti G, and Giugliano D. Weight loss reduces interleukin-18 levels in obese women. *J Clin Endocrinol Metab* 2002;87:3864-6.
142. Marfella R, Esposito K, Siniscalchi M, Cacciapuoti F, Giugliano F, Labriola D, Ciotola M, Di Palo C, Misso L, and Giugliano D. Effect of weight loss on cardiac synchronization and proinflammatory cytokines in premenopausal obese women. *Diabetes Care* 2004;27:47-52.
143. Escobar-Morreale HF, Botella-Carretero JI, Villuendas G, Sancho J, and San Millan JL. Serum interleukin-18 concentrations are increased in the polycystic ovary syndrome: relationship to insulin resistance and to obesity. *J Clin Endocrinol Metab* 2004;89:806-11.
144. Marfella R, Siniscalchi M, Esposito K, Sellitto A, De Fanis U, Romano C, Portoghese M, Siciliano S, Nappo F, Sasso FC, Mininni N, Cacciapuoti F, Lucivero G, Giunta R, Verza M, and Giugliano D. Effects of stress hyperglycemia on acute myocardial infarction: role of inflammatory immune process in functional cardiac outcome. *Diabetes Care* 2003;26:3129-35.
145. Esposito K, Nappo F, Marfella R, Giugliano G, Giugliano F, Ciotola M, Quagliaro L, Ceriello A, and Giugliano D. Inflammatory cytokine concentrations are acutely increased by hyperglycemia in humans: role of oxidative stress. *Circulation* 2002;106:2067-72.
146. Nicoletti F, Conget I, Di Marco R, Speciale AM, Morinigo R, Bendtzen K, and Gomis R. Serum levels of the interferon-gamma-inducing cytokine interleukin-18 are increased in individuals at high risk of developing type I diabetes. *Diabetologia* 2001;44:309-11.
147. Moriwaki Y, Yamamoto T, Shibutani Y, Aoki E, Tsutsumi Z, Takahashi S, Okamura H, Koga M, Fukuchi M, and Hada T. Elevated levels of interleukin-18 and tumor necrosis factor-alpha in serum of patients with type 2 diabetes mellitus: relationship with diabetic nephropathy. *Metabolism* 2003;52:605-8.
148. Aso Y, Okumura K, Takebayashi K, Wakabayashi S, and Inukai T. Relationships of plasma interleukin-18 concentrations to hyperhomocysteinemia and carotid intimal-media wall thickness in patients with type 2 diabetes. *Diabetes Care* 2003;26:2622-7.
149. Esposito K, Marfella R, and Giugliano D. Plasma interleukin-18 concentrations are elevated in type 2 diabetes. *Diabetes Care* 2004;27:272.

- 150.** Jaffe EA, Nachman RL, Becker CG, and Minick CR. Culture of human endothelial cells derived from umbilical veins. Identification by morphologic and immunologic criteria. *J Clin Invest* 1973;52:2745-56.
- 151.** Chamley-Campbell JH, Campbell GR, and R.Ross. The smooth muscle cell in culture. *Physiological Reviews* 1979;58:1-61.
- 152.** Fazio S, and Linton MF. Mouse models of hyperlipidemia and atherosclerosis. *Front Biosci* 2001;6:D515-25.
- 153.** Daugherty A, and Whitman SC. Quantification of atherosclerosis in mice. *Methods Mol Biol* 2003;209:293-309.
- 154.** Zhou X, Paulsson G, Stemme S, and Hansson GK. Hypercholesterolemia is associated with a T helper (Th) 1/Th2 switch of the autoimmune response in atherosclerotic apo E-knockout mice. *J Clin Invest* 1998;101:1717-25.
- 155.** Jawien J, Nastalek P, and Korbut R. Mouse models of experimental atherosclerosis. *J Physiol Pharmacol* 2004;55:503-17.
- 156.** Rosenfeld ME, Carson KG, Johnson JL, Williams H, Jackson CL, and Schwartz SM. Animal models of spontaneous plaque rupture: the holy grail of experimental atherosclerosis research. *Curr Atheroscler Rep* 2002;4:238-42.
- 157.** Zhou Y, Chen R, Catanzaro SE, Hu L, Dansky HM, and Catanzaro DF. Differential effects of angiotensin II on atherogenesis at the aortic sinus and descending aorta of apolipoprotein-E-deficient mice. *Am J Hypertens* 2005;18:486-92.
- 158.** Zhang SH, Reddick RL, Piedrahita JA, and Maeda N. Spontaneous hypercholesterolemia and arterial lesions in mice lacking apolipoprotein E. *Science* 1992;258:468-71.
- 159.** Plump AS, Smith JD, Hayek T, Aalto-Setala K, Walsh A, Verstuyft JG, Rubin EM, and Breslow JL. Severe hypercholesterolemia and atherosclerosis in apolipoprotein E-deficient mice created by homologous recombination in ES cells. *Cell* 1992;71:343-53.
- 160.** Ishibashi S, Brown MS, Goldstein JL, Gerard RD, Hammer RE, and Herz J. Hypercholesterolemia in low density lipoprotein receptor knockout mice and its reversal by adenovirus-mediated gene delivery. *J Clin Invest* 1993;92:883-93.
- 161.** Glaccum MB, Stocking KL, Charrier K, Smith JL, Willis CR, Maliszewski C, Livingston DJ, Peschon JJ, and Morrissey PJ. Phenotypic and functional characterization of mice that lack the type I receptor for IL-1. *J Immunol* 1997;159:3364-71.
- 162.** Hoshino K, Tsutsui H, Kawai T, Takeda K, Nakanishi K, Takeda Y, and Akira S. Generation of IL-18 receptor-deficient mice: evidence for IL-1 receptor-related protein as an essential IL-18 binding receptor. *J Immunol* 1999;162:5041-4.
- 163.** Morse HC, 3rd. Genetic nomenclature for loci controlling surface antigens of mouse hemopoietic cells. *J Immunol* 1992;149:3129-34.
- 164.** Takeda K, Tsutsui H, Yoshimoto T, Adachi O, Yoshida N, Kishimoto T, Okamura H, Nakanishi K, and Akira S. Defective NK cell activity and Th1 response in IL-18-deficient mice. *Immunity* 1998;8:383-90.
- 165.** Li P, Allen H, Banerjee S, Franklin S, Herzog L, Johnston C, McDowell J, Paskind M, Rodman L, Salfeld J, Towne E, Tracey D, Wardwell S, Wei F-Y, Wong W, Kamen R, and Seshadri T. Mice deficient in IL-1 β -converting enzyme are defective in production of mature IL-1 β and resistant to endotoxic shock. *Cell* 1995;80:401-11.

- 166.** Mach F, Schonbeck U, Sukhova GK, Atkinson E, and Libby P. Reduction of atherosclerosis in mice by inhibition of CD40 signalling. *Nature* 1998;394:200-3.
- 167.** Vidal-Vanaclocha F, Fantuzzi G, Mendoza L, Fuentes AM, Anasagasti MJ, Martin J, Carrascal T, Walsh P, Reznikov LL, Kim SH, Novick D, Rubinstein M, and Dinarello CA. IL-18 regulates IL-1beta-dependent hepatic melanoma metastasis via vascular cell adhesion molecule-1. *Proc Natl Acad Sci U S A* 2000;97:734-9.
- 168.** Amirghofran Z, and Ghaderi AA. Characterization of a murine monoclonal antibody reactive with a leukocyte common antigen and its application to bone marrow transplantation. *Transplant Proc* 1995;27:2657-8.
- 169.** Kirii H, Niwa T, Yamada Y, Wada H, Saito K, Iwakura Y, Asano M, Moriwaki H, and Seishima M. Lack of interleukin-1beta decreases the severity of atherosclerosis in ApoE-deficient mice. *Arterioscler Thromb Vasc Biol* 2003;23:656-60.
- 170.** Schönbeck U, Mach F, and Libby P. Generation of biologically active IL-1 beta by matrix metalloproteinases: a novel caspase-1-independent pathway of IL-1 beta processing. *J Immunol* 1998;161:3340-6.
- 171.** McQuibban GA, Gong JH, Wong JP, Wallace JL, Clark-Lewis I, and Overall CM. Matrix metalloproteinase processing of monocyte chemoattractant proteins generates CC chemokine receptor antagonists with anti-inflammatory properties in vivo. *Blood* 2002;100:1160-7.
- 172.** Konishi K, Tanabe F, Taniguchi M, Yamauchi H, Tanimoto T, Ikeda M, Orita K, and Kurimoto M. A simple and sensitive bioassay for the detection of human interleukin-18/interferon-gamma-inducing factor using human myelomonocytic KG-1 cells. *J Immunol Methods* 1997;209:187-91.
- 173.** Warner SJC, Friedman GB, and Libby P. Immune interferon inhibits proliferation and induces 2'-5'-oligoadenylate synthetase gene expression in human vascular smooth muscle cells. *J Clin Invest* 1989;83:1174-82.
- 174.** Hansson GK, Jonasson L, Holm J, Clowes MK, and Clowes A. Gamma interferon regulates vascular smooth muscle proliferation and Ia expression in vivo and in vitro. *Circ Research* 1988;63:712-19.
- 175.** Hansson GK, Hellstrand M, Rymo L, Rubbia L, and Gabbiani G. Interferon-gamma inhibits both proliferation and expression of differentiation-specific alpha-smooth muscle actin in arterial smooth muscle cells. *J Exp Med* 1989;170:1595-608.
- 176.** Robinson BW, McLemore TL, and Crystal RG. Gamma interferon is spontaneously released by alveolar macrophages and lung T lymphocytes in patients with pulmonary sarcoidosis. *J Clin Invest* 1985;75:1488-95.
- 177.** Di Marzio P, Puddu P, Conti L, Belardelli F, and Gessani S. Interferon gamma upregulates its own gene expression in mouse peritoneal macrophages. *J Exp Med* 1994;179:1731-6.
- 178.** van Der Loos CM, Houtkamp MA, de Boer OJ, Teeling P, van Der Wal AC, and Becker AE. Immunohistochemical Detection of Interferon-gamma. Fake or fact? *J Histochem Cytochem* 2001;49:699-710.
- 179.** Tenger C, Sundborger A, Jawien J, and Zhou X. IL-18 accelerates atherosclerosis accompanied by elevation of IFN-gamma and CXCL16 expression independently of T cells. *Arterioscler Thromb Vasc Biol* 2005;25:791-6.

- 180.** Huang YH, Ronnelid J, and Frostegard J. Oxidized LDL induces enhanced antibody formation and MHC class II-dependent IFN-gamma production in lymphocytes from healthy individuals. *Arterioscler Thromb Vasc Biol* 1995;15:1577-83.
- 181.** Varadhancharay AS, Monestier M, and Salgame P. Reciprocal induction of IL-10 and IL-12 from macrophages by low-density lipoprotein and its oxidized forms. *Cell Immunol* 2001;213:45-51.
- 182.** Morel JC, Park CC, Woods JM, and Koch AE. A novel role for interleukin-18 in adhesion molecule induction through NF kappa B and phosphatidylinositol (PI) 3-kinase-dependent signal transduction pathways. *J Biol Chem* 2001;276:37069-75.
- 183.** Liebau C, Merk H, Schmidt S, Roesel C, Karreman C, Prisack JB, Bojar H, and Baltzer AW. Interleukin-12 and interleukin-18 change ICAM-I expression, and enhance natural killer cell mediated cytotoxicity of human osteosarcoma cells. *Cytokines Cell Mol Ther* 2002;7:135-42.
- 184.** Stuyt RJ, Netea MG, Geijtenbeek TB, Kullberg BJ, Dinarello CA, and van der Meer JW. Selective regulation of intercellular adhesion molecule-1 expression by interleukin-18 and interleukin-12 on human monocytes. *Immunology* 2003;110:329-34.
- 185.** Gutzmer R, Langer K, Mommert S, Wittmann M, Kapp A, and Werfel T. Human dendritic cells express the IL-18R and are chemoattracted to IL-18. *J Immunol* 2003;171:6363-71.
- 186.** Kaser A, Kaser S, Kaneider NC, Enrich B, Wiedermann CJ, and Tilg H. Interleukin-18 attracts plasmacytoid dendritic cells (DC2s) and promotes Th1 induction by DC2s through IL-18 receptor expression. *Blood* 2004;103:648-55.
- 187.** Khovidhunkit W, Kim MS, Memon RA, Shigenaga JK, Moser AH, Feingold KR, and Grunfeld C. Effects of infection and inflammation on lipid and lipoprotein metabolism: mechanisms and consequences to the host. *J Lipid Res* 2004;45:1169-96.
- 188.** Hakkinen T, Karkola K, and Yla-Hertuala S. Macrophages, smooth muscle cells, endothelial cells, and T-cells express CD40 and CD40L in fatty streaks and more advanced human atherosclerotic lesions. Colocalization with epitopes of oxidized low-density lipoprotein, scavenger receptor, and CD16 (Fc gammaRIII). *Virchows Arch* 2000;437:396-405.
- 189.** Bersot TP, Innerarity TL, Pitas RE, Rall SC, Jr., Weisgraber KH, and Mahley RW. Fat feeding in humans induces lipoproteins of density less than 1.006 that are enriched in apolipoprotein [a] and that cause lipid accumulation in macrophages. *J Clin Invest* 1986;77:622-30.
- 190.** Whitman SC, Ravisankar P, and Daugherty A. Interleukin-18 enhances atherosclerosis in apolipoprotein E(-/-) mice through release of interferon-gamma. *Circ Res* 2002;90:E34-8.
- 191.** Mallat Z, Corbaz A, Scoazec A, Graber P, Alouani S, Esposito B, Humbert Y, Chvatchko Y, and Tedgui A. Interleukin-18/interleukin-18 binding protein signaling modulates atherosclerotic lesion development and stability. *Circ Res* 2001;89:E41-5.
- 192.** Elhage R, Jawien J, Rudling M, Ljunggren HG, Takeda K, Akira S, Bayard F, and Hansson GK. Reduced atherosclerosis in interleukin-18 deficient apolipoprotein E-knockout mice. *Cardiovasc Res* 2003;59:234-40.

- 193.** de Nooijer R, von der Thusen JH, Verkleij CJ, Kuiper J, Jukema JW, van der Wall EE, van Berkel JC, and Biessen EA. Overexpression of IL-18 decreases intimal collagen content and promotes a vulnerable plaque phenotype in apolipoprotein-E-deficient mice. *Arterioscler Thromb Vasc Biol* 2004;24:2313-9.
- 194.** Libby P, Friedman GB, and Salomon RN. Cytokines as modulators of cell proliferation in fibrotic diseases. *Amer Rev Resp Dis* 1989;140:1114-17.
- 195.** Libby P (1990). Inflammatory and immune mechanisms in atherogenesis. *Atherosclerosis Reviews*. Leaf A, and Weber P. New York, Raven Press. 21: 79-89.
- 196.** Dunn E, Sims JE, Nicklin MJ, and O'Neill LA. Annotating genes with potential roles in the immune system: six new members of the IL-1 family. *Trends Immunol* 2001;22:533-6.
- 197.** Sims JE. IL-1 and IL-18 receptors, and their extended family. *Curr Opin Immunol* 2002;14:117-22.
- 198.** Diem R, Hobom M, Grotsch P, Kramer B, and Bahr M. Interleukin-1 beta protects neurons via the interleukin-1 (IL-1) receptor-mediated Akt pathway and by IL-1 receptor-independent decrease of transmembrane currents in vivo. *Mol Cell Neurosci* 2003;22:487-500.
- 199.** Touzani O, Boutin H, LeFeuvre R, Parker L, Miller A, Luheshi G, and Rothwell N. Interleukin-1 influences ischemic brain damage in the mouse independently of the interleukin-1 type I receptor. *J Neurosci* 2002;22:38-43.
- 200.** Boutin H, Kimber I, Rothwell NJ, and Pinteaux E. The expanding interleukin-1 family and its receptors: do alternative IL-1 receptor/signaling pathways exist in the brain? *Mol Neurobiol* 2003;27:239-48.
- 201.** Pan G, Risser P, Mao W, Baldwin DT, Zhong AW, Filvaroff E, Yansura D, Lewis L, Eigenbrot C, Henzel WJ, and Vandlen R. IL-1H, an interleukin 1-related protein that binds IL-18 receptor/IL-1R α . *Cytokine* 2001;13:1-7.
- 202.** Kumar S, Hanning CR, Brigham-Burke MR, Rieman DJ, Lehr R, Khandekar S, Kirkpatrick RB, Scott GF, Lee JC, Lynch FJ, Gao W, Gambotto A, and Lotze MT. Interleukin-1F7B (IL-1H4/IL-1F7) is processed by caspase-1 and mature IL-1F7B binds to the IL-18 receptor but does not induce IFN-gamma production. *Cytokine* 2002;18:61-71.
- 203.** Lin L, and Peng SL. Interleukin-18 receptor signaling is not required for autoantibody production and end-organ disease in murine lupus. *Arthritis Rheum* 2005;52:984-6.
- 204.** Neumann D, Del Giudice E, Ciaramella A, Boraschi D, and Bossu P. Lymphocytes from autoimmune MRL lpr/lpr mice are hyperresponsive to IL-18 and overexpress the IL-18 receptor accessory chain. *J Immunol* 2001;166:3757-62.
- 205.** Sugawara S, Uehara A, Nochi T, Yamaguchi T, Ueda H, Sugiyama A, Hanzawa K, Kumagai K, Okamura H, and Takada H. Neutrophil proteinase 3-mediated induction of bioactive IL-18 secretion by human oral epithelial cells. *J Immunol* 2001;167:6568-75.
- 206.** Fantuzzi G, Ku G, Harding MW, Livingston DJ, Sipe JD, Kuida K, Flavell RA, and Dinarello CA. Response to local inflammation of IL-1 β converting enzyme-deficient mice. *J Immunol* 1997;158:1818 - 24.
- 207.** Nylander-Lundqvist E, and Egelrud T. Formation of active IL-1 beta from pro-IL-1 beta catalyzed by stratum corneum chymotryptic enzyme in vitro. *Acta Derm Venereol* 1997;77:203-6.

208. Fink SL, and Cookson BT. Apoptosis, pyroptosis, and necrosis: mechanistic description of dead and dying eukaryotic cells. *Infect Immun* 2005;73:1907-16.
209. Tone M, Thompson SA, Tone Y, Fairchild PJ, and Waldmann H. Regulation of IL-18 (IFN-gamma-inducing factor) gene expression. *J Immunol* 1997;159:6156-63.
210. Knox JB, Sukhova GK, Whittemore AD, and Libby P. Evidence for altered balance between matrix metalloproteinases and their inhibitors in human aortic diseases. *Circulation* 1997;95:205-12.
211. Wallakovits LA, Moore VL, Bhardwaj N, Gallick GS, and Lark MW. Detection of stromelysin and collagenase in synovial fluid from patients with rheumatoid arthritis and posttraumatic knee injury. *Arthritis Rheum* 1992;35:35-42.
212. Clark IM, Powell LK, Ramsey S, Hazleman BL, and Cawston TE. The measurement of collagenase, tissue inhibitor of metalloproteinases (TIMP), and collagenase-TIMP complex in synovial fluids from patients with osteoarthritis and rheumatoid arthritis. *Arthritis Rheum* 1993;36:372-79.
213. Yoshihara Y, Obata K, Fujimoto N, Yamashita K, Hayakawa T, and Shimmel M. Increased levels of stromelysin-1 and tisause inhibitor of metalloproteinases-1 in sera from patients with rheumatoid arthritis. *Arthritis Rheum* 1995;38:969-75.
214. Ishiguro N, Ito T, Obata K, Fujimoto N, and Iwata H. Determination of stromelysin-1, 72 and 92 kDa type IV collagenase, tissue inhibitor of metalloproteinase-1 (TIMP-1), and TIMP-2 in synovial fluid and serum from patients with rheumatoid arthritis. *J Rheumatol* 1996;23:1599-604.
215. Blaser J, Triebel S, Maasjosthusmann U, Romisch J, Krahl-Mateblowski U, Freudenberg W, Fricke R, and Tschesche H. Determination of metalloproteinases, plasminogen-activators and their inhibitors in the synovial fluids of patients with rheumatoid arthritis during chemical synoviorthesis. *Clin Chim Acta* 1996;244:17-33.
216. Freestone T, Turner RJ, Coady A, Higman DJ, Greenhalgh RM, and Powell JT. Inflammation and matrix metalloproteinases in the enlarging abdominal aortic aneurysm. *Arteriosclerosis, Thrombosis & Vascular Biology* 1995;15:1145-51.
217. Ahrens D, Koch AE, Pope RM, Stein-Picarella M, and Niedbala MJ. Expression of matrix metalloproteinase 9 (92-kd gelatinase B) in human rheumatoid arthritis. *Arthritis Rheum* 1996;39:1576 - 87.
218. Okada Y, Takeuchi N, Tomita K, Nakanishi I, and Nagase H. Immunolocalization of matrix metalloproteinase 3 (stromelysin) in rheumatoid synovioblasts (B cells): correlation with rheumatoid arthritis. *Ann Rheum Dis* 1989;48:645 - 51.
219. Dean DD, Martel-Pelletier J, Pelletier J-P, Howell DS, and Woessner J. Evidence for matrix metalloproteinase and metalloproteinase inhibitor imbalance in human osteoarthritic cartilage. *J Clin Invest* 1989;84:678 - 83.
220. Shah PK, Falk E, Badimon JJ, Fernandez-Ortiz A, Mailhac A, Villareal-Levy G, Fallon JT, Regnstrom J, and Fuster V. Human monocyte-derived macrophages induce collagen breakdown in fibrous caps of atherosclerotic plaques. Potential role of matrix-degrading metalloproteinases and implications for plaque rupture. *Circulation* 1995;92:1565-9.
221. Young JL, Sukhova GK, Foster D, Kisiel W, Libby P, and Schonbeck U. The serpin proteinase inhibitor 9 is an endogenous inhibitor of interleukin 1beta-converting enzyme (caspase-1) activity in human vascular smooth muscle cells. *J Exp Med* 2000;191:1535-44.

Acknowledgements

First and foremost, I cannot thank Uwe Schönbeck enough for teaching and guiding me over the past years. You have been a constant source of knowledge, solutions, challenges, and enormous motivation. Thank you also for not considering all your “deadlines” literally, as I would not be alive today otherwise. Also, I would like to apologize to your wife and kids for my shortcomings costing them valuable time with you.

I would like to thank Peter Libby for the opportunity to work in his laboratory. It has been a very enjoyable journey over these years in your group. Discussions with you not only advanced my scientific insight but also fostered my interest into the clinical implications of our research. Thank you also for all the advice and support.

I am also very grateful to Professor Helmut W. Klein for mentoring this thesis and discussing the progress during my visits to Cologne.

Thanks also to Professor Jens Brüning for agreeing to review this thesis.

I am extremely thankful to the Ernst Schering Research Foundation in Berlin for entrusting me with a Scholarship for a substantial time of this thesis work.

Karen Williams’ editorial assistance was of tremendous help during the final preparation of this thesis. The work of Elissa Simon-Morrissey made organization of lab work much easier. David and Mark for making the office a fun place to visit. Marysia Muszynski, Irina Chulsky, Neil Tritman, Nomeda Vaisviliene, and Michelle Rodrigue for invaluable help over all the years in the cell culture core. Galina Sukhova and Eugenia Shvartz for sharing their expertise and knowledge of immunohistochemistry. Thank you all.

I thank Dr. John Randle and Vertex Pharmaceuticals for kindly providing the recombinant pro-IL-18, Dr. Winnie Wong for providing Caspase-1 deficient mice, and Eric Spooner of the Functional Proteomics Center at the Department of Pathology at Harvard Medical School for his invaluable assistance with the mass spectrometric analysis and for taking the time to help me to understand it.

Lindsey MacFarlane, Rebecca Reynolds, and Samantha LaClair must be thanked for putting up with me and all of my little furry friends. Analyzing atherosclerosis in hundreds of mice has been fun because of you guys. Thanks!

It has been a pleasure to work with Krishna Aragam. I hope it wasn't too dire to be the first student guided by me. Thank you for all the effort and discussions.

I am also very grateful to Andreas "Mr. Cheers" Zirlik for being an ever helpful colleague and great friend and for constantly reminding me that "Life is no picnic".

This thesis would not be printed at this very moment without the help of so many people in the last weeks, days, hours and minutes. Especially, Andreas and Lindsey.
THANKS!

Thanks to all the current and former members of the Schönbeck, Libby, and Plutzky labs, especially Udo, Kikuo, Jimmy, Dan, Meagan, Brendan, Rebecca, Nerea, Mike, Vedika, Fabrice, Rene (and everybody I forgot to list here) for providing help, friendship, and more laughs than I can remember.

I want to thank the "World Series Champions" Boston Red Sox letting me become a fan of the game of baseball, which I previously thought of as impossible, and for finally letting me witness them ending the 86 years-long title drought.

I am enormously thankful to my parents and siblings, who always supported me wherever they could. I am sorry that my "three month internship" ended in this six year journey and is still not returning home yet. Danke!

Finally, Christin, thank you for everything. For your courage to move to Boston, your endurance to stay here, and your craziness to be willing to stick with me. There are too many things and not enough pages here to express my gratefulness and love.

Statement of research

English

I verify, that I prepared this present dissertation independently and that all resources and parts of this work, including tables, maps, or figures, which are inferred from other sources, are fully disclosed as such. This dissertation has not previously been submitted to any other faculty or university. Furthermore, this dissertation has not been and will not be published before the conclusion of the conferral of the doctorate with the exception of the partial publications disclosed below. I am aware of the regulations detailed in the “Promotionsordnung”.

This present dissertation was mentored by Professor Helmut W. Klein.

German:

Ich versichere, daß ich die von mir vorgelegte Dissertation selbständig angefertigt, die benutzten Quellen und Hilfsmittel vollständig angegeben und die Stellen der Arbeit - einschließlich Tabellen, Karten und Abbildungen -, die anderen Werken im Wortlaut oder dem Sinn nach entnommen sind, in jedem Einzelfall als Entlehnung kenntlich gemacht habe; dass diese Dissertation noch keiner anderen Fakultät oder Universität zur Prüfung vorgelegen hat; daß sie - abgesehen von unten angegebenen Teilpublikationen - noch nicht veröffentlicht worden ist sowie, daß ich eine solche Veröffentlichung vor Abschluß des Promotionsverfahrens nicht vornehmen werde. Die Bestimmungen dieser Promotionsordnung sind mir bekannt. Die von mir vorgelegte Dissertation ist von Herrn Professor Helmut W. Klein betreut worden.

Boston, 15. Mai 2005

(Norbert Gerdes)

Original Articles:

Gerdes N, Sukhova GK, Libby P, Young JL, Reynolds RS, Schönbeck U. Expression of interleukin (IL)-18 and functional IL-18 receptor on human vascular endothelial cells, smooth muscle cells, and macrophages: implications for atherogenesis. *J. Exp. Med.* 2002, 195(2):245-257.

Abstracts:

Gerdes N, Sukhova GK, Libby P, Young JL, Schönbeck U. Expression of functional IL-18 and IL-18 receptor on endothelial cells, smooth muscle cells, and macrophages: Implications in Atherogenesis. *Scand. J Immunol.* 2001; 54,Suppl.1: 98.

Gerdes N, Libby P, Reynolds R, Kilbride M, Sukhova GK, Akira S, Schönbeck U. Diminished atherosclerosis in IL-18 gene-deficient mice. *Circulation.* 2002, 106(19): II-250.

Gerdes N, Aragam KG, LaClair SJ, MacFarlane LA, Libby P, Schönbeck U. Caspase-1-independent activation of interleukin-18 by matrix metalloproteinases as a novel proatherogenic pathway . *Circulation.* 2004, 110(17): III-312.

Presentations:

11th International Congress of Immunology, July 22-27, 2001, Stockholm, Sweden.

75th Scientific Sessions of the American Heart Association, November 17-20, 2002, Chicago, USA.

77th Scientific Sessions of the American Heart Association, November 7-10, 2004, New Orleans, USA.

Curriculum vitae

Name:	Norbert Gerdes
Date of Birth:	3. October 1974
Place of Birth:	48341 Altenberge, Germany
Citizenship:	German
Education:	
1981 - 1985	St. Johannes-Grundschule, Altenberge, Germany (Elementary School)
1985 - 1994	Gymnasium Paulinum, Münster, Germany (High School)
1994 – 1995	Mandatory civil service, University Hospital, Münster, Germany
1995 - 1997	Studies of Biology, Westfälische-Wilhelms-University, Münster, Germany
1997	Pre-examination in Biology (Vordiplom), Westfälische-Wilhelms-University, Münster, Germany
1997 - 2000	Advanced Studies of Biology, University of Cologne, Germany
2000	Examination in Biology (Diplom; equivalent to <i>Masters of Science</i>)
2000 –2001	Diploma thesis in Biology, performed at Brigham & Women's Hospital and Harvard Medical School, Boston, USA Instructor: Prof. Dr. Peter Libby, Brigham & Women's Hospital and Harvard Medical School Supervisor: Prof. Dr. Jonathan C. Howard, University of Cologne
Since 2001	Doctoral thesis in Biology, performed at Brigham & Women's Hospital and Harvard Medical School, Boston, USA Instructor: Prof. Dr. Uwe Schönbeck, Brigham & Women's Hospital and Harvard Medical School Supervisor: Prof. Dr. Helmut W. Klein, Institute of Biochemistry, University of Cologne